Regulation of (De)Ubiquitination Enzymes involved in Translesion Synthesis

Shreya Dharadhar

551327-L-bw-Dharadhar
Processed on: 30-12-2020

Colofon
Regulation of (De)Ubiquitination Enzymes involved in Translesion Synthesis
Shreya Dharadhar
ISBN/EAN: 9789464191042

Copyright © 2020 Shreya Dharadhar
All rights reserved. No part of this thesis may be reproduced, stored or transmitted in any way or by any means without the prior permission of the author, or when applicable, of the publishers of the scientific papers.

Cover design and Layout and design by Birgit Vredenburg, persoonlijkproefschrift.nl
Printing: Gildeprint Enschede, gildeprint.nl

Regulation of (De)Ubiquitination Enzymes involved in Translesion Synthesis

De regulatie van (de-)ubiquitinering-enzymen die betrokken zijn in translesiesynthese

Proefschrift

ter verkrijging van de graad van doctor aan de
Erasmus Universiteit Rotterdam
op gezag van de
rector magnificus

Prof.dr. F.A. van der Duyn Schouten

en volgens besluit van het College voor Promoties.
De openbare verdediging zal plaatsvinden op

vrijdag 5 februari 2021 om 10.30 uur

door

Shreya Dharadhar
geboren te Mumbai, India.

Erasmus University Rotterdam

PROMOTIECOMMISSIE:

Promotoren:	Prof. dr. T.K. Sixma
	Prof. dr. A. Perrakis
Overige leden:	Dr.Ir. J.A.F. Marteijn
	Prof. dr. C.P. Verrijzer
	Prof. dr. N. Dekker

TABLE OF CONTENTS

CHAPTER 1

INTRODUCTION

GENERAL INTRODUCTION

Ubiquitination of proteins is essential for optimal functioning of almost every cellular pathway in eukaryotes. Post-translational modification of a protein with ubiquitin can be used to trigger different processes. During replication, the ubiquitination of PCNA at K164 is a crucial step in the regulation of several DNA damage tolerance pathways. This thesis studies the enzymes involved in the mono-ubiquitination of PCNA and how this specific mark is generated and removed. A combination of mechanistic and structural studies is used to get insight in the regulation of this process. To place it into context this introduction first describes the ubiquitination process followed by a brief introduction of the essential players involved in DNA damage bypass.

Ubiquitination is a post-translational modification which involves the attachment of ubiquitin on either the lysine residues or the N-terminus of target proteins. Ubiquitin modifications are extremely modular since ubiquitin itself has 7 lysine residues in addition to its N-terminus which allows for the formation of homotypic, heterotypic and branched ubiquitin chains apart from the simpler mono-ubiquitination marks. Examples are K-48 linked ubiquitin chains, which are the most abundant form of ubiquitination and lead to proteasomal degradation of the target protein whereas mono-ubiquitination and K63-linked chains are non-degradative signals involved in several cellular pathways, e.g. DNA damage pathways and innate immunity (Thrower *et al*, 2000; Hoege *et al*, 2002; Galan & Haguenauer-Tsapis, 1997). Recently, many reports have identified new phenotypes for the lesser known atypical chains which highlights the incredible diversity of the ubiquitin system (Swatek & Komander, 2016).

Attachment of ubiquitin to target proteins is performed by the sequential action of enzymes belonging to the ubiquitin activating enzymes (E1), ubiquitin conjugating enzymes (E2) and the ubiquitin ligases (E3) respectively. In this process, the E3 ligases control catalytic efficiency and substrate specificity. On the other hand, the removal of ubiquitin is carried out by a class of proteases called deubiquitinating enzymes (DUBs) which carry the catalytic as well as the substrate binding component.

The large numbers of (de)-ubiquitination enzymes are necessary to direct a vast array of ubiquitin linkages to a diverse set of substrates while ensuring specificity. Their action leads to the timely attachment and removal of ubiquitin linkages which is essential for proper functioning of the respective pathways. Further regulation of these enzymes can add another layer of control. This is important, as unchecked activity can have disastrous consequences for the cell. Different forms of regulation, including PTMS, effects of the substrate and intra-enzyme allosteric regulation have been observed and described

551327-L-bw-Dharadhar
Processed on: 30-12-2020
PDF page: 8

in a number of review articles (Sahtoe & Sixma, 2015; Zheng & Shabek, 2017). In the following sections we will highlight the importance of E3 ligases and DUBs in catalyzing their respective reactions and dictating substrate specificity.

UBIQUITINATING ENZYMES

The ubiquitination cascade is initiated by an E1 enzyme which activates the C-terminal tail of ubiquitin by forming a thioester bond with its active site cysteine residue in an ATP dependent manner. This is followed by the transfer of ubiquitin to the active site cysteine of one of ~35 different E2 enzymes. E3 ligases then bind ubiquitin-loaded E2's and mediate the transfer of ubiquitin to the substrate.

E3 ligases are divided in three classes with distinct mechanisms for ubiquitin transfer, the HECT (homologous to E6-AP carboxy terminus) ligases directly catalyze ubiquitin transfer through their own enzymatic activity whereas the RING (really interesting new gene) E3's act as intermediates and enhance the rate of ubiquitin transfer from the E2 to the substrate (Metzger *et al*, 2014; Scheffner & Kumar, 2014; Deshaies & Joazeiro, 2009). The third class of E3 ligases called RBR's (RING-IBR-RING) display a RING-HECT hybrid mechanism to facilitate ubiquitin transfer (Wenzel *et al*, 2011). RING mediated transfer of ubiquitin from E2 to substrate is the most commonly used mechanism as RING E3's are the largest family of E3 ligases with over 600 members.

The RING E3's are composed of a zinc binding domain called the RING domain which contains highly conserved cysteine and histidine residues that co-ordinate two zinc atoms within its central core in a cross braced manner (Deshaies & Joazeiro, 2009). This peculiar fold allows the RING domain to act as a central axis for protein-protein interactions which is essential for its activity since both the E2 and the charged ubiquitin interact through this domain. RING E3s are a diverse group where some are active as single subunit RINGs while others require RING dimerization to exhibit full activity. Dimerization has been shown to be important for ligase activity as the non-E2 binding RING monomer is important for preferential binding of the ubiquitin-loaded E2 and subsequent catalysis (Plechanovová *et al*, 2011). In monomeric RINGs like the Cbl family, an additional ubiquitin interacting component which is external to the RING domain is necessary for optimal transfer of ubiquitin from the charged E2 (Dou *et al*, 2013).

Several variants of the RING domain have been identified, some of these lack one or most of the conserved residues but retain a similar fold while others have a similar conserved amino acid pattern but lack the distinct RING fold (Borden & Freemont, 1996). One of the notable variants is the U-box domain which does not bind zinc but has a similar fold

551327-L-bw-Dharadhar
Processed on: 30-12-2020
PDF page: 9

as the RING domain and is also able to independently recruit E2 enzymes (Aravind & Koonin, 2000; Vander Kooi *et al*, 2006). In addition to the RING domain, most RING E3's also contains a substrate interaction domain but, in some cases, they reside in multi subunit complexes where specificity is dictated by another subunit of the complex.

The RING domain does not contain an active site but it enhances the rate of transfer of charged ubiquitin from E2 to target substrate by several folds. This activation occurs upon binding of the RING domain to both the E2 and ubiquitin which results in the immobilization of the previously flexible donor ubiquitin. The RING imposed conformational selection also positions the C-terminal tail of ubiquitin with respect to the E2 active site such that the thioester is now prone to attack from the target lysine (Plechanovová *et al*, 2012; Pruneda *et al*, 2012; Dou *et al*, 2012). RING E3 ligases share this mechanism of E2~Ub binding and activation among themselves but their mode of substrate recruitment is very diverse and thus far less understood. The mechanistic details of substrate specificity are understood for a few cases but these cannot be applied to such a broad class of enzymes until more research with different combinations of E3's and substrates is carried out.

DEUBIQUITINATING ENZYMES (DUBS)

DUBs are isopeptidases that cleave ubiquitin or ubiquitin-like molecules from their target substrates. DUBs counteract the activity of ubiquitin ligases so their role is defined by the nature of the substrate and the type of modification being processed. They also play a role in maintaining the free ubiquitin pool and formation of mature ubiquitin monomers. There are nearly 100 DUBs encoded in the human genome and they are divided into seven families based on their sequence and catalytic fold. The ubiquitin-specific proteases (USPs), the ovarian tumor proteases (OTUs), the ubiquitin C-terminal hydrolases (UCHs), the Josephin's, MINDY's and ZUFSP are cysteine proteases while the seventh DUB family is the JAMM (JAB1/MPN/Mov34) domain zinc-dependent metalloprotease family (Mevissen & Komander, 2017; Hermanns *et al*, 2018; Kwasna *et al*, 2018).

DUBs can cleave ubiquitin modifications either directly from their target substrate or they can modify ubiquitin signals by trimming ubiquitin chains. Many DUBs including the USPs do not exhibit chain specificity for ubiquitin dimers and cleave all types of chains. However, a subset, e.g. the OTU family, has exquisite chain specificity, even at the dimer level. Moreover, most USPs that have been tested on longer chains displayed some level of chain selectivity. In addition to their catalytic domains, many DUBs carry domains which allows them to either recognize specific linkage type or the target from which the linkage needs to be cleaved. In some cases, these internal domains don't

551327-L-bw-Dharadhar
Processed on: 30-12-2020
PDF page: 10

affect target recruitment but instead regulate DUB function by modulating their intrinsic catalytic activity.

Regulation of DUB activity by affecting target recruitment or catalytic activity can also be carried out by external proteins that associate with DUBs in multi subunit complexes (Sahtoe & Sixma, 2015; Leznicki & Kulathu, 2017). Multiple subunits of the SAGA DUB module act together to increase yeast USP Ubp8 activity while one subunit also facilitates substrate recognition (Lee *et al*, 2005; Morgan *et al*, 2016). UCH-L5 activity is regulated both positively and negatively by binding to RPN13 and INO80G respectively. Structural studies have shown how both these regulators affect UCH-L5 substrate binding leading to opposite outcomes (Sahtoe *et al*, 2015; VanderLinden *et al*, 2015). Another well know example is the activation of USP1/12/46 by WDR48 where binding leads to increased catalytic turnover of the USPs (Cohn *et al*, 2007). USP12 and USP46 also bind another activator called WDR20 which leads to further activation of these complexes (Kee *et al*, 2010). Structures of DUBs from each subfamily have been reported in the past decade that highlight the distinct architecture and activity mechanism of each class. However, the mechanisms involved in allosteric regulation and substrate specificity are still poorly understood for most DUBs.

SUBSTRATE SPECIFICITY

The ubiquitin machinery performs its function on a broad group of substrates with a high degree of specificity. If (de)-ubiquitination enzymes were not acting specifically on their respective substrates then this would lead to a complete breakdown in cellular functioning. E3 ligases and DUBs are the principal determinants of target specificity for ubiquitin attachment and removal respectively. Over the past few decades many reports have emerged that describe the role of specific regions in recruitment of these enzymes to their respective substrates. These regions could either be specialized domains within the enzymes itself or they can be “external” proteins that interact with the enzyme (Zheng & Shabek, 2017). However, there is far less understanding of the mechanistic details involved in specific lysine targeting especially when there are other lysine’s also present in the vicinity of the ubiquitin thioester. Some breakthroughs have been achieved for a handful of RING E3’s as mechanisms describing the role of protein-protein interactions with substrate in orienting the charged ubiquitin in the vicinity of the target lysine have been elucidated (McGinty *et al*, 2014; Streich & Lima, 2016). In case of DUBs, the first structure reported was of the SUMO specific SENP2 with its substrate RanGAP1-SUMO. The authors identified interaction surfaces on the protease that are important for RanGAP1 specific activity (Reverter & Lima, 2006). Recently, the structure of the SAGA-DUB module on ubiquitinated (K120) histone H2B highlighted

551327-L-bw-Dharadhar
Processed on: 30-12-2020
PDF page: 11

the molecular determinants for substrate specificity in yeast Ubp8 (USP22 in humans) (Morgan *et al*, 2016).

Many examples of substrates that show modification of specific lysine residues have emerged for e.g. ubiquitin modification of K164 in PCNA, K561 and K523 in FANCD2 and FANCI, K519 in SMAD4 etc (Mattiroli & Sixma, 2014). One of the best studied substrates for site specific (de)-ubiquitination is the nucleosome, more specifically the histone H2A. There are three distinct sites on H2A (K13/K15; K118/K119; K125/K127/K129) which are ubiquitinated specifically by three different E3 ligases which lead to different biological outcomes (Wang *et al*, 2004; Mattiroli *et al*, 2012; Gatti *et al*, 2012; Kalb *et al*, 2014). Conversely, the removal of ubiquitin from these three sites also seems to be performed by different DUBs as it has been reported that BAP1 (Scheuermann *et al*, 2010; Sahtoe *et al*, 2016) and USP16 (Joo *et al*, 2007) specifically deubiquitinate the K118/K119 site while USP44 (Mosbech *et al*, 2013) and USP51 (Wang *et al*, 2016) have been implicated in the deubiquitination of the K13/K15 site. Recently, USP48 was identified to be preferentially involved in counteracting the role of BRCA1/BARD1 ubiquitination of K125/K127/K129 (Uckelmann *et al*, 2018). Another substrate that is selectively modified at a specific lysine residue is PCNA which is mono-ubiquitinated at K164 by the E2-E3 pair RAD6-RAD18 (Hoege *et al*, 2002) and deubiquitinated by USP1 (Huang *et al*, 2006). In chapters 4 and 5, we have identified regions in both USP1 and RAD18 which play a role in PCNA interaction directly and also through their association with DNA.

PCNA (DE)-UBIQUITINATION

Proliferating cell nuclear antigen (PCNA) is a ring-shaped protein that orchestrates a large plethora of functions at the replication fork. It is also known as the sliding clamp since its architecture enables it to encircle the DNA and slide bi-directionally on it to perform multiple functions, primarily by recruitment of replication and repair factors. A 5-protein complex called the replication factor complex (RFC) ensures efficient loading of PCNA on DNA in an ATP dependent manner (Yoder & Burgers, 1991). PCNA lacks any enzymatic activity by itself but it plays a role in varied processes by recruiting a wide range of proteins (Moldovan *et al*, 2007). PCNA interacts with a large number of proteins by binding to a conserved motif called the PCNA interacting peptide (PIP) motif. The consensus PIP sequence is Q-X-X-Ψ-X-X-ϑ-ϑ, in which Ψ is a moderately hydrophobic amino acid (L, V, I, or M) and ϑ is an aromatic residue (Y or F) (De Biasio & Blanco, 2013). Many proteins have different versions of the PIP which deviate from the consensus sequence as a result of which they can have different affinities for PCNA.

551327-L-bw-Dharadhar
Processed on: 30-12-2020
PDF page: 12

The primary function of PCNA is in DNA replication where it tethers the polymerase to DNA which leads to an increase in replication processivity. The sliding clamp also plays a crucial role in non-replicative processes mostly dealing with DNA repair and genomic stability (Choe & Moldovan, 2017). One such process is the translesion synthesis (TLS) pathway where cells employ low fidelity polymerases (for eg; Pol η, Pol κ, Rev1) to bypass damaged lesions which cannot be processed by normal replicative polymerases. TLS is tolerated by the cell as it prefers the use of error prone polymerases instead of replication fork stalling which can lead to formation of more toxic double stranded breaks if replication is not restarted (Cipolla *et al*, 2016). In TLS, PCNA gets mono-ubiquitinated at lysine 164 by RAD6-RAD18 upon fork stalling at DNA lesions (Fig.1), this leads to the recruitment of specialized TLS polymerases that allow for damage bypass and continuation of replication (Hoege *et al*, 2002; Watanabe *et al*, 2004; Kannouche *et al*, 2004). Since unchecked recruitment of these polymerase can be highly mutagenic, cells employ the deubiquitinase USP1 which removes the mono-ubiquitin mark from PCNA (Fig.2) and allows the entry of normal replicative polymerases resulting in more faithful replication of the DNA once the damage has been bypassed.

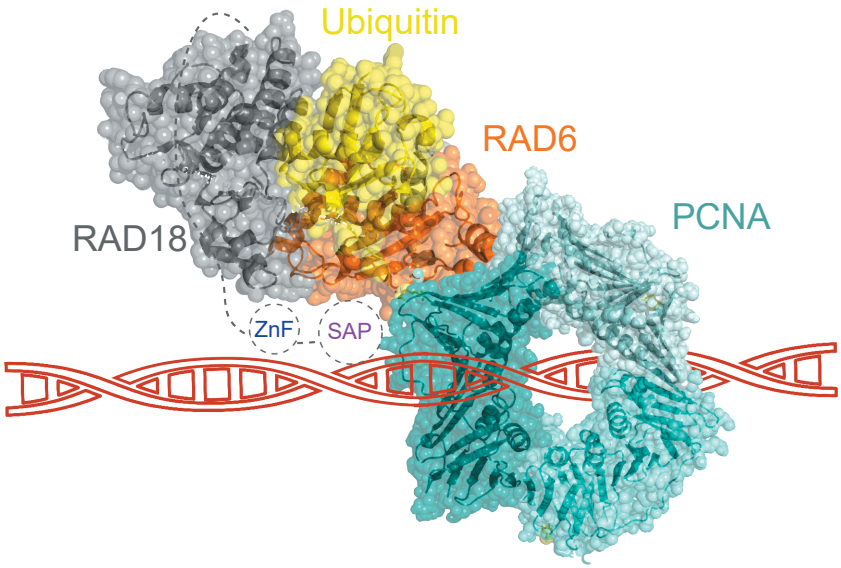

Fig.1) Structural model of RAD6_Ub-RAD18 bound to PCNA (PDB: 1AXC chains A,C,E) loaded on DNA. Model of RAD6_Ub-RAD18 is based on RNF4-RNF4-Ub~E2 (PDB: 4AP4), the RAD18 RING domain (PDB: 2Y43) was superimposed on RNF4 and RAD6 (PDB: 2YBF chain A) was superimposed on the E2 before removing the RNF4 and E2 structures. The current model lacks the Zinc finger (ZnF) and SAP domain (shown here) along with the C-terminal region of RAD18 which contains the RAD6 and Pol η binding domain.

RAD6-RAD18

RAD18 is a multi-domain RING E3 ligase that is active upon homodimerization mediated by its N-terminal RING domain. This domain is also important for RAD6 (E2) interaction along with another specialized RAD6 binding domain (R6BD) that is present at the C-terminus of RAD18. Additionally, RAD18 also contains a zinc-finger (ZnF) domain, SAP domain and a Pol η interaction domain (Hedglin & Benkovic, 2015). RAD6-RAD18 form a stable asymmetric complex where one RAD6 molecule binds one RAD18 homodimer (Bailly *et al*, 1997; Huang *et al*, 2011). RAD6 is capable of forming ubiquitin chains through non covalent interactions with the "backside" ubiquitin binding site but RAD18 binds to this site through its R6BD and prevents "backside" binding thereby inhibiting RAD6 chain formation activity (Hibbert *et al*, 2011). The mono-ubiquitination activity of RAD6-RAD18 is low on free PCNA but it is strongly stimulated when PCNA is loaded onto the DNA (Fig.1) (Garg & Burgers, 2005). The mechanistic details of this activation were still unknown so we have tried to address this by performing quantitative mono-ubiquitination assays on DNA-loaded PCNA in chapter 5.

In spite of the large number of ubiquitination enzymes, RAD6-RAD18 is essential for carrying out PCNA mono-ubiquitination. This ubiquitination mark acts as a trigger for TLS upon replication fork stalling. Stalling of the replication fork leads to a buildup of ssDNA which is quickly bound by the heterotrimeric RPA protein. This induces the recruitment of RAD6-RAD18 to the stalled replication fork by a direct interaction between RPA and RAD18 (Niimi *et al*, 2008). The binding of RAD18 to RPA takes place through its N- terminal region which includes the RING domain but not the ZnF or the SAP domain (Davies *et al*, 2008). However, RAD18 binds DNA through its SAP domain which has been shown to be important for its activity on PCNA (Notenboom *et al*, 2007; Tsuji *et al*, 2008; Nakajima *et al*, 2006). Altogether, this suggests that both DNA and RPA interactions are necessary for RAD18 ligase activity on PCNA. The interaction region for PCNA on RAD18 has been broadly mapped to the N-terminal region spanning from residue 16-366 but the exact residues involved are not known. This leads us to the important question of how several of these RAD18 interactions co-operate to achieve specific PCNA mono-ubiquitination at K164 (Fig.1). In Chapter 5, we identify several molecular features within RAD18 that allow for activity on DNA-loaded PCNA and uncover new mechanisms involved in RAD18 activity.

USP1 AND ITS PARALOGS

USP1 acts as a negative regulator of TLS by deubiquitinating monoubiquitinated PCNA (PCNA-Ub) thereby preventing the unscheduled recruitment of TLS polymerases (Fig.2) (Huang *et al*, 2006). USP1 also acts as a negative regulator of another DNA repair

551327-L-bw-Dharadhar
Processed on: 30-12-2020
PDF page: 14

pathway i.e. the Fanconi Anemia pathway where it deubiquitinates monoubiquitinated FANCD2 (Nijman *et al*, 2005). The USP1 knockout mice show a severe Fanconi Anemia phenotype with defects in homologous recombination and heightened PCNA-Ub levels confirming the importance of USP1 in genomic stability (Kim *et al*, 2009). Due to its role in DNA repair, USP1 has emerged as an attractive drug target in cancer research and several studies have shown that inhibition of its enzymatic activity can reverse the chemoresistance of non-small cell lung cancer cells to cisplatin which is a commonly used anticancer drug (Chen *et al*, 2011). Recently, USP1 mediated PCNA deubiquitination in TLS was shown to be important for maintaining replication fork stability in the absence of BRCA1. This gives rise to an interesting synthetic lethal relationship and suggests that USP1 inhibitors might help in treatment of BRCA1 deficient tumors (Lim *et al*, 2018). Additionally, USP1 has been proposed to have an important role in stabilizing a number of proteins involved in diverse cellular pathways like autophagy, cell division, antiviral immunity, AKT signaling, β-catenin signaling and stem cell maintenance (Raimondi *et al*, 2019; Jung *et al*, 2016; Yu *et al*, 2017; Zhang *et al*, 2012; Ma *et al*, 2019; Williams *et al*, 2011). The various USP1 functions and its clinical potential make it an interesting member of the USP family to study mechanistically.

USP1 is a multi-domain protein of 785 amino acid residues and belongs to the largest family of DUBs called the USPs. This family of DUBs has cysteine protease activity in a conserved catalytic domain. The USP catalytic domain can be divided into 3 subdomains which are known as the finger, palm and thumb domains. Its catalytic center has a catalytic triad involving a cysteine (Cys), a histidine (His) and an aspartate or asparagine (Asp or Asn). In some USPs the third catalytic residue (Asp or Asn) is missing but the regions containing the Cys and His residues are highly conserved among all family members. The mode of catalysis in USPs is similar to that observed in the Papain protease families where an acyl intermediate is formed between the catalytic Cys and C-terminal glycine of ubiquitin which is hydrolyzed upon nucleophilic attack by a water molecule (Komander *et al*, 2009). Alternatively, it was proposed that USP1 activity takes place through general base catalysis which is different from the mode of action of the papain family (Villamil *et al*, 2012a).

The catalytic triad of USPs is located at the interface of the palm and thumb subdomains while the finger domain binds the ubiquitin molecule that is linked via its C-terminus to a lysine residue of a target protein or another ubiquitin molecule. Several structures of USP catalytic domains with and without ubiquitin have been solved which not only highlight the conservation of the catalytic fold but also demonstrate unique structural features among USPs. In these structures, some USPs are found in an inactive conformation in

551327-L-bw-Dharadhar
Processed on: 30-12-2020
PDF page: 15

the Apo form, where either the catalytic residues are misaligned or the ubiquitin binding region is blocked. These USPs achieve a catalytic competent state upon binding of ubiquitin or specialized domains (internal or external) to the USP catalytic domain. One such example is that of USP7 where binding of ubiquitin leads to changes in several structural elements surrounding the catalytic cleft which realigns the active site residues (Hu *et al*, 2002). There is no structural information of the USP1 protein as of now but it is very likely that its catalytic domain would be similar to that of other members of this family (Fig.2). However, the presence of large inserts within its catalytic domain makes the overall structure of USP1 very interesting as it can inform us on the specific positioning and role of these inserts in USP1 activity.

USP1 activity is regulated at multiple levels since it is a crucial regulator of important cellular pathways. It has been proposed that exposure to UV irradiation leads to an autocleavage event within USP1 resulting in loss of activity and thus a prolonged TLS (Huang *et al*, 2006). Importantly, USP1 activity is regulated by a WD40 repeat protein called UAF1 (USP1-associated factor) which binds and enhances USP1 catalytic activity. UAF1 is a WD40 domain containing protein which is composed of an N-terminal 8-bladed β-propeller and two C-terminal domains namely, SLD1 and SLD2. The N-terminal β-propeller region is responsible for binding to USP1 that leads to a several fold increase in k_{cat} while there is no significant change in K_M on a minimal substrate. This suggests that UAF1 binding results in increased catalytic turnover of USP1 and no change in affinity for ubiquitin (Cohn *et al*, 2007). It was later shown that UAF1 activates USP1 by realigning the active site residues into a productive confirmation (Villamil *et al*, 2012a). The C-terminal domains of UAF1 have also been implicated in USP1 function on both PCNA-Ub and FANCD2-Ub. The SLD2 domain of UAF1 binds to the SIM motif on FANCI and hElg1 which ensures targeted recruitment of USP1 to FANCD2-Ub and PCNA-Ub respectively (Yang *et al*, 2011).

UAF1 binds and activates two other USPs which are paralogs of USP1 namely, USP12 and USP46 (Cohn *et al*, 2009). Both these USPs are much smaller than USP1 as they are mainly composed of the USP catalytic domain and lack the large inserts found in USP1. USP12 and USP46 share high sequence similarity (88%) with each other and 31% sequence similarity with USP1. The cellular substrates of USP12 and USP46 are not well defined with multiple reports implicating them in divergent cellular pathways. USP46 plays an important role in neurobiology as studies have linked it to behavioral phenotypes in mice and in the regulation of AMPA receptors which are crucial for brain function (Imai *et al*, 2013; Zhang *et al*, 2011; Huo *et al*, 2015). USP46 has also been shown to be essential for proliferation of HPV transformed cells making it a target for the treatment

551327-L-bw-Dharadhar
Processed on: 30-12-2020
PDF page: 16

of HPV induced cancers (Kiran *et al*, 2018). On the other hand, USP12 acts on the T cell receptor (TCR) adaptor proteins LAT and Trat1 thereby regulating TCR expression at the cell surface (Jahan *et al*, 2016). It is also proposed to promote LPS induced macrophage responses and act as a negative regulator of the Notch signaling pathway (Kumar *et al*, 2017; Moretti *et al*, 2012). Additionally, some reports have identified considerable overlap in USP12 and USP46 function which is to be expected due to the high degree of similarity. Both USP46 and USP12 have been implicated in deubiquitination of histone H2A and H2B in *Xenopus*, in the regulation of Akt phosphatases (PHLPP and PHLPPL1) and in the regulation of immune response upon exposure to the Epstein Barr virus (Joo *et al*, 2011; Gangula & Maddika, 2013; Li *et al*, 2013; Ohashi *et al*, 2015).

The activation of USP12 and USP46 by UAF1 takes place solely by an increase in k_{cat} which is similar to what is observed in USP1. But USP12 and USP46 undergo a second activation step upon binding another WD40 repeat protein called WDR20 (Kee *et al*, 2010). WDR20 is composed of a 7 bladed β-propeller domain and together with UAF1 stimulates the catalytic activity of USP12 and USP46 to its maximum state. Interestingly, USP1 lacks WDR20-mediated hyperactivation presumably due to its inability to bind this protein which suggests significant differences in USP1 activity regulation compared to USP12 and USP46. Several structures of USP12 and USP46 with and without their activators have been solved in the last few years. These have shed more light on the mechanistic details of this activation (Yin *et al*, 2015; Li *et al*, 2016; Dharadhar *et al*, 2016). In chapter 3, we present the structure of USP12-Ub+UAF1 and show that UAF1 has a secondary binding site on USP12 which is conserved among its paralogs, USP46 and USP1.

Our structure is identical to the USP46-Ub+UAF1 structure where the authors also observed the second UAF1 binding but did not pursue it as the second UAF1 binding does not affect the catalytic activity of these USPs. Altogether, these structures highlighted the mechanistic details of UAF1 binding in this subfamily of USPs and revealed the interfaces involved in catalytic activation. The USP12 and USP46 showed no structural changes with and without UAF1 as all these structures were bound to ubiquitin suicide probes which trap the USP in an active conformation. However, it was observed that these USPs get activated when UAF1 binds to the finger sub-domain which is very distant from the active site suggesting an allosteric activation mechanism. In another study, the apo structures of USP12 and USP12+UAF1 were solved which when compared to each other showed subtle rearrangements of various structural elements within the USP12 catalytic domain upon UAF1 binding. Additionally, the same study also presented the

551327-L-bw-Dharadhar
Processed on: 30-12-2020
PDF page: 17

structure of the USP12+UAF1+WDR20 complex showing that WDR20 binds the palm domain of USP12 which is still very distant from the catalytic center (Li *et al*, 2016).

Understanding the mechanistic details of USP1 activation by UAF1 has proven to be elusive so far due to lack of any structural information of USP1 itself. However, the structures of its paralogs with and without UAF1 do reveal the activation interface on USP1 along with the understanding that the activation mechanism is highly dynamic in this sub class of USPs. Further correlation of the findings in USP12/USP46 to USP1 is complicated since USP1 is a much larger protein due to its inserts which are interspersed within its catalytic domain. Additionally, USP1 does not have a secondary activation step upon interaction with WDR20 like its paralogs which indicates that certain distinct mechanisms might be employed by USP1 upon UAF1 binding. In Chapter 4, we describe the role of USP1 inserts in regulating its intrinsic activity and reveal how this regulation is closely linked to UAF1 mediated activation.

Apart from UAF1-mediated activation of USP1 there are other external factors that have been proposed to play a role in USP1 regulation. Phosphorylation of serine 313 located in the large insert of USP1 seemed essential for UAF1 recruitment and activation (Villamil *et al*, 2012b) but this does not explain why USP1 lacking this region can still bind to and get activated by UAF1. Moreover, USP12 and USP46 lack this region within their corresponding insert and still bind UAF1 and mutational analysis suggests that binding is conserved within this sub-family of USPs (Yin *et al*, 2015; Li *et al*, 2016). Another factor that was recently reported to regulate USP1 activity was DNA binding to the large insert of USP1. DNA binding was reported to stimulate USP1-UAF1 activity three-fold by enhancing ubiquitin binding and catalytic turnover (Lim *et al*, 2018). Since USP1 deubiquitinates a number of DNA bound substrates this kind of regulation seems feasible but the total activation is small and we could not reproduce it (chapter 4). In Chapter 4, we present a detailed analysis of the effect of both DNA binding and phosphorylation on USP1 activity against a minimal substrate.

The regulation of USP catalytic activity has been mostly studied on minimal substrates which are mainly composed of a ubiquitin molecule attached to a fluorophore at the C-terminus. These kind of activity assays do not allow us to study the role of substrates in regulation of USP intrinsic activity. Furthermore, recognition of molecular determinants within USPs for their respective substrates is also not possible with this experimental setup. Many USPs have multiple natural substrates thus identifying specific interaction motifs will help in targeted inhibition of USP function rather than inhibiting all catalytic activity which is the most commonly used method of targeting USPs. Biochemical and

551327-L-bw-Dharadhar
Processed on: 30-12-2020
PDF page: 18

structural studies of USPs with their natural substrates is an exciting area of research which can help answer a lot of these questions and can aid in the development of a new class of specific USP inhibitors. This avenue is currently technically challenging to explore as it requires the production of a well-defined singly modified substrate. Additionally, several other factors have to be considered which have been explained in detail along with an example of studying USP activity on natural substrate in Chapter 2 of this thesis.

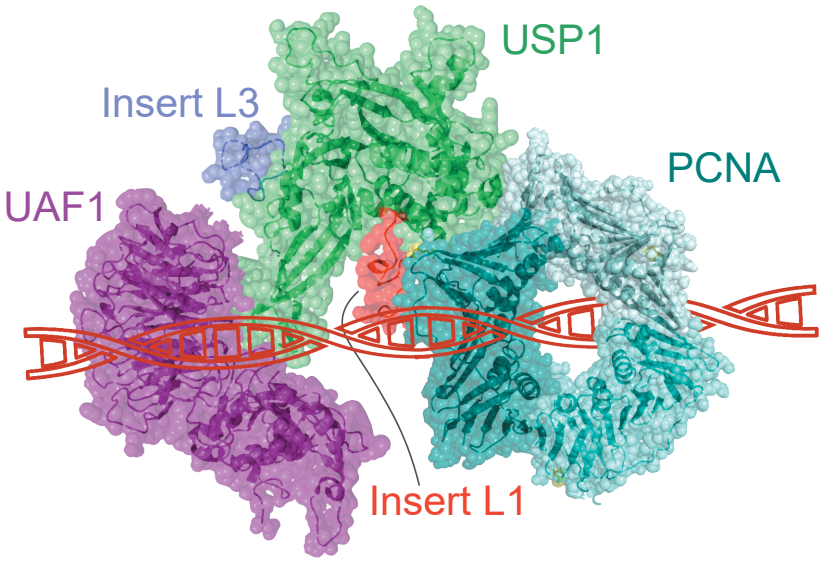

Fig.2) Structural model of USP1-UAF1 bound to PCNA (PDB: 1AXC chain A,C,E) loaded on DNA. A homology model of USP1-UAF1 was created based on the USP12-UAF1 structure (PDB: 5K1C chain A,B); USP1 has three inserts, i.e. L1, L2 (not shown here) and L3, these inserts are absent in USP1 paralogs USP12 and USP46.

USP1 has gained interest for clinical applications due to its role in two essential DNA repair pathways i.e. Fanconi Anemia pathway and Translesion synthesis pathway. USP1 deubiquitinates monoubiquitinated FANCD2 and PCNA respectively in these pathways and both these substrates can be purified in large amounts biochemically. This presents an opportunity to uncover mechanistic details of USP1 function on its natural substrate which will not only aid in the development of specific inhibitors but also answer some basic concepts of substrate mediated catalysis in USP function. The activity of USP1 on FANCD2 has been examined in significant detail and FANCD2 recognition elements have been identified in USP1 (Arkinson *et al*, 2018). Moreover, it was also shown that DNA is an essential cofactor for efficient FANCD2 deubiquitination by USP1-UAF1 where the activation is solely dependent on the DNA binding role of UAF1 (Liang *et al*, 2019).

551327-L-bw-Dharadhar
Processed on: 30-12-2020
PDF page: 19

Similar analysis of USP1 activity on PCNA has not yielded any new insights and the role of DNA loading of PCNA on deubiquitination has not been explored yet. This is most likely due to the technical challenges in the loading of PCNA-Ub on DNA and the subsequent purification of this complex for biochemical analysis. In Chapter 4, we describe a protocol for large scale purification of DNA-loaded PCNA-Ub and uncover a secondary activation step in USP1 which takes place upon interaction with DNA-loaded PCNA-Ub.

This thesis brings to light several aspects involved in the allosteric regulation of USP1 both by its activator UAF1 and its natural substrate DNA-loaded PCNA-Ub. It also highlights the role of DNA-loaded PCNA on regulating activity of RAD6-RAD18 and identifies PCNA interacting regions on both RAD18 and USP1. Altogether, this helps in understanding basic mechanisms of substrate mediated catalysis in E3's and DUB's and provides new hotspots for specific targeting of this important pathway.

OUTLINE OF THE THESIS

Chapter 2 provides a detailed framework for quantitative characterization of USP activity with complete protocols for purification of USPs and their kinetic analysis on both minimal and more natural substrates. The advantages and limitations of various in vitro binding assays that could be used for studying USP interactions are also discussed.

In **Chapter 3** we report the crystal structure of the USP12-Ub/UAF1 and show that the USP12/UAF1 complex has a 1:2 stoichiometry in solution with a two-step binding that is conserved in USP1 and USP46. We also show that the high affinity interface is essential for UAF1 mediated activation in USP12 while the low affinity interface does not affect catalytic activity.

In **Chapter 4** we describe the mechanistic details of USP1 activation by UAF1 and show how UAF1 binding alone brings USP1 to an activated state that resembles WDR20 activation in USP12/USP46. We also discover a secondary activation step within USP1 that is triggered only upon interaction with DNA-loaded PCNA-Ub. Moreover, we identify the region within USP1 responsible for DNA and PCNA interaction and show that these are necessary for the secondary activation of USP1.

In **Chapter 5** we perform a biochemical analysis of RAD6-RAD18 activity on DNA-loaded PCNA and identify molecular motifs that are important for its activity in the presence and absence of DNA. We propose that activation on DNA-loaded PCNA is solely due to DNA binding of RAD18 and also that the interface for ubiquitin transfer in RAD18 is unique from what is observed in other RING ligases.

551327-L-bw-Dharadhar
Processed on: 30-12-2020
PDF page: 20

Chapter 6 closes the thesis with a general discussion of the results presented here along with its significance in the broader ubiquitin field and a brief deliberation on ideas for future research.

551327-L-bw-Dharadhar
Processed on: 30-12-2020

REFERENCES

Aravind L & Koonin E V. (2000) The U box is a modified RING finger - A common domain in ubiquitination [1]. *Curr. Biol.* **10:** 132–134

Arkinson C, Chaugule VK, Toth R & Walden H (2018) Specificity for deubiquitination of monoubiquitinated FANCD2 is driven by the N-terminus of USP1. *Life Sci. Alliance* **1:** 1–15

Bailly V, Lauder S, Prakash S & Prakash L (1997) Yeast DNA repair proteins Rad6 and Rad18 form a heterodimer that has ubiquitin conjugating, DNA binding, and ATP hydrolytic activities. *J. Biol. Chem.* **272:** 23360–23365

De Biasio A & Blanco FJ (2013) Proliferating cell nuclear antigen structure and interactions: Too many partners for one dancer? 1st ed. Elsevier Inc.

Borden KLB & Freemont PS (1996) The RING finger domain: A recent example of a sequence-structure family. *Curr. Opin. Struct. Biol.* **6:** 395–401

Chen J, Dexheimer TS, Ai Y, Liang Q, Villamil MA, Inglese J, Maloney DJ, Jadhav A, Simeonov A & Zhuang Z (2011) Selective and cell-active inhibitors of the USP1/ UAF1 deubiquitinase complex reverse cisplatin resistance in non-small cell lung cancer cells. *Chem. Biol.* **18:** 1390–1400

Choe KN & Moldovan GL (2017) Forging Ahead through Darkness: PCNA, Still the Principal Conductor at the Replication Fork. *Mol. Cell* **65:** 380–392

Cipolla L, Maffia A, Bertoletti F & Sabbioneda S (2016) The regulation of DNA damage tolerance by ubiquitin and ubiquitin-like modifiers. *Front. Genet.* **7:** 1–12

Cohn MA, Kee Y, Haas W, Gygi SP & D'Andrea AD (2009) UAF1 is a subunit of multiple deubiquitinating enzyme complexes. *J. Biol. Chem.* **284:** 5343–5351

Cohn MA, Kowal P, Yang K, Haas W, Huang TT, Gygi SP & D'Andrea AD (2007) A UAF1-Containing Multisubunit Protein Complex Regulates the Fanconi Anemia Pathway. *Mol. Cell* **28:** 786–797

Davies AA, Huttner D, Daigaku Y, Chen S & Ulrich HD (2008) Activation of Ubiquitin-Dependent DNA Damage Bypass Is Mediated by Replication Protein A. *Mol. Cell* **29:** 625–636

Deshaies RJ & Joazeiro C a P (2009) RING domain E3 ubiquitin ligases. *Annu. Rev. Biochem.* **78:** 399–434

Dharadhar S, Clerici M, Dijk WJ Van, Fish A & Sixma TK (2016) A conserved two-step binding for the UAF1 regulator to the USP12 deubiquitinating enzyme. *J. Struct. Biol.*

Dou H, Buetow L, Sibbet GJ, Cameron K & Huang DT (2012) BIRC7-E2 ubiquitin conjugate structure reveals the mechanism of ubiquitin transfer by a RING dimer. *Nat. Struct. Mol. Biol.* **19:** 876–883

Dou H, Buetow L, Sibbet GJ, Cameron K & Huang DT (2013) Essentiality of a non-RING element in priming donor ubiquitin for catalysis by a monomeric E3. *Nat. Struct. Mol. Biol.* **20:** 982–986

Galan JM & Haguenauer-Tsapis R (1997) Ubiquitin Lys63 is involved in ubiquitination of a yeast plasma membrane protein. *EMBO J.* **16:** 5847–5854

Gangula NR & Maddika S (2013) WD repeat protein WDR48 in complex with deubiquitinase USP12 suppresses akt-dependent cell survival signaling by stabilizing ph domain leucine-rich repeat protein phosphatase 1 (PHLPP1). *J. Biol. Chem.* **288:** 34545–34554

Garg P & Burgers PM (2005) Ubiquitinated proliferating cell nuclear antigen activates translesion DNA polymerases η and REV1. *Proc. Natl. Acad. Sci. U. S. A.* **102:** 18361–18366

Gatti M, Pinato S, Maspero E, Soffientini P, Polo S & Penengo L (2012) A novel ubiquitin mark at the N-terminal tail of histone H2As targeted by RNF168 ubiquitin ligase. *Cell Cycle* **11:** 2538–2544

Hedglin M & Benkovic SJ (2015) Regulation of Rad6/Rad18 Activity During DNA Damage Tolerance. *Annu. Rev. Biophys.* **44:** 207–228

Hermanns T, Pichlo C, Woiwode I, Klopffleisch K, Witting KF, Ovaa H, Baumann U & Hofmann K (2018) A family of unconventional deubiquitinases with modular chain specificity determinants. *Nat. Commun.* **9:**

551327-L-bw-Dharadhar
Processed on: 30-12-2020
PDF page: 22

Hibbert RG, Huang A, Boelens R & Sixma TK (2011) E3 ligase Rad18 promotes monoubiquitination rather than ubiquitin chain formation by E2 enzyme Rad6. *Proc. Natl. Acad. Sci. U. S. A.* **108:** 5590–5595

Hoege C, Pfander B, Moldovan GL, Pyrowolakis G & Jentsch S (2002) RAD6-dependent DNA repair is linked to modification of PCNA by ubiquitin and SUMO. *Nature* **419:** 135–141

Hu M, Li P, Li M, Li W, Yao T, Wu JW, Gu W, Cohen RE & Shi Y (2002) Crystal structure of a UBP-family deubiquitinating enzyme in isolation and in complex with ubiquitin aldehyde. *Cell* **111:** 1041–1054

Huang A, Hibbert RG, De Jong RN, Das D, Sixma TK & Boelens R (2011) Symmetry and asymmetry of the RING-RING dimer of Rad18. *J. Mol. Biol.* **410:** 424–435

Huang TT, Nijman SMB, Mirchandani KD, Galardy PJ, Cohn M a, Haas W, Gygi SP, Ploegh HL, Bernards R & D'Andrea AD (2006) Regulation of monoubiquitinated PCNA by DUB autocleavage. *Nat. Cell Biol.* **8:** 339–347

Huo Y, Khatri N, Hou Q, Gilbert J, Wang G & Man HY (2015) The deubiquitinating enzyme USP46 regulates AMPA receptor ubiquitination and trafficking. *J. Neurochem.* **134:** 1067–1080

Imai S, Kano M, Nonoyama K & Ebihara S (2013) Behavioral Characteristics of Ubiquitin-Specific Peptidase 46-Deficient Mice. *PLoS One* **8:** 0–8

Jahan AS, Lestra M, Swee LK, Fan Y, Lamers MM, Tafesse FG, Theile CS, Spooner E, Bruzzone R, Ploegh HL & Sanyal S (2016) Usp12 stabilizes the T-cell receptor complex at the cell surface during signaling. *Proc. Natl. Acad. Sci.* **113:** 201521763

Joo HY, Jones A, Yang C, Zhai L, Smith IV AD, Zhang Z, Chandrasekharan MB, Sun ZW, Renfrow MB, Wang Y, Chang C & Wang H (2011) Regulation of histone H2A and H2B deubiquitination and xenopus development by USP12 and USP46. *J. Biol. Chem.* **286:** 7190–7201

Joo HY, Zhai L, Yang C, Nie S, Erdjument-Bromage H, Tempst P, Chang C & Wang H (2007) Regulation of cell cycle progression and gene expression by H2A deubiquitination. *Nature* **449:** 1068–1072

Jung JK, Jang SW & Kim JM (2016) A novel role for the deubiquitinase USP1 in the control of centrosome duplication. *Cell Cycle* **15:** 584–592

Kalb R, Mallery DL, Larkin C, Huang JTJ & Hiom K (2014) BRCA1 is a histone-H2A-specific ubiquitin ligase. *Cell Rep.* **8:** 999–1005

Kannouche PL, Wing J & Lehmann AR (2004) Interaction of human DNA polymerase η with monoubiquitinated PCNA: A possible mechanism for the polymerase switch in response to DNA damage. *Mol. Cell* **14:** 491–500

Kee Y, Yang K, Cohn MA, Haas W, Gygi SP & D'Andrea AD (2010) WDR20 regulates activity of the USP12.UAF1 deubiquitinating enzyme complex. *J. Biol. Chem.* **285:** 11252–11257

Kim JM, Parmar K, Huang M, Weinstock DM, Ruit CA, Kutok JL & D'Andrea AD (2009) Inactivation of Murine Usp1 Results in Genomic Instability and a Fanconi Anemia Phenotype. *Dev. Cell* **16:** 314–320

Kiran S, Dar A, Singh SK, Lee KY & Dutta A (2018) The Deubiquitinase USP46 Is Essential for Proliferation and Tumor Growth of HPV-Transformed Cancers. *Mol. Cell* **72:** 823-835.e5

Komander D, Clague MJ & Urbé S (2009) Breaking the chains: Structure and function of the deubiquitinases. *Nat. Rev. Mol. Cell Biol.* **10:** 550–563

Vander Kooi CW, Ohi MD, Rosenberg JA, Oldham ML, Newcomer ME, Gould KL & Chazin WJ (2006) The Prp19 U-box crystal structure suggests a common dimeric architecture for a class of oligomeric E3 ubiquitin ligases. *Biochemistry* **45:** 121–130

Kumar T, Nayak S, Alamuru-yellapragada NP & Parsa KVL (2017) Biochemical and Biophysical Research Communications Deubiquitinase USP12 promotes LPS induced macrophage responses through inhibition of I k B a. **:** 1–6

551327-L-bw-Dharadhar
Processed on: 30-12-2020
PDF page: 23

Kwasna D, Abdul Rehman SA, Natarajan J, Matthews S, Madden R, De Cesare V, Weidlich S, Virdee S, Ahel I, Gibbs-Seymour I & Kulathu Y (2018) Discovery and Characterization of ZUFSP/ZUP1, a Distinct Deubiquitinase Class Important for Genome Stability. *Mol. Cell* **70:** 150-164.e6

Lee KK, Florens L, Swanson SK, Washburn MP & Workman JL (2005) The Deubiquitylation Activity of Ubp8 Is Dependent upon Sgf11 and Its Association with the SAGA Complex. *Mol. Cell. Biol.* **25:** 1173–1182

Leznicki P & Kulathu Y (2017) Mechanisms of regulation and diversification of deubiquitylating enzyme function. *J. Cell Sci.* **130:** 1997–2006

Li H, Lim KS, Kim H, Hinds TR, Jo U, Mao H, Weller CE, Sun J, Chatterjee C, D'Andrea AD & Zheng N (2016) Allosteric Activation of Ubiquitin-Specific Proteases by β-Propeller Proteins UAF1 and WDR20. *Mol. Cell* **63:** 249–260

Li X, Stevens PD, Yang H, Gulhati P, Wang W, Evers BM & Gao T (2013) The deubiquitination enzyme USP46 functions as a tumor suppressor by controlling PHLPP-dependent attenuation of Akt signaling in colon cancer. *Oncogene* **32:** 471–478

Liang F, Miller AS, Longerich S, Tang C, Maranon D, Williamson EA, Hromas R, Wiese C, Kupfer GM & Sung P (2019) DNA requirement in FANCD2 deubiquitination by USP1-UAF1-RAD51AP1 in the Fanconi anemia DNA damage response. *Nat. Commun.* **10:** 1–8

Lim KS, Li H, Roberts EA, Gaudiano EF, Clairmont C, Sambel LA, Ponnienselvan K, Liu JC, Yang C, Kozono D, Parmar K, Yusufzai T, Zheng N & D'Andrea AD (2018) USP1 Is Required for Replication Fork Protection in BRCA1-Deficient Tumors. *Mol. Cell* **72:** 925-941.e4

Ma A, Tang M, Zhang L, Wang B, Yang Z, Liu Y, Xu G, Wu L, Jing T, Xu X, Yang S & Liu Y (2019) USP1 inhibition destabilizes KPNA2 and suppresses breast cancer metastasis. *Oncogene* **38:** 2405–2419

Mattiroli F & Sixma TK (2014) Lysine-targeting specificity in ubiquitin and ubiquitin-like modification pathways. *Nat. Struct. Mol. Biol.* **21:** 308–316

Mattiroli F, Vissers JHA, Van Dijk WJ, Ikpa P, Citterio E, Vermeulen W, Marteijn JA & Sixma TK (2012) RNF168 ubiquitinates K13-15 on H2A/H2AX to drive DNA damage signaling. *Cell* **150:** 1182–1195

McGinty RK, Henrici RC & Tan S (2014) Crystal structure of the PRC1 ubiquitylation module bound to the nucleosome. *Nature* **514:** 591–596

Metzger MB, Pruneda JN, Klevit RE & Weissman AM (2014) RING-type E3 ligases: Master manipulators of E2 ubiquitin-conjugating enzymes and ubiquitination. *Biochim. Biophys. Acta - Mol. Cell Res.* **1843:** 47–60

Mevissen TET & Komander D (2017) Mechanisms of Deubiquitinase Specificity and Regulation. *Annu. Rev. Biochem.* **86:** annurev-biochem-061516-044916

Moldovan GL, Pfander B & Jentsch S (2007) PCNA, the Maestro of the Replication Fork. *Cell* **129:** 665–679

Moretti J, Chastagner P, Liang CC, Cohn MA, Israël A & Brou C (2012) The ubiquitin-specific protease 12 (USP12) is a negative regulator of notch signaling acting on notch receptor trafficking toward degradation. *J. Biol. Chem.* **287:** 29429–29441

Morgan MT, Haj-Yahya M, Ringel AE, Bandi P, Brik A & Wolberger C (2016) Structural basis for histone H2B deubiquitination by the SAGA DUB module. *Science (80-.).* **351:** 725–728

Mosbech A, Lukas C, Bekker-Jensen S & Mailand N (2013) The deubiquitylating enzyme USP44 counteracts the DNA double-strand break response mediated by the RNF8 and RNF168 ubiquitin ligases. *J. Biol. Chem.* **288:** 16579–16587

Nakajima S, Lan L, Kanno SI, Usami N, Kobayashi K, Mori M, Shiomi T & Yasui A (2006) Replication-dependent and -independent Responses of RAD18 to DNA damage in human cells. *J. Biol. Chem.* **281:** 34687–34695

551327-L-bw-Dharadhar
Processed on: 30-12-2020
PDF page: 24

Niimi A, Brown S, Sabbioneda S, Kannouche PL, Scott A, Yasui A, Green CM & Lehmann AR (2008) Regulation of proliferating cell nuclear antigen ubiquitination in mammalian cells. *Proc. Natl. Acad. Sci. U. S. A.* **105:** 16125–16130

Nijman SMB, Huang TT, Dirac AMG, Brummelkamp TR, Kerkhoven RM, D'Andrea AD & Bernards R (2005) The deubiquitinating enzyme USP1 regulates the fanconi anemia pathway. *Mol. Cell* **17:** 331–339

Notenboom V, Hibbert RG, van Rossum-Fikkert SE, Olsen J V., Mann M & Sixma TK (2007) Functional characterization of Rad18 domains for Rad6, ubiquitin, DNA binding and PCNA modification. *Nucleic Acids Res.* **35:** 5819–5830

Ohashi M, Holthaus AM, Calderwood MA, Lai CY, Krastins B, Sarracino D & Johannsen E (2015) The EBNA3 Family of Epstein-Barr Virus Nuclear Proteins Associates with the USP46/USP12 Deubiquitination Complexes to Regulate Lymphoblastoid Cell Line Growth. *PLoS Pathog.* **11:** 1–33

Plechanovová A, Jaffray EG, McMahon SA, Johnson KA, Navrátilová I, Naismith JH & Hay RT (2011) Mechanism of ubiquitylation by dimeric RING ligase RNF4. *Nat. Struct. Mol. Biol.* **18:** 1052–1059

Plechanovová A, Jaffray EG, Tatham MH, Naismith JH & Hay RT (2012) Structure of a RING E3 ligase and ubiquitin-loaded E2 primed for catalysis. *Nature* **489:** 115–120

Pruneda JN, Littlefield PJ, Soss SE, Nordquist KA, Chazin WJ, Brzovic PS & Klevit RE (2012) Structure of an E3:E2~Ub Complex Reveals an Allosteric Mechanism Shared among RING/U-box Ligases. *Mol. Cell* **47:** 933–942

Raimondi M, Cesselli D, Di Loreto C, La Marra F, Schneider C & Demarchi F (2019) USP1 (ubiquitin specific peptidase 1) targets ULK1 and regulates its cellular compartmentalization and autophagy. *Autophagy* **15:** 613–630

Reverter D & Lima CD (2006) Structural basis for SENP2 protease interactions with SUMO precursors and conjugated substrates. *Nat. Struct. Mol. Biol.* **13:** 1060–1068

Sahtoe DD, van Dijk WJ, Ekkebus R, Ovaa H & Sixma TK (2016) BAP1/ASXL1 recruitment and activation for H2A deubiquitination. *Nat. Commun.* **7:** 10292

Sahtoe DD & Sixma TK (2015) Layers of DUB regulation. *Trends Biochem. Sci.* **40:** 456–67

Sahtoe DD, vanDijk WJ, ElOualid F, Ekkebus R, Ovaa H & Sixma TK (2015) Mechanism of UCH-L5 Activation and Inhibition by DEUBAD Domains in RPN13 and INO80G. *Mol. Cell* **57:** 887–900

Scheffner M & Kumar S (2014) Mammalian HECT ubiquitin-protein ligases: Biological and pathophysiological aspects. *Biochim. Biophys. Acta - Mol. Cell Res.* **1843:** 61–74

Scheuermann JC, De Ayala Alonso AG, Oktaba K, Ly-Hartig N, McGinty RK, Fraterman S, Wilm M, Muir TW & Müller J (2010) Histone H2A deubiquitinase activity of the Polycomb repressive complex PR-DUB. *Nature* **465:** 243–247

Streich FC & Lima CD (2016) Capturing a substrate in an activated RING E3/E2-SUMO complex. *Nature* **536:** 304–308

Swatek KN & Komander D (2016) Ubiquitin modifications. *Cell Res.* **26:** 399–422

Thrower J., Hoffman L, Rechsteiner M & Pickart CM (2000) Recognition of the polyubiquitin proteolytic signal. *EMBO J.* **19:** 94–102

Tsuji Y, Watanabe K, Araki K, Shinohara M, Yamagata Y, Tsurimoto T, Hanaoka F, Yamamura K ichi, Yamaizumi M & Tateishi S (2008) Recognition of forked and single-stranded DNA structures by human RAD18 complexed with RAD6B protein triggers its recruitment to stalled replication forks. *Genes to Cells* **13:** 343–354

Uckelmann M, Densham RM, Baas R, Winterwerp HHK, Fish A, Sixma TK & Morris JR (2018) USP48 restrains resection by site-specific cleavage of the BRCA1 ubiquitin mark from H2A. *Nat. Commun.* **9:** 229

551327-L-bw-Dharadhar
Processed on: 30-12-2020
PDF page: 25

VanderLinden RT, Hemmis CW, Schmitt B, Ndoja A, Whitby FG, Robinson H, Cohen RE, Yao T & Hill CP (2015) Structural Basis for the Activation and Inhibition of the UCH37 Deubiquitylase. *Mol. Cell* **57:** 901–911

Villamil MA, Chen J, Liang Q & Zhuang Z (2012a) A noncanonical cysteine protease USP1 is activated through active site modulation by USP1-associated factor 1. *Biochemistry* **51:** 2829–2839

Villamil MA, Liang Q, Chen J, Choi YS, Hou S, Lee KH & Zhuang Z (2012b) Serine phosphorylation is critical for the activation of ubiquitin-specific protease 1 and its interaction with WD40-repeat protein UAF1. *Biochemistry* **51:** 9112–9113

Wang H, Wang L, Hediye, Erdjument-Bromage Miguel V, Paul T, Richard SJ & Zhang Y (2004) Role of histone H2A ubiquitination in Polycomb silencing. *Nature* **431:** 862–868

Wang Z, Zhang H, Liu J, Cheruiyot A, Lee J, Ordog T, Lou Z, You Z & Zhang Z (2016) USP51 deubiquitylates H2AK13,15ub and regulates DNA damage response. **:** 946–959

Watanabe K, Tateishi S, Kawasuji M, Tsurimoto T, Inoue H & Yamaizumi M (2004) Rad18 guides polη to replication stalling sites through physical interaction and PCNA monoubiquitination. *EMBO J.* **23:** 3886–3896

Wenzel DM, Lissounov A, Brzovic PS & Klevit RE (2011) UBCH7 reactivity profile reveals parkin and HHARI to be RING/HECT hybrids. *Nature* **474:** 105–108

Williams SA, Maecker HL, French DM, Liu J, Gregg A, Silverstein LB, Cao TC, Carano RAD & Dixit VM (2011) USP1 deubiquitinates ID proteins to preserve a mesenchymal stem cell program in osteosarcoma. *Cell* **146:** 918–930

Yang K, Moldovan GL, Vinciguerra P, Murai J, Takeda S & D'Andrea AD (2011) Regulation of the Fanconi anemia pathway by a SUMO-like delivery network. *Genes Dev.* **25:** 1847–1858

Yin J, Schoeffler AJ, Wickliffe K, Newton K, Starovasnik MA, Dueber EC & Harris SF (2015) Structural Insights into WD-Repeat 48 Activation of Ubiquitin-Specific Protease 46. *Structure* **23:** 2043–2054

Yoder BL & Burgers PMJ (1991) Saccharomyces cerevisiae replication factor C. I. Purification and characterization of its ATPase activity. *J. Biol. Chem.* **266:** 22689–22697

Yu Z, Song H, Jia M, Zhang J, Wang W, Li Q, Zhang L & Zhao W (2017) USP1-UAF1 deubiquitinase complex stabilizes TBK1 and enhances antiviral responses. *J. Exp. Med.* **214:** 3553–3563

Zhang W, Tian QB, Li QK, Wang JM, Wang CN, Liu T, Liu DW & Wang MW (2011) Lysine 92 amino acid residue of USP46, a gene associated with 'behavioral despair' in mice, influences the deubiquitinating enzyme activity. *PLoS One* **6:** 2–7

Zhang Z, Qinghui Y, Zhang Y, Zhang J, Xin Z, Haiying M & Yuepeng G (2012) USP1 regulates AKT phosphorylation by modulating the stability of PHLPP1 in lung cancer cells. *J. Cancer Res. Clin. Oncol.* **138:** 1231–1238

Zheng N & Shabek N (2017) Ubiquitin Ligases: Structure, Function, and Regulation. *Annu. Rev. Biochem.* **86:** 129–157

551327-L-bw-Dharadhar
Processed on: 30-12-2020
PDF page: 26

CHAPTER 2

Quantitative analysis of USP activity *in vitro*

Shreya Dharadhar, Robbert Q. Kim†, Michael Uckelmann‡, Titia K. Sixma

Division of Biochemistry and Oncode Institute, Netherlands Cancer Institute, Plesmanlaan 121, 1066 CX Amsterdam, The Netherlands.

†Current address: Department of Cell and Chemical Biology and Oncode Institute, Leiden University Medical Center, Leiden, The Netherlands.
‡Current address: Department of Biochemistry and Molecular Biology, Monash Biomedicine Discovery Institute, Monash University, Melbourne, Victoria, Australia.

Adapted from: Methods in Enzymology, 2019, 618:281-319

ABSTRACT

Ubiquitin-specific proteases (USPs) are an important class of deubiquitinating enzymes (DUBs) that carry out critical roles in cellular physiology and are regulated at multiple levels. Quantitative characterization of USP activity is crucial for mechanistic understanding of USP function and regulation. This requires kinetic analysis using *in vitro* activity assays on minimal and natural substrates with purified proteins. In this chapter we give advice for efficient design of USP constructs and their optimal expression, followed by a series of purification strategies. We then present protocols for studying USP activity quantitatively on minimal and more natural substrates, and we discuss how to include possible regulatory elements such as internal USP domains or external interacting proteins. Lastly, we examine different binding assays for studying USP interactions and discuss how these can be included in full kinetic analyses.

551327-L-bw-Dharadhar
Processed on: 30-12-2020
PDF page: 30

INTRODUCTION

Ubiquitination of proteins has become one of the most widely studied aspects of cellular physiology in eukaryotes. This is due to its crucial role in regulating a plethora of cellular pathways ranging from DNA damage responses to cell migration. The (de)-ubiquitinating enzymes orchestrating the ubiquitination cycle were first described in the 1980's (Hershko, Heller, Elias, & Ciechanover, 1983; Pickart & Rose, 1985), and since then considerable progress has been made in understanding their role as essential components of many, if not all cellular pathways. Deubiquitinating enzymes (DUBs) are proteases that cleave ubiquitin from their target substrates, and sometimes can also remove closely-related ubiquitin-like proteins such as NEDD8. They play a role in the formation of mature ubiquitin monomers by processing C-terminally extended ubiquitin precursors, and they maintain a free ubiquitin pool by recycling unanchored polyubiquitin chains into free ubiquitin. Apart from being important for ubiquitin maintenance, DUBs also cleave ubiquitin marks from their target proteins, which counteracts the activities of ubiquitin-ligating enzymes. This leads to distinct roles for DUBs depending on the type of ubiquitin modification and the nature of substrate being cleaved. Cleavage of Lys-48 linked ubiquitin chains prevents proteasome-mediated degradation of the target proteins, while cleaving "non-degradative" ubiquitin linkages turns off the signal created by particular ubiquitin-substrate attachments. Finally, DUBs can also partially trim ubiquitin chains, which leads to modification of ubiquitin chain architecture and changes in downstream signaling (Reyes-Turcu, Ventii, & Wilkinson, 2009).

There are approximately 100 DUBs encoded in the human genome, which are subdivided into smaller families based on their sequences and catalytic mechanisms (Leznicki & Kulathu, 2017). Seven families of DUBs are characterized by structurally distinct catalytic folds, six of which are cysteine proteases and one a metalloprotease, the so-called JAMM domain (Mevissen & Komander, 2017; Hermanns et al., 2018; Hewings et al., 2018; Kwasna et al., 2018). The Ubiquitin-Specific Proteases (USPs) form the largest family of DUBs, and in this chapter we focus on this group.

USPs contain a conserved catalytic core which has a papain-like fold that is comprised of approximately 350 residues. This catalytic domain adopts a conformation which resembles an extended open hand, subdivided into fingers, palm and thumb subdomains (Hu et al., 2002). USPs have a catalytic triad composed of cysteine, histidine and aspartate/asparagine residues that come from regions remote in the primary sequence. Many USPs have insertions of various sizes in their catalytic domains (Ye, Scheel, Hofmann, & Komander, 2009), as well as substantial N- and C-terminal extensions. These additional regions can play major roles in the catalysis and regulation of the USPs. A well-

551327-L-bw-Dharadhar
Processed on: 30-12-2020
PDF page: 31

studied example is USP7 in which an N-terminal TRAF domain is crucial for interaction with its substrates (Holowaty, Sheng, Nguyen, Arrowsmith, & Frappier, 2003; Sheng et al., 2006), while the C-terminal region is important for regulating its catalytic activity as well as substrate binding (Fernández-Montalván et al., 2007; Faesen et al., 2011; Cheng et al., 2015; Pfoh et al., 2015).

The physiological functions of USPs are slowly emerging. Many USPs are involved in pathways that are dysregulated in human diseases such as cancer and neurodegenerative diseases. (Clague, Coulson, & Urbe, 2012; Heideker & Wertz, 2015). For example, USP1, USP3, USP11, USP16, USP28, USP47, USP48 are involved in DNA damage repair pathways; USP2, USP4, USP15, USP34 participate in Wnt signaling; and USP8, USP15, USP30, USP32 are implicated in the autophagy of mitochondria (mitophagy) (Fraile, Quesada, Rodríguez, Freije, & López-Otín, 2012; Bingol et al., 2014; Cornelissen et al., 2014; Durcan et al., 2014; Wang et al., 2015). How most USPs select their respective substrates is unclear, which makes it hard to infer any specific function from their sequence or structure; this is further complicated by their tendency to function on multiple substrates. A quantitative analysis of USP activity on different substrates (especially natural substrates) can yield deeper insights into how specific USP targets are selected.

Since USPs are essential biological regulators, they themselves have to be tightly regulated to ensure proper functioning. Different modes of regulation exist, affecting catalytic activity, subcellular localization, or cellular abundance of these enzymes. Regulation can be orchestrated by internal factors (domains within the USPs), external factors (binding partners, substrate, post-translational modifications) as well as transcriptional control; many different modes of regulation may contribute to activity of a single USP (Sahtoe & Sixma, 2015; Leznicki & Kulathu, 2017; Mevissen & Komander, 2017). Continuing with the example of USP7, substrate binding and catalytic activity are regulated by its internal domains but it can be further modulated by an external protein called GMPS that enhances its activity and affects its subcellular localization (Van Der Knaap et al., 2005; Faesen et al., 2011; Reddy et al., 2014). There are many examples where multiple modes of regulation are employed for a single USP and these have been extensively reviewed elsewhere (Sahtoe & Sixma, 2015; Leznicki & Kulathu, 2017; Mevissen & Komander, 2017).

To understand how internal and external regulatory factors modulate catalytic activity of USPs it is important to perform quantitative analysis of USP activity. *In vitro* analysis can be very valuable here, as it allows separating individual functions by performing assays in the presence and absence of the regulatory elements. These kinds of analyses shed

551327-L-bw-Dharadhar
Processed on: 30-12-2020
PDF page: 32

light on the mechanism of activity modulation and in some cases inform us on how concerted action of multiple regulatory elements brings about changes in USP function.

In this chapter we give a detailed workflow for quantitative analysis of USP function. We discuss expression systems and present a series of examples of USP purification. We then describe how USP catalytic activity can be quantitatively analyzed on different substrates, i.e., minimal substrates and natural substrates. We also present a detailed workflow for generating fluorescently labelled ubiquitinated substrate for quantitative analysis of DUB activity. Furthermore, we review the use of activity assays to study how internal and external factors modulate USP catalytic activity. Finally, we discuss the importance of studying USP interactions with their substrates and/or cofactors quantitatively *in vitro* and highlight the advantages and limitations of commonly used binding assays.

PURIFICATION OF USPS

For the *in vitro* characterization of USPs it is important to carefully purify the USP in question. The first step is expression of the protein, but as yields vary in a protein-specific manner we do not present a general protocol, but rather suggest testing different expression systems. As USPs are intracellular proteins, either bacteria or insect cells usually work well for expression. In bacterial expression, there will be no eukaryote-specific post-translational modifications taking place, whereas this may happen during expression of USPs in insect cells. As these may affect activity, this needs to be carefully examined. Moreover, DUBs purified from insect cells may bind tightly to regulatory proteins that are hard to remove; a notable example is USP1, that carries along its activator UAF1 (WDR48). A related problem occurs when purifying the activators: it is difficult to purify GMPS from insect cells without carrying along a fraction of USP7.

To efficiently test different affinity tags and expression systems we make use of a coherent set of ligation-independent expression vectors (Luna-Vargas et al., 2011), most of which are available from Addgene (www.addgene.org). Unless post-translational modifications are important, we prefer bacteria for expression as procedures are faster. Therefore, we first test if the protein of interest can be expressed in bacteria in small-scale expression tests under a set of different conditions. In these assays we vary the choice of affinity tag, expression strain, growth medium, and induction conditions. If none of these conditions yield soluble protein, then we try insect cells, where we again start with small scale tests. Expression is read out after the initial affinity purification by analysis on sodium dodecyl sulphate-polyacrylamide gel electrophoresis (SDS-PAGE).

551327-L-bw-Dharadhar
Processed on: 30-12-2020
PDF page: 33

If specific protein domains have to be expressed, or if soluble full-length protein is not expressed in any of the tested conditions, one needs to design the specific region to be expressed. In the following sections we will reflect on the design of the expression construct that can aid in obtaining pure USP proteins or protein fragments and describe three case studies to show what a USP purification protocol can look like.

Determination of a well behaved USP catalytic domain construct

Protocol

1. Look up the USP of interest in e.g. UniProt. Here protein sequences are stored, including splicing variants, as well as additional information from the literature: scroll through the page and follow links to published papers or second party websites. Especially when there is structural information known, we recommend checking the linked page of the Protein Databank (PDB) and if applicable the accompanying paper(s) for expression constructs and domain information.
2. If the literature assessment has not yielded defined construct boundaries, we highly recommend looking at the sequence analysis by Ye et. al. (Ye et al., 2009). Here the catalytic domains (CDs) of all (human) USPs have been aligned and annotated in the supplemental information. Search for the USP of interest and note the active-site residues as well as the presence of any zinc-binding motifs. This information is useful for the actual purification and analysis.
3. The alignment in Ye et. al.,2009 shows boundaries for the catalytic core. These boundaries have been obtained by sequence comparison and in our experience, they give a good starting point to design a construct that yields a soluble catalytic domain. However, the actual domain boundaries vary more than expected from the sequence alignments alone and may require optimization.
4. We use sequence conservation and secondary structure to define the borders of the constructs. As a tool we make use of the Crystallographic Construct Designer (CCD, https://ccd.rhpc.nki.nl) (Mooij, Mitsiki, & Perrakis, 2009) as this shows the results from multiple analyses and suggests potential cloning primers.
5. Usually the N-terminal end of the catalytic construct does not need a lot of adaptation, but the C-terminal boundaries may vary. We generally extend the construct by up to forty residues as this can improve heterologous expression. As an example, USP7 has a large α-helix just C-terminal of the CD. Inclusion of this region was helpful for soluble bacterial expression (Kim, Dijk, & Sixma, 2016). As an extra check, one can run a protein structure prediction program on the final construct (e.g. Phyre2 (Kelley, Mezulis, Yates, Wass, & Sternberg, 2015)).

551327-L-bw-Dharadhar
Processed on: 30-12-2020

The designed construct should yield the USP domain, possibly with small N- and C-terminal extensions.

6. Order primers and clone the designed constructs into expression vectors. We recommend testing several constructs, with varying start and end points.
7. Using a codon-optimised sequence should also be considered. Codon-optimisation can increase the chances of successful heterologous expression. It can be done for multiple expression systems through various suppliers (e.g. GenScript, Integrated DNA technologies).

Note: Remember that any protease used to cleave off an affinity tag requires an unobstructed recognition sequence: a slightly extended N- or C-terminus in the construct can help this.

General purification protocol for USPs

For the expression and purification of the designed USP constructs we refer the reader to the many handbooks available (eg. Strategies for Protein Purification by GE Healthcare, etc.). In general, the protocols supplied by manufacturers suffice for initial purification trials, and optimization is done from this starting point. Here we describe three case studies to give examples of purification of USPs in bacteria, insect cells and co-purification of a USP with its regulator in insect cells.

Note: The practical guidelines mentioned in the notes should be applied for all the purification protocols described in this chapter.

Note: Since USPs are cysteine proteases, it is important that all purification buffers should contain reducing agents because oxidation by reactive oxygen species (ROS) has been shown to inactivate a large number of USPs (Cotto-Rios, Békés, Chapman, Ueberheide, & Huang, 2012; Lee, Baek, Soetandyo, & Ye, 2013).

Case Study– a) Expression of a USP in E. coli: USP7

The full length codon-optimized USP7 sequence is cloned into a pGEX-6p vector containing a 3C protease-cleavable N-terminal GST tag (Faesen et al., 2011). Transform the sequence-verified expression construct into *Escherichia Coli* BL21 Rosetta2 (DE3) T^{1R} cells and grow the transformed cells in 4 liters of Terrific Broth growth medium, which allows growing to high density. When cells reach an $O.D._{600nm}$ of 1.8 add 0.2 mM IPTG to induce and incubate overnight at 18°C.

551327-L-bw-Dharadhar
Processed on: 30-12-2020
PDF page: 35

Buffers

- Lysis buffer - 50 mM HEPES (pH 7.5) + 150 mM NaCl + 1 mM EDTA + 1 mM DTT + 0.1 mM PMSF + DNase I (Roche)

Note: DNAse should be omitted if the USP will be tested for binding or activity against DNA.

- GST Wash buffer - 50 mM HEPES (pH 7.5) + 250 mM NaCl + 1 mM EDTA + 1 mM DTT
- GST Elution buffer - 50 mM HEPES (pH 7.5) + 250 mM NaCl + 1 mM EDTA + 1 mM DTT + 15 mM glutathione
- IEX buffer A - 10 mM HEPES (pH 7.5) + 50 mM NaCl + 1 mM DTT
- IEX buffer B - 10 mM HEPES (pH 7.5) + 1 M NaCl + 1 mM DTT
- Gel filtration buffer - 25 mM HEPES (pH 7.5) + 100 mM NaCl + 1 mM DTT

Protocol

1. Harvest cells by centrifugation at 5300 x *g* for 15 minutes and resuspend in Lysis buffer. For expressions in TB we use 30 mL of buffer per expressed liter.
2. Lyse the resuspended cells by homogenization using a cell homogenizer (e.g. Avestin Emulsiflex-C5) which is precooled to 4°C.

Note: We use the emulsiflex and sonicator both. Results are mostly interchangeable, but occasionally a protein seems to respond better to one or the other treatment.

3. Spin down the lysed cell suspension at 53000 x *g* for 40 mins in a pre-cooled centrifuge at 4°C and collect the supernatant. Collect samples of the supernatant and pellet and dilute them tenfold for analysis by SDS-PAGE along with samples from step 6-7.
4. Add 5 ml of GST-Sepharose beads (GE Healthcare) to a gravity flow column (Bio-Rad) and equilibrate with 5 column volumes (CV) of GST Wash buffer at 4°C. Determine the amount of GST beads to use based on protein yields from the first small scale prep. We use 1 ml of GST beads for 10 mg of GST tagged protein but this might differ for individual proteins depending on their size.
5. Add the lysate and incubate by rotating at 4°C for 30 minutes.
6. Allow the lysate to pass through the column by gravity flow and collect the flowthrough. Take a sample of the flowthrough for SDS-PAGE analysis.
7. Wash the column with 20 CV of Wash buffer and elute with 5 x 0.8 CV of Elution buffer. Collect wash and elution fractions and take samples for SDS-PAGE.

551327-L-bw-Dharadhar
Processed on: 30-12-2020
PDF page: 36

8. Perform SDS-PAGE with all the collected samples to determine which fractions contain USP7. If all the steps are performed properly then protein should be in the elution fractions.
9. Pool elution fractions containing USP7 and set aside a sample for comparison with the 3C protease post-cleavage sample by SDS-PAGE.

Note: Estimate the absolute amount of protein after every step during the purification. This will help in identifying if unusual amounts of protein are lost in any step.

10. Add 3C protease to the pooled USP7 sample and transfer the mixture to a dialysis tube, Incubate at 4°C while dialyzing overnight against 2 liters of IEX buffer. Make sure the molecular weight cut-off does not allow the 3C protease to go through (MWCO < 20 kDa).

Note: Cleavage times can vary depending on the sample and the amount of enzyme added; it is usually most convenient to incubate the sample overnight. Adding 1 µg of 3C protease for 100 µg of protein is sufficient for complete cleavage under these conditions.

11. Equilibrate a 10 ml POROS Q anion exchange column with sequential washes of 2 CV IEX buffer A, 2 CV IEX buffer B and 2 CV IEX buffer A at 4°C. The size of the column can vary depending upon the purification scale.
12. Check if 3C protease cleavage is complete by analyzing samples from before and after cleavage on SDS-PAGE. If it is already known that cleavage is complete under these conditions, then this step can be skipped.
13. Spin down the cleaved protein sample and load the supernatant on the column followed by washing with 3 CV of IEX buffer A.
14. Elute USP7 by using a salt gradient of 20 CV from 50 mM to 1 M NaCl; full-length human USP7 typically elutes around 150-250 mM NaCl.
15. Collect samples corresponding to all the significant peaks as measured by UV absorbance at 280 nM (UV280) and analyze them by SDS-PAGE.
16. Equilibrate a Superdex 200 10/300 size exclusion column (GE Healthcare) with Gel filtration buffer at 4°C. The size of column is based on the amount of protein being purified (for e.g. if USP7 ≥ 10 mg then we use the 16/60 column and for ≤ 10 mg we use the 10/300 column).

Note: If a larger column is used, then make sure that equilibration is started earlier so that it is ready to use as soon as the sample is concentrated.

551327-L-bw-Dharadhar
Processed on: 30-12-2020
PDF page: 37

17. Concentrate the pooled fractions from the anion-exchange column at 4°C using a Amicon Ultra-15 centrifugal filter unit with a 30 kDa cutoff (Merck) until a final volume of 500 µl is reached.
18. Load the concentrated sample on the pre-equilibrated size exclusion column.
19. Collect samples corresponding to the UV280 peaks and analyze them by SDS-PAGE.
20. Combine fractions containing pure USP7 (128 kDa) and concentrate at 4°C in a Amicon Ultra-15 centrifugal filter unit with a 30 kDa cutoff (Merck) to a final concentration of 10 mg/ml.
21. Aliquot the concentrated protein and flash freeze in liquid nitrogen for long term storage at -80°C. If protein is to be used for functional studies, then make aliquots of 10 µl; if protein is to be used for crystallography, then make aliquots of 40 µl.

Note: It is not recommended to refreeze the protein aliquot after assays as this can influence the activity and stability.

Case Study – b) Expression of a USP in insect cells: USP46

Many USPs are not expressed in bacteria or have very low expression and solubility levels. In such cases, expression and purification in insect cells can be a good alternative, frequently improving expression levels as well as solubility. We employ *Spodoptera frugiperda* (Sf9) insect cells for protein expression using the baculovirus expression system. Sf9 cells are more sensitive to variations in culture conditions compared to bacterial cells; our reproducibility improved when we appointed a single person to maintain the insect cell cultures. This helps to avoid contamination, makes it possible to efficiently expand cultures for protein expression, and ensures that new stock cultures are started before the passage limit is reached.

Production of recombinant bacmids and baculoviruses is carried out based on protocols in the Invitrogen manual (Bac-to-Bac® Baculovirus Expression Systems) for insect cell expression. The titre of the P1 viral stock is not calculated and it is assumed to be in the range of 1×10^6 to 1×10^7. Optimal infection conditions for large-scale expression vary for each recombinant baculovirus. Therefore, small-scale expression tests are performed, varying virus amounts. Additionally, different expression times are tested at constant virus levels and only after determining these two parameters is large-scale expression initiated.

The full length USP46 cDNA is cloned into a pFastbac vector with a cleavable N-terminal His tag. Transform the sequence-verified construct into DH10Bac bacterial cells for bacmid preparation. Purify the recombinant bacmid and use it for transfection of Sf9

551327-L-bw-Dharadhar
Processed on: 30-12-2020
PDF page: 38

insect cells to produce the recombinant baculovirus. We don't normally determine virus titer, but rather rely on small-scale expression tests to decide on the necessary amount of USP46 P2 viral stock to add. Here we use 4 ml of the P2 virus per 2 liters of Sf9 culture at 2 x 10^6 cells/ml and harvest after 72 hours.

Buffers

- Lysis buffer – 50 mM Tris-HCl (pH 7.5) + 200 mM NaCl + 2 mM Tris(2-carboxyethyl) phosphine (TCEP) + Pierce™ Protease Inhibitor Mini Tablets, EDTA Free (1 tablet/50 ml)
- His wash buffer – 50 mM Tris-HCl (pH 7.5) + 150 mM NaCl + 2 mM TCEP + 50 mM Imidazole (pH 8.0)
- His elution buffer – 50 mM Tris-HCl (pH 7.5) + 150 mM NaCl + 2 mM TCEP + 500 mM Imidazole (pH 8.0)
- IEX dilution buffer - 50 mM Tris-HCl (pH 7.5) + 50 mM NaCl + 2 mM TCEP
- IEX buffer A - 20 mM Tris-HCl (pH 7.5) + 50 mM NaCl + 2 mM DTT
- IEX buffer B - 20 mM Tris-HCl (pH 7.5) + 1 M NaCl + 2 mM DTT
- Gel filtration buffer – 20 mM HEPES (pH 7.5) + 150 mM NaCl + 2 mM DTT

Protocol

1. Harvest Sf9 cells by spinning them down at 750 x *g* for 15 minutes at room temperature and resuspend the cells in 50 ml of Lysis buffer.We generally use 25 ml of Lysis buffer to harvest 1 liter of Sf9 cells (2 x 10^6 cells/ml).
2. Add the resuspended cells to a 125 ml metal beaker immersed in ice, and lyse by sonicating with a pre-cooled sonicator (Qsonica Q700 with 12.7 mm probe) . The lysis conditions are as follows, Amp -50; Pulse on -15 seconds; Pulse off - 45 seconds; Total Time – 2 minutes.
3. Spin down the lysed cell suspension at 53000 x *g* for 40 mins in a pre-cooled centrifuge at 4°C and collect the supernatant. Collect and dilute samples of the supernatant and pellet for analysis by SDS-PAGE along with samples from step 6-7.
4. Add 2 ml of Ni^{2+}-Sepharose beads (GE Healthcare) in a gravity flow column and equilibrate with 4 CV of Lysis Buffer (without protease inhibitors) at 4°C.

Note: Nickel and Talon beads are most commonly used for His affinity purification. They have somewhat different affinity and this can be optimized for individual constructs.

Note: The amount of beads used depends on the estimated yields based on small scale expression tests. It is important to note that Nickel and Talon beads can act as ion exchangers and can bind to random proteins. It is therefore important to limit the quantity

551327-L-bw-Dharadhar
Processed on: 30-12-2020
PDF page: 39

of beads and better to underestimate than to overestimate. This may result in not binding all the protein of interest, but what is purified is much cleaner.

5. Add the lysate and incubate with rotation at 4°C for 30 minutes.
6. Allow the lysate to pass through the column by gravity flow and collect the flowthrough. Take a sample of the flowthrough for SDS-PAGE analysis.
7. Wash the column with 50 CV of Wash buffer and elute with 5 x 0.8 CV of Elution buffer. Collect wash and elution fractions and take aliquots for SDS-PAGE.

Note: Some His-tagged proteins start eluting at 50 mM imidazole therefore always check if this is the case before using 50 mM imidazole in the wash buffers.

8. Perform SDS-PAGE with all the collected samples to determine which fractions contain USP46.
9. Equilibrate a 10 ml POROS Q anion exchange column with sequential washes of 2 CV IEX buffer A, 2 CV IEX buffer B and 2 CV IEX buffer A at 4°C.
10. Pool elution fractions containing USP46 and dilute the pooled sample with an equal volume of IEX dilution buffer.

Note: The final salt concentration of the buffer should be significantly lower than the salt concentration at which the protein is expected to elute from the column. Don't dilute more than necessary as some proteins might precipitate.

11. Load the diluted USP46 sample on the column followed by washing with 3 CV of IEX buffer A.
12. Elute USP46 by using a salt gradient of 20 CV from 50 mM to 1 M NaCl.
13. Collect samples corresponding to all the significant UV280 fractions and analyze them by SDS-PAGE. USP46 typically elutes around 200-300 mM NaCl.
14. Equilibrate a Superdex 200 16/60 size exclusion column (GE Healthcare) with Gel filtration buffer at 4°C.
15. Concentrate the pooled fractions at 4°C using a Amicon Ultra-15 centrifugal filter unit with a 10 kDa cutoff (Merck) until a final volume of 500 µl is reached.
16. Load the concentrated sample on the pre equilibrated size exclusion column. A single UV280 peak with a leading shoulder will be obtained. The shoulder contains USP46 bound to its interacting proteins from insect cells such as UAF1.
17. Collect fractions corresponding to the shoulder and peak for analyzing them by SDS-PAGE.

551327-L-bw-Dharadhar
Processed on: 30-12-2020
PDF page: 40

18. Combine peak fractions containing pure USP46 and concentrate at 4°C in a Amicon Ultra-15 centrifugal filter unit with a 10 kDa cutoff (Merck) to a final concentration of 10 mg/ml.
19. Aliquot the concentrated protein and flash freeze in liquid nitrogen for long term storage at -80°C. If protein is to be used for activity assays, then make aliquots of 10 µl, and if protein is to be used for crystallography, then make aliquots of 40 µl.

Case Study – c) Co expression of a USP with a regulatory protein in insect cells: USP1-UAF1

USP1 was cloned into a pFastBac vector with a cleavable N-terminal His tag, UAF1 into a pFastBac vector with a cleavable N-terminal Strep II tag. Transform the sequence-verified constructs separately into DH10Bac cells for bacmid preparation. Purify the recombinant USP1 and UAF1 bacmids and use each for transfection of *Spodoptera frugiperda* (Sf9) insect cells to produce recombinant baculoviruses. Perform small-scale expression tests with different ratios of USP1 and UAF1 viruses and check if both proteins are expressed equally. Based on the small-scale expression tests, select appropriate amounts of P2 viral stock. Here we use 4 ml of USP1 P2 viral stock and 2 ml of UAF1 P2 viral stock in 2 liters of Sf9 culture at $2x10^6$ cells/ml and harvest after 72 hours.

Buffers

- Lysis buffer – 50 mM Tris-HCl (pH 7.5) + 150 mM NaCl + 2 mM TCEP + Pierce™ Protease Inhibitor Mini Tablets, EDTA Free (1 tablet/50 ml)
- His wash buffer – 50 mM Tris-HCl (pH 7.5) + 150 mM NaCl + 2 mM TCEP + 50 mM Imidazole (pH 8.0)
- His elution buffer – 50 mM Tris-HCl (pH 7.5) + 150 mM NaCl + 2 mM TCEP + 500 mM Imidazole (pH 8.0)
- Strep wash buffer – 50 mM Tris-HCl (pH 7.5) + 150 mM NaCl + 2 mM TCEP
- Strep elution buffer – 50 mM Tris-HCl (pH 7.5) + 150 mM NaCl + 2 mM TCEP + 2.5 mM Desthiobiotin
- Gel filtration buffer – 20 mM HEPES (pH 7.5) + 150 mM NaCl + 2 mM DTT

Protocol

1. Harvest cells by spinning them down at 750 x *g* for 15 minutes at room temperature and resuspend the cells in 100 ml of Lysis buffer.
2. Add the resuspended cells to a 125 ml metal beaker immersed in ice, and lyse by sonicating with a pre-cooled sonicator (Qsonica Q700 with 12.7 mm probe). We use lysis conditions as follows, Amp -50; Pulse on -15 seconds; Pulse off - 45 seconds; Total Time – 2 minutes.

551327-L-bw-Dharadhar
Processed on: 30-12-2020
PDF page: 41

3. Spin down the lysed cell suspension at 53000 x *g* for 40 mins in a pre-cooled centrifuge at 4°C and collect the supernatant. Collect and dilute samples of the supernatant and pellet for analysis by SDS-PAGE along with samples from step 7-8.
4. Add 2 ml of Ni^{2+}-Sepharose beads (GE Healthcare) to a gravity flow column (Bio-Rad) and equilibrate with 4 CV of Lysis Buffer (without protease inhibitors) at 4°C.
5. Load the lysate and incubate by rotating at 4°C for 30 minutes.
6. Allow the lysate to pass through the column by gravity and collect the flowthrough. Take a sample of the flowthrough for SDS-PAGE analysis.
7. Wash the column with 50 CV of His wash buffer and elute with 5 x 0.8 CV of His elution buffer. Collect wash and elution fractions and take aliquots for SDS-PAGE.
8. Perform SDS-PAGE with all the collected samples to determine which fractions contain USP1-UAF1.
9. Add 5 ml of Streptactin sepharose beads (IBA Life Sciences) to a gravity flow column and equilibrate with 5 CV of Strep wash buffer at 4°C. The amount of beads used depends on the estimated protein yields. Generally 1 ml of Streptactin sepharose beads bind up to 100 nmol of strep-tagged protein.
10. Combine and load the USP1-UAF1 fractions on the column without disturbing the Streptactin beads. Allow the sample to pass through the column slowly by gravity and reload the flowthrough at least once on the column. Collect the flowthrough and take a sample for SDS-PAGE.
11. Wash the column with 2 CV of Strep wash buffer and elute with 6 x 0.8 CV of Strep elution buffer.

Note: Excessive washing of the Streptactin column should be avoided as contaminating proteins get easily washed away in 1-2 CV due to lack of nonspecific interactions. More importantly, excessive washing will lead to loss of the strep tagged protein since the affinity between the strep tag and the streptactin beads is in the low micromolar range.

12. Perform SDS-PAGE with all the collected samples to determine which fractions contain the USP1-UAF1 complex.
13. Combine the elution fractions and take a sample for comparison with the post-cleavage sample by SDS-PAGE.
14. Add His-tagged 3C protease to the pooled USP1-UAF1 sample and incubate overnight at 4°C. Save a sample and check for cleavage on SDS-PAGE.
15. Add 4 ml of Ni^{2+}-Sepharose beads (GE Healthcare) to a gravity flow column and equilibrate with 4 CV of Lysis Buffer (without protease inhibitors) at 4°C.

551327-L-bw-Dharadhar
Processed on: 30-12-2020
PDF page: 42

16. Perform a reverse Ni^{2+}-affinity purification by adding the cleaved sample to the column. The cleaved USP1-UAF1 should not bind, while the His-tagged protease will bind to the column.
17. Allow the sample to go through the column slowly by gravity flow and reload the flowthrough at least once on the column. Collect the flowthrough and take a sample for SDS-PAGE.
18. Wash the column with 5 x 1 CV of His wash buffer and elution is done with 3 x 0.8 CV of His elution buffer.
19. Perform SDS-PAGE with all the collected samples to determine which fractions to collect for the next step; pure USP1-UAF1 should be in the flowthrough and wash fractions.
20. Equilibrate the Superdex 200 10/300 size exclusion column (GE Healthcare) with Gel filtration buffer at 4°C.
21. Pool and concentrate the fractions at 4°C using a Amicon Ultra-15 centrifugal filter unit with a 50 kDa cutoff (Merck) until a final volume of 500 µl is reached.
22. Load the concentrated sample on a pre-equilibrated size exclusion column.
23. Collect fractions corresponding to the UV280 peak and analyze them by SDS-PAGE.
24. Combine fractions containing pure USP1-UAF1 and concentrate at 4°C in a Amicon Ultra-15 centrifugal filter unit with a 50 kDa cutoff (Merck) to a final concentration of 5 mg/ml.
25. Aliquot the concentrated protein and flash freeze in liquid nitrogen for storage at -80°C.

CHARACTERIZATION OF USPS

After purification of the USP of interest, or a USP domain or USP-regulator complex, one would like to assess the quality of the particular protein preparation. Methods to assess protein stability and stoichiometry have been described extensively elsewhere (Wen, Arakawa, & Philo, 1996; Senisterra & Finerty, 2009); for this analysis of USPs, we focus on the enzymatic activity.

Besides using an activity assay for quality control, these assays can also provide insight into the mechanisms of USP activity by yielding key enzymatic parameters. Here we describe our protocols to determine parameters such as K_M and k_{cat}, using a minimal substrate and a more “realistic” one. Furthermore, we indicate how these activity assays could help to understand the effect of ancillary domains or interactors on the USP protein.

551327-L-bw-Dharadhar
Processed on: 30-12-2020
PDF page: 43

USP activity on a minimal substrate

Ubiquitin-specific proteases specifically cleave ubiquitin (Ub) from targets, with ubiquitin being the minimally recognized entity as a substrate. As such the minimal substrate to use in activity assays consists of ubiquitin with its C-terminus conjugated to a readout molecule, usually a quenched fluorophore that increases in fluorescence when released or a moiety that can trigger a secondary, luminescent signal (Orcutt, Wu, Eddins, Leach, & Strickler, 2013). For an activity assay, the ubiquitin needs to have a peptide(-like) linkage to the C-terminal leaving group to allow processing by the USP. One possibility is assessment using a fluorescence polarization assay (FP, see section 3.4.4) in which the release of fluorescently tagged ubiquitin from a substrate is measured by the change in polarization.

Here we use two commonly used quenched fluorophores, rhodamine (Rho) or 7-amino-4-methylcoumarin (AMC), which are conjugated to ubiquitin. Ubiquitin rhodamine (UbRho) or Ubiquitin 7-amino-4-methylcoumarin (UbAMC) are commercially available and often used in the DUB-field (Hassiepen et al., 2007). As the released compound from these model substrates is a direct readout of cleaved product, we can use the time-resolution of a plate reader to determine the enzymatic parameters.

Here, we use a PheraStar plate reader (BMG LabTech), but other machines could be suitable as well. Make sure that the plate reader has the required filters or monochromators to measure rhodamine (Rho) or 7-amino-4-methylcoumarin (AMC) fluorescence and that it can measure the fluorescence intensity (FI) over an extended period of time. Some plate readers, like the PheraStar, also have an injection option, which sometimes can be useful. The injector allows detection of early events of the reaction, which is necessary for very active USPs or when they display unexpected behavior ((Clerici, Luna-Vargas, Faesen, & Sixma, 2014; Haahr et al., 2018); Kim et al, 2019). For enzymes with normal Michaelis-Menten behavior, the procedure described here, where we prepare the plates manually, leaving a delay time between the addition of substrate or enzyme and the start of the measurement, is sufficient.

Deubiquitination assay as a quality control step

For a simple check of deubiquitinating activity for a new protein construct, one would simply add the newly purified enzyme to the minimal substrate and monitor the fluorescence increase. If this is a new purification of an already analyzed USP, take into account the assay conditions (concentration, buffer) already established for the protein (see 3.1.3).

551327-L-bw-Dharadhar
Processed on: 30-12-2020
PDF page: 44

Materials

- Freshly thawed protein, make sure it has reduced cysteines

Note: Using fresh DTT ensures the cysteines (including the active site) are reduced, which is essential for the enzyme to be active.

Note: Try not to refreeze enzymes as they lose activity. It is better to make small aliquots and thaw only once.

- UbRho (from e.g. Boston BioChem (US), or UbiQ Bio (Europe)); for these quality control assays, we use an 8 µM stock.

Note: Upon 1:1 dilution in the assay, this will result in an end concentration of 4 µM, which is around the K_D for many USPs.

- Protein storage buffer: the exact composition depends on the USP of interest. Generally a buffer containing 20 mM HEPES (pH 7.5); 150 mM NaCl and 1 mM DTT suffices.
- Low Volume 384-Well Black Flat Bottom Polystyrene NBS™ Microplate (Corning, catalogue number: 3820)

Protocol

1. Add 10 µL UbRho to two wells of the plate.
2. At the plate reader, check the settings and the program, take care to select the proper wells. Time-wise the result of the experiment will be clear within 10 minutes, but we usually measure longer.

Note: Rhodamine: excitation maximum- 485 nm, emission maximum- 530 nm. AMC: excitation maximum- 380 nm, emission maximum- 480 nm.

3. Add 10 µL buffer to one well (blank) and 10 µL of protein solution to the other.
4. Insert the plate and start the program, monitoring the fluorescence increase over time.
5. If correct, the blank will show a steady, low baseline fluorescent signal over time, indicating no cleavage is taking place. The other well will show, if there is an active DUB, an increasing fluorescence intensity signal, levelling off as the substrate is consumed.

551327-L-bw-Dharadhar
Processed on: 30-12-2020
PDF page: 45

Preparatory analysis for quantitation of UbRho cleavage
To convert the obtained fluorescence units into concentration (μM) a calibration curve for the batch of UbRho has to be determined. Keep in mind that such a calibration curve differs with the machine and 'gain' settings used. We use the same machine with one particular gain setting per batch of minimal substrate.

Determine optimal gain

1. Decide on the highest concentration of UbRho you are planning to use. 30 μM is generally sufficient for K_M determination for most USPs.
2. Prepare UbRho at this concentration and add a known active DUB, preferably at a high concentration so hydrolysis proceeds quickly. We generally use USP7, but other very active USPs such as USP21 will work too and are available at reasonable price from a supplier such as Boston BioChem.
3. Add the sample to a micro well plate and measure fluorescence in the plate reader.
4. If the signal reaches the detection limit, restart the measurement using a lower gain setting. Wait until the signal increase levels off, all substrate is now hydrolyzed.
5. Use the plate reader's auto-gain function, setting the FI signal of the well to 90%.
6. Make a note of the gain setting, or alternatively save this in a method file to be used by the plate reader.

Note: UbRho concentrations higher than 30 μM are tricky to work with. It can give unreliable readings, possibly due to aggregation of the fluorophore.

Determine a calibration curve of Rhodamine fluorescence as a function of substrate concentration
Once the optimal gain has been determined, one can run the calibration that gives the conversion factor to calculate product concentrations from the fluorescence readings.

1. Make a dilution range of your UbRho stock in the range of 0.25-30 μM.
2. Add an active DUB to each well.
3. Monitor the fluorescence using the plate reader and wait until the signal is stable.

Note: The optimal gain can also be determined here by using the plate readers auto-gain function on the highest concentration of substrate once the fluorescence signal is stable. Alternatively, one can also use a stock of free rhodamine to determine the optimal gain.

4. After the measurements, assess the reactions using a spectrophotometer (e.g. Nanodrop) at their excitation wavelength. Using Beer's law and the extinction

551327-L-bw-Dharadhar
Processed on: 30-12-2020
PDF page: 46

coefficient of the cleaved fluorescent product, one can determine the product (and thus the starting substrate) concentration.

5. Get the FI readings of the plateau (in AU) for each UbRho dilution and plot them against the used substrate concentration.
6. Fit the points linearly to get a conversion factor, converting AU to µM.

Optimal USP concentration for kinetic analysis of enzyme activity

In order to quantify USP kinetics, the experiment must be performed under optimal sample conditions. To determine enzyme parameters such as K_M and k_{cat}, the enzyme and substrate concentrations have to be within the Michaelis-Menten domain ([E]<<[S]; (Michaelis & Menten, 1913)). In general, this means that the enzyme concentration should be at least two orders of magnitude lower than the substrate concentration. Due to the detection limits of the released fluorophore, the substrate concentration must be between 100 nM and 30 µM. This places initial constraints on the enzyme concentration in the assay. Moreover, the assay needs to sample the full range of activity, if there is too much enzyme, we cannot get the initial velocity (V0) of the reaction; if there is too little enzyme it will take too long before the signal appears.

Materials

- The purified protein, with a known concentration (UV280 or Bradford assay)
- UbRho, for this optimization assay we use an 8 µM stock
- Protein storage buffer

Note: Make sure to have fresh reducing agent in both the buffer and protein stock.

- Low Volume 384 Well Black Flat Bottom Polystyrene NBS™ Microplate (Corning, catalogue number: 3820)
- PCR tubes, preferably in a strip for easy use with a multichannel pipette

Protocol

1. Make a concentration range of the USP protein in an 8 strip of PCR tubes. We usually make a ten-fold dilution range going down from 2 µM to 2 nM or even pM with very active enzymes.
2. For every concentration to be tested add 10 µL UbRho stock into a well.
3. At the plate reader, check the settings and the program, take care to select the proper wells. We generally run this experiment for 1 hour.
4. Using a multichannel pipette, add 10 µL of the protein samples into the wells.
5. Insert the plate and start the measurement.

551327-L-bw-Dharadhar
Processed on: 30-12-2020
PDF page: 47

Analysis

6. Observe the FI increase over time. For the highest concentration the signal will probably level off within seconds: with this concentration no V0 can be determined. Try to find the curve with the optimal protein concentration; this curve will preferably reach a plateau right before the end of your measurement (see note).
7. Note down the optimal concentration or fine-tune it by repeating the experiment with a narrower dilution range.

Note: If the signal reaches a plateau it gives you an internal experiment control within this one measurement. When converting the plateau value (in AU) to µM using the calibration curve (3.1.2), it should yield the used UbRho concentration.

Determining steady-state enzymatic parameters using minimal substrate

Here we describe steady-state kinetic analysis of USP7 activity on a minimal substrate. The protocol can be used for other USPs as well, but buffer conditions and protein concentrations may have to be optimized (see 3.1.3).

Materials

- Reaction buffer: 20 mM HEPES 7.5; 100 mM NaCl; 1 mM DTT; 0.05% Tween-20
- UbRho stock (1 mM, in DMSO)
- USP7 protein stock
- Low Volume 384 Well Black Flat Bottom Polystyrene NBS™ Microplate (Corning, catalogue number: 3820)
- PCR tubes, preferably in a strip for easy use with a multichannel pipette
- Data fitting software: GraphPad Prism 7

Protocol

1. Prepare reaction buffer, using fresh DTT.

Note: Using fresh DTT ensures the cysteines (including the active site) are reduced, which is essential for the enzyme to be active. The Tween-20 is included to prevent proteins or compounds from sticking to the walls of the plate.

2. Thaw stocks and determine the protein concentration (For USP7: 1 OD280 = 7.96 µM).
3. Make a 2 nM USP7 stock. Make sure to make enough volume-wise, for one single measurement, we make 100 µL.

551327-L-bw-Dharadhar
Processed on: 30-12-2020

Note: Do NOT take too large dilution steps. We usually do sequential dilutions starting with a 1 µM dilution (measure for certainty using a NanoDrop), then dilute 25-fold (40 nM) and then 20-fold (2 nM). This helps prevent aggregation.

4. Make serial two-fold dilutions of UbRho (starting at 16 µM) in an 8-strip of PCR tubes. Make sure the minimal amount is 10 µL for each reaction. E.g. make 25 µL of 16 µM UbRho, then do a serial dilution transferring 12.5 µL to the next well with 12.5 µL buffer.
5. Add 10 µL of 2 nM USP7 into the wells of the assay plate - note down the wells.
6. At the plate reader, check the settings and the program, take care to select the proper wells.

Note: Rhodamine: excitation maximum- 485 nm, emission maximum- 530 nm. AMC: excitation maximum- 380 nm, emission maximum- 480 nm. Gain setting as determined in 3.1.2.

7. Using the multichannel pipette, add 10 µL of the substrate into the wells.
8. Start the program, and monitor the fluorescence increase.

Analysis

9. Get the data from the machine (.xls or .csv file) and copy them into Prism 7.
10. Using the determined conversion rate (section 3.1.2), convert the AU values into µM and plot them (as converted substrate vs time).
11. Examine the plot to assess the quality of the experiment. Are there curves where the signal increase does not seem to follow the dilution steps and do the plateaus reached (see note in 3.1.3) match the substrate concentrations used? Also find the time range to determine the initial velocity (V0); this range encompasses the linear part of the curve right after the start.
12. If the linear range cannot be properly determined, look into optimizing the experiment (section 3.1.3).
13. Use the determined time range to linearly fit that part of the data and acquire the V0 for each substrate concentration tested. Then plot these velocities against substrate concentration to obtain a Michaelis-Menten plot. The data can also be fitted using the built-in Michaelis-Menten equation to obtain the K_M and V_{max}.

Note: Modern computers do not require linearization of the data for fitting Michaelis-Menten data. Linearization creates large artefacts and should be avoided.

551327-L-bw-Dharadhar
Processed on: 30-12-2020
PDF page: 49

14. The curve and the fit statistics will indicate whether you have sufficient plateaus at the top and bottom of the curve. Take this into account in the next experiments for the tested enzyme, extending the substrate dilution range if necessary.
15. Convert the V_{max} value to k_{cat} by dividing it with the enzyme concentration used and calculate the catalytic efficiency k_{cat}/K_M.

Measuring deubiquitination of a natural target

Minimal substrates such as ubiquitin-AMC or ubiquitin-rhodamine are convenient for initial enzymological characterization of DUBs. However, activities on minimal substrates do not always translate directly to activities on a physiological target (Uckelmann et al., 2018; Kim et al.,provisionally accepted), and substrates may affect the reaction itself. Since regulation of deubiquitinating enzymes is often achieved through modulating their activities (Sahtoe & Sixma, 2015; Mevissen & Komander, 2017), it is ultimately necessary to study the enzymology of DUBs on their physiological targets. The identification of physiological targets for some DUBs and advanced tools for modelling enzyme kinetics allow one to study target-specific deubiquitination in some systems.

Quantitative analysis is assisted by a well-defined singly modified substrate. To make such a substrate, requires a properly characterized ubiquitination site, known to be used *in vivo*, knowledge of the natural ubiquitin modification (monomer or polymer and if the latter what linkages), and a way to consistently produce labelled substrate. In our USP7 case study (Kim et al., provisionally accepted), we investigated its interaction with p53, for which the ubiquitination sites and USP7 recognition sites were well defined in literature. This protein sequence and the advanced methods in chemical ubiquitin synthesis allowed the generation of a fluorescently labelled, homogeneous, peptide substrate. We could use this tool, along with the kinetic modelling program KinTek (Johnson, Simpson, & Blom, 2009), to quantitatively study the effect of target recognition on the enzyme kinetics of USP7.

Here we describe a different approach to measuring substrate-specific deubiquitination. We employ a gel-based setup, enzymatically ubiquitinated target proteins (H2A in nucleosomal core particles) with a fluorescently labelled ubiquitin and a laser-based fluorescence gel scanner for quantification of the signal. In this experimental system we exploit the fact that ubiquitination of H2A by BRCA1/BARD1 is unusually site-specific. This allows tracking of H2A deubiquitination by the BRCA1-site-specific DUB USP48. The three steps necessary for measuring specific deubiquitination of nucleosomes are described in detail:

551327-L-bw-Dharadhar
Processed on: 30-12-2020
PDF page: 50

1. Labelling of ubiquitin
2. Generation of the ubiquitinated nucleosome substrate
3. Measurement of site-specific deubiquitination

Note: Here we make use of a well characterized system that allows tracking specific ubiquitination and deubiquitinating events. For every new experimental system, it is worth considering some very basic questions:

What exactly constitutes the substrate?

- *Are there different distinct ubiquitination sites (different lysines ubiquitinated) on the target protein?*
- *Should different sites be treated as distinct targets?*
- *Can the experimental setup distinguish between different sites?*
- *Are the sites mono-ubiquitinated or will ubiquitin chains be formed?*

Once the substrate is identified, can it be produced in high purity?

- *Can the ubiquitinated substrate be produced synthetically or enzymatically?*
- *Are there side products of the ubiquitination reaction that need to be considered (e.g. formation of nonspecific ubiquitin chains)?*
- *Can the product be purified after the ubiquitination reaction?*
- *Will substrate preparation yield a homogeneous substrate?*

Finally, does the selected assay readout report on the deubiquitination of the site of interest?

Labelling ubiquitin

To enable labelling of ubiquitin with cysteine-reactive fluorescent dyes, a mutant ubiquitin construct carrying a cysteine as the second residue (^{Cys}ubiquitin) is used; ubiquitin has no native Cys residues. Any dye carrying a cysteine-reactive moiety can in principle be used. In the following example we used a tetramethylrhodamine dye (TAMRA) with a Cys-reactive maleimide moiety to generate ^{TAMRA}ubiquitin which was suitable for our specific purpose and economical when considering the large amounts of fluorophore used in the study.

Purification of ^{Cys}ubiquitin

The ^{Cys}Ubiquitin construct is cloned into the pETNKI-His-SUMO2-kan vector (Luna-Vargas et al., 2011). Transform the sequence-verified expression construct into *Escherichia Coli*

551327-L-bw-Dharadhar
Processed on: 30-12-2020

BL21 (DE3) T^{1R} cells and grow the transformed cells in 1 liter of Lysogeny Broth (LB) growth medium. When cells reach an $O.D._{600nm}$ of 0.8 add 0.2 mM IPTG to induce and incubate at 37°C for 4 hours.

Buffers

- Lysis buffer - 50 mM Tris-HCl (pH 7.5) + 150 mM NaCl + 1 mM TCEP + 5 mM Imidazole + Pierce™ Protease Inhibitor Mini Tablets, EDTA Free (1 tablet/50 ml)
- Wash buffer - 50 mM Tris-HCl (pH 7.5) + 150 mM NaCl + 1 mM TCEP + 20 mM Imidazole
- Elution buffer -50 mM Tris-HCl (pH 7.5) + 150 mM NaCl + 1 mM TCEP + 350 mM Imidazole
- Dialysis buffer 1 - 50 mM Tris-HCl (pH 7.5) + 150 mM NaCl + 1 mM TCEP
- Dialysis buffer 2 - 50 mM Ammonium Acetate (pH 4.5) + 1 mM DTT
- IEX buffer A - 50 mM Ammonium Acetate (pH 4.5) + 2 mM DTT
- IEX buffer B - 50 mM Ammonium Acetate (pH 4.5) + 500 mM NaCl + 2 mM DTT
- GF buffer - 50 mM Tris-HCl (pH 7.5) + 150 mM NaCl + 5 mM DTT

Protocol

1. Spin down cells at 5300 x *g* for 15 minutes at room temperature and resuspend in 50 ml lysis buffer.
2. Lyse cells by sonicating with a pre-cooled sonicator (Qsonica Q700 with 12.7 mm probe) . The lysis conditions are as follows, Amp -80; Pulse on -15 seconds; Pulse off - 45 seconds; Total Time – 4 minutes.
3. Centrifuge the lysate at 53000 x g for 30 minutes at 4 °C.
4. Add 8 ml chelating sepharose beads (Roche) charged with Ni^{2+} to the supernatant, load onto a sealed gravity-flow column (Bio-Rad), let the beads settle by force of gravity, then open the column and let the supernatant flow through.
5. Wash the beads with 3 x 80 ml of wash buffer.
6. Elute the sample in 25 ml of elution buffer.
7. Add His-tagged SENP2 protease to a final concentration of 3 µg/ml, transfer sample to a 3500 – 5000 Da cutoff Spectra/Por dialysis tube (Spectrum) and dialyze against 2 x 2 L of dialysis buffer 1 at 4 °C. After 4 hours replace the buffer with 2 L of fresh dialysis buffer 1 and let this second dialysis step proceed overnight.
8. To remove the His-SUMO, uncleaved protein and SENP2, add 8 ml chelating sepharose beads charged with Ni^{2+} to the dialysed sample and load on a gravity-flow column. Let the beads settle by force of gravity and collect the flow-through containing ubiquitin (His-SUMO, uncleaved SUMO-^{Cys}Ubiquitin and His-SENP2 will

remain bound to the beads). Wash beads with 8 ml of dialysis buffer 1 and collect in the same tube.

9. While stirring the sample on ice, add perchloric acid dropwise until a final concentration of 2 % v/v is reached. Most proteins will precipitate at this stage, while ^{Cys}Ubiquitin will stay in solution.
10. Centrifuge at 53000 x *g* at 4 °C for 30 minutes and collect the supernatant.
11. Dialyze the supernatant against 2 L Dialysis Buffer 2 overnight at 4 °C.
12. Load sample on a 5 ml HiTrap SP HP ion exchange column (GE healthcare) in IEX-buffer A at 4 °C.
13. Elute sample using a linear gradient ranging from 0 % IEX-buffer B to 100 % IEX-buffer B in 12 column volumes.
14. Combine fractions containing ^{Cys}Ubiquitin and gel filter on a Superdex 75 16/60 column (GE healthcare) .
15. Combine fractions containing ^{Cys}Ubiquitin, concentrate in an Amicon Ultra-15 centrifugal filter unit with a 3 kDa cutoff (Merck) to a concentration of ~1 mM, snap-freeze 50 µl aliquots in liquid nitrogen and store at -80 °C.

Materials

- Fresh DTT
- Labelling buffer: 50 mM Tris-HCl pH 7.5, 150 mM NaCl
- Purified ^{Cys}ubiquitin
- TAMRA-maleimide
- Storage buffer: 25 mM HEPES, 150 mM NaCl, 1 mM DTT
- Spectra/Por 3500 – 5000 D cutoff dialysis tubing (Spectrum)

Protocol

Note: Throughout the protocol, wherever possible, keep the fluorophore and the fluorescently labelled protein protected from direct light.

1. Thaw the desired amount of ^{Cys}ubiquitin to be labelled.
2. Add 5 mM of fresh DTT to the sample to reduce the cysteine residue for labelling.

Note: It is critical the cysteine residues are reduced, otherwise labelling will not be possible.

3. Dialyze reduced ^{Cys}ubiquitin against at least three changes of 2 L labelling buffer to remove residual DTT which would interfere with labelling. Ideally the second dialysis step should be carried out overnight.

551327-L-bw-Dharadhar
Processed on: 30-12-2020

Note: Removal of residual DTT is critical as it would otherwise react with the maleimide group and compete with cysteine labeling. TCEP should not interfere with maleimide-dependent labelling reactions as it does not contain thiols. However, we have never tested labelling in the presence of TCEP and the reader is advised to conduct their own pilot experiments if the reducing agent is to be changed. For faster removal of DTT, a buffer exchange column or desalting spin column can be used.

4. For the labelling reaction, add a 5-fold molar excess of TAMRA-maleimide over ubiquitin and incubate for 2 hours at room temperature, followed by overnight incubation at 4°C.

Note: The ratio of fluorophore over ubiquitin is critical for high labelling efficiency. The optimal ratio can vary between batches of protein and fluorophore. When feasible, the reader is advised to conduct small-scale pilot experiments, varying the ratio incrementally between 2:1 and 8:1 and assess labelling efficiency as described later on. Similarly, different incubation times and temperatures can be tested. We had good success with the suggested ratios and incubation.

5. Quench the labelling reaction with a 3-fold molar excess of DTT over fluorophore.
6. Centrifuge the sample at 20000 x *g* to remove aggregated material and collect the supernatant.
7. Dialyze the supernatant against three changes of 2 L storage buffer to remove excess dye.
8. To remove residual dye that might be present even after extensive dialysis, purify the sample on an appropriate size-exclusion column (Superdex S75 or comparable) using FPLC or a commercially available dye-removal spin column.

Note: Removal of residual dye is a crucial step in order to be able to estimate concentrations of labelled ubiquitin accurately. The suggested procedure using FPLC allowed us to obtain exceptionally pure sample. If purification by FPLC is not an option, or if the protocol needs speeding up, commercially available dye-removal spin columns are a good alternative. High amounts of free fluorophore might necessitate the use of two successive column steps.

9. If using FPLC, be aware that fluorescent dyes can be very sticky and adhere to the column resin, especially when present in high concentration during size exclusion chromatography. Extensive column washes are necessary to remove residual dye.

551327-L-bw-Dharadhar
Processed on: 30-12-2020
PDF page: 54

10. Concentrate sample to the desired concentration;. the concentration is best calculated using the fluorophores absorbance at 542 nm and the corresponding extinction coefficient of 101000 $cm^{-1}M^{-1}$

Note: This combination of maximum absorbance and extinction coefficient is true for the particular fluorophore used in this study. Make sure you use the right absorbance and extinction coefficient for the fluorophore you are using. This might differ from the stated values here, even if the fluorophore is a TAMRA-based fluorophore.

11. Assess labelling efficiency by determining concentration of dye and protein. To determine the dye concentration measure absorption at the appropriate wavelength. Estimation of ubiquitin concentration is best done on a SDS gel. As a standard, run a titration series of known amounts of unlabelled ubiquitin. To determine the ubiquitin concentration in your labelled sample, run several dilutions on the same gel and compare to the standard. Divide this estimate of the ubiquitin concentration by the dye concentration to estimate the labelling efficiency.
12. Flash freeze sample aliquots and store at -80°C.

Note: The labelled ubiquitin can be used not only for measuring deubiquitination, but is equally suited for E3 ligase ubiquitination reactions. It can further be used for binding assays reliant on fluorescence polarization.

Generating ubiquitinated nucleosomes

We describe here the ubiquitination of nucleosome core particles (NCPs) using truncated BRCA1/BARD1 as the E3 ligase. If other E3-substrate combinations are used, concentrations of components may vary and pilot experiments need to be conducted to establish reaction conditions. However, in our experience, the stated conditions are appropriate for all H2A-specific E3 ligases and should provide a reasonable starting point for other systems as well.

Materials

- E1: hUBA1 purified from *E.Coli* (Uckelmann et al., 2018), also commercially available (Boston Biochem)
- E2: UBCH5C purified from *E.Coli* (Uckelmann et al., 2018), also commercially available (Boston Biochem)
- E3: $BRCA1^{1-306}$/$BARD1^{26-302}$ purified from *E.Coli* (Uckelmann et al., 2018)
- Purified recombinant *Xenopus laevis* H2A, H2B, H3 and H4 (Luger, Rechsteiner, & Richmond, 1999)

551327-L-bw-Dharadhar
Processed on: 30-12-2020
PDF page: 55

- Purified 147 bp DNA for nucleosome reconstitution (Vasudevan, Chua, & Davey, 2010)
- Labelled ubiquitin
- EDTA, pH 8 (500 mM)
- ATP, pH 7.5 (100 mM)
- Ubiquitination reaction buffer: 25 mM HEPES (pH 7.5) + 150 mM NaCl + 3 mM $MgCl_2$ + 1 mM DTT (fresh)
- Gel filtration buffer: 25 mM HEPES (pH 7.5) + 150 mM NaCl + 1 mM DTT
- 50 kDa cutoff Amicon ultra-15 centrifugal filter unit (Merck)

Protocol

Note: Throughout the protocol, wherever possible keep the fluorophore and the fluorescently labelled protein protected from direct light.

1. Reconstitute recombinant nucleosome core particles (NCP) according to a previously published protocol (Luger et al., 1999).
2. For the ubiquitination reaction, combine 0.5 µM of hUBA1, 1 µM UBCH5C, 1 µM $BRCA1^{1-306}$ / $BARD1^{26-302}$, 5 µM NCP and 40 µM ^{TAMRA}ubiquitin in Ubiquitination reaction buffer.
3. Start the reaction by adding ATP to a final concentration of 3 mM.
4. Incubate at 30°C for 45 minutes.
5. Stop the reaction by putting the sample on ice and adding EDTA to a final concentration of 5 mM.
6. Purify the ubiquitinated nucleosomes by size exclusion on a Superose 6 increase column (GE Healthcare) in gel filtration buffer.

Note: This step removes excess ubiquitin, ATP, E1 and E2 enzymes but ubiquitinated NCP cannot be resolved from non-ubiquitinated NCP. However, the reaction conditions of the ubiquitination reaction have been optimized to yield a mix of mono- di- and triubiquitinated NCP and a negligible amount of non-ubiquitinated NCP. This heterogeneous mix of different ubiquitination states is appropriate for the following USP48 analysis as mono-, di-, and triubiquitinated species can be resolved on a SDS-PAGE gel, which allows to discern individual catalytic rates for different ubiquitination states.

7. Check for ubiquitination by running a SDS-PAGE gel and combine fractions that contain ubiquitinated nucleosomes. Concentrate sample to ~10 µM using a 50 kDa cutoff concentrator.

551327-L-bw-Dharadhar
Processed on: 30-12-2020
PDF page: 56

8. Ideally the ubiquitinated nucleosomes are used immediately. However, storage of up to a week at 4°C leads to only minor deterioration in sample quality. Never freeze reconstituted nucleosomes.

Quantitative analysis of USP activity: Deubiquitination of Nucleosome core particles by USP48

To enable quantitation of kinetic parameters, full data sets are needed under Michaelis-Menten conditions. However, an interesting alternative approach is the modelling of kinetic parameters (with e.g., Kintek explorer (Johnson et al., 2009)) based on reaction velocities while sampling over a wide range of substrate and enzyme concentrations. A 4 x 3 grid of enzyme and substrate concentrations (Table 1) was sufficient to reliably estimate kinetic parameters for NCP deubiquitination by USP48. It will become obvious during the fitting process how much data is necessary for proper restraint of the model parameters for the particular system studied (for details see (Johnson et al., 2009)).

Table 1: Combinations of enzyme and substrate concentrations used to determine kinetic parameters for NCP deubiquitination by USP48

USP48 12.5 nM NCP 500 nM	USP48 25 nM NCP 500 nM	USP48 50 nM NCP 500 nM	USP48 100 nM NCP 500 nM
USP48 12.5 nM NCP 2000 nM	USP48 25 nM NCP 2000 nM	USP48 50 nM NCP 2000 nM	USP48 100 nM NCP 2000 nM
USP48 12.5 nM NCP 3000 nM	USP48 25 nM NCP 3000 nM	USP48 50 nM NCP 3000 nM	USP48 100 nM NCP 3000 nM

For the sake of clarity, we describe the experimental setup used to record a single time course for only one combination of enzyme and substrate concentration (25 nM USP48, 2000 nM NCP). For the complete grid of different combinations, the reader is referred to Table 1.

Material

- Full length USP48 purified from Sf-9 insect cells (Uckelmann et al., 2018); 80 µM
- Purified NCP ubiquitinated with ^{TAMRA}ubiquitin; 15 µM
- DUB-reaction buffer: 25 mM HEPES, 150 mM NaCl, 2 mM DTT (fresh)
- 4x Laemmli sample buffer

Protocol

Note: Throughout the protocol, wherever possible keep the fluorophore and the fluorescently labelled protein protected from direct light.

551327-L-bw-Dharadhar
Processed on: 30-12-2020
PDF page: 57

1. Prepare a 30 µl aliquot containing 50 nM USP48 in DUB-reaction buffer.
2. Prepare a 27.5 µl aliquot of 4 µM ubiquitinated NCP (NCP^{Ub}) in DUB-reaction buffer.

Note: Make sure DTT in the reaction buffer is added freshly

3. Pre-warm USP48 and NCP^{Ub} to 30°C.

Note: Assays are best done using thin-walled PCR tubes and a PCR machine set to incubate at 30°C.

4. Time points will be taken after 0, 1, 2, 4, 8, 16, and 45 minutes. The reaction will be stopped at each time point by transferring 5 µl of the reaction to a tube pre-filled with 1.7 µl of 4x Laemmli sample buffer. While samples are pre-warming, prepare "stop-tubes" for each time point by adding 1.7 µl 4x Laemmli sample buffer to 200 µl PCR-tubes.
5. For the time point 0, add 2.5 µl reaction buffer and 2.5 µl of the pre-incubating NCP^{Ub} dilution to the appropriate stop-tube.
6. Start the reaction by adding 25 µl from the USP48 dilution to the now 25 µl of the NCP^{Ub} dilution and incubate at 30°C.

Note: In experimental systems where the fluorophore tends to aggregate and form precipitate, addition of 0.05 % TWEEN20 v/v can help prevent aggregation

7. At each time-point, take 5 µl from the reaction mixture and add to the appropriate stop-tube.

Note: Several reactions can easily be streamlined by using a multichannel pipette so that different enzyme-substrate combinations can be recorded simultaneously.

8. Boil the samples and run 5 µl on a 4-12% gradient SDS-gel.
9. For quantitative readout a laser-based fluorescence gel scanner is suggested.
10. Quantify the bands in each lane using programs such as ImageJ. Each band represents a fraction of the total concentration of labelled ubiquitin (and thus ubiquitinated substrate) used in the reaction. Note, however, that this represents the molar amounts of ubiquitin present in each band. If the interest lies with the molar amounts of substrate, the quantification needs to be corrected for the number of ubiquitins present on each substrate species. For example, to calculate molar amounts for the species corresponding to di-ubiquitinated H2A, the molar amounts

551327-L-bw-Dharadhar
Processed on: 30-12-2020
PDF page: 58

quantified from the fluorescence signal need to be divided by two, as there are two ubiquitins on the di-ubiquitinated H2A.

Note: More details on analysis and interpretation of the kinetic data generated this way can be found in ((Johnson et al., 2009; Uckelmann et al., 2018)*; Kim et al., in revision)*

Regulation of USP activity

USPs are usually large multi-domain proteins where the accessory domains can play a vital role in regulation of the USPs either by modulating their catalytic rates or by altering their affinity for ubiquitin or their natural substrates. Additionally, USP activity can be regulated upon binding to regulatory proteins in *trans.* To investigate the potential effects of any regulatory element on DUB activity, a first step is to assess differences in USP activity in the presence and absence of the regulatory element.

Estimation of K_D based on activity assays

For determining kinetic parameters of USP activity in the presence of regulatory factors it is important to estimate the K_D between the USP and the regulatory factor. This gives us an idea of the concentration required to saturate the binding so that the effect caused by this regulatory binding can be observed. Here we describe a general protocol for estimating K_D that is based on change in USP catalytic activity upon binding to its regulator.

Note: Activation assays done with domains added in trans will yield an apparent K_D for the in trans interaction, in a covalently linked setting the affinities can differ.

Materials

- Purified regulatory protein (e.g. UAF1) or a domain (e.g. UBL domains of USP7)
- Purified USP full length or catalytic domain
- UbRho (8 µM stock)
- Reaction Buffer (20 mM HEPES (pH 7.5) + 100 mM NaCl + 5 mM DTT + 0.05% Tween 20)
- Low Volume 384 Well Black Flat Bottom Polystyrene NBS™ Microplate (Corning, catalogue number: 3820)

Protocol

1. Determine the protein concentration of the USP and the regulatory protein.
2. Prepare a USP stock (refer to 3.1.3) in reaction buffer.

551327-L-bw-Dharadhar
Processed on: 30-12-2020
PDF page: 59

3. Prepare a two-fold dilution series of the regulatory protein in reaction buffer. Each dilution should have a volume of 10 µl.
4. Add 10 µl of the USP stock to each dilution and let the sample incubate for 10-15 minutes at room temperature.
5. Prepare an 8 µM stock of UbRho in reaction buffer.
6. Add 10 µl of USP + regulator into the wells; each dilution goes into a separate well.
7. Using a multichannel pipette, add 10 µL of the substrate into the wells.
8. Start the program, and monitor the fluorescence increase.
9. If the regulatory effect is saturated at the lowest concentrations of regulator or if saturation is not reached even at the highest concentration then adjust the concentration range of the regulator and perform the experiment again.
10. Determine the apparent K_D by calculating the initial rates and plotting them against the concentration of regulator.

Note: Since this assay includes ubiquitin, the K_D obtained here could be different for the ubiquitin-USP intermediate then for the USP alone. For non-ubiquitin-based affinity experiments refer to section 3.4.

Quantitative assessment of activity modulation

Here we describe the case study of USP1-UAF1, in which we determine the steady-state kinetic parameters for this complex. The protocol can be used for other USP complexes as well, although the buffer and protein concentrations may have to be optimized (see 3.1.3).

Materials

- Purified USP1 (65 µM) and UAF1 (75 µM)
- UbRho stock (1 mM, in DMSO)
- Reaction Buffer (20 mM HEPES 7.5 + 100 mM NaCl + 5mM DTT + 0.05% Tween 20)
- Low Volume 384 Well Black Flat Bottom Polystyrene NBS™ Microplate (Corning, catalogue number: 3820)
- PCR tubes, in a strip
- Data fitting software: GraphPad Prism 7

Note: Follow the same guidelines for sample and buffer preparation provided in the notes of section 3.1.4.

Protocol

1. Determine the concentration of USP1 and UAF1.

551327-L-bw-Dharadhar
Processed on: 30-12-2020
PDF page: 60

2. Prepare a 40 nM USP1 stock and a 400nM UAF1 stock in reaction buffer. Make at least 60 µl of each stock solution.

Note: The K_D for USP1-UAF1 binding is around 10 nM, but we still use 10 times more UAF1 to USP1 to ensure all of the USP1 is bound. For every USP complex, perform the experiment at varying concentrations of regulator (3.3.1) to determine the concentration of regulator to use.

3. Mix 50 µl of the USP1 stock with 50 µl of the UAF1 stock, and incubate at room temperature for 10 minutes.
4. Make a two-fold dilution range of UbRho (starting at 60 µM) in an 8-strip of PCR tubes. Make sure the minimal amount is 10 µL for each reaction. For example, prepare 25 µL of 60 µM UbRho, then do a serial dilution transferring 12.5 µL to the next well containing 12.5 µL buffer.
5. Add 10 µL of USP1/UAF1 stock solution into the wells of the assay plate – note down the wells.
6. At the plate reader, check the settings and the program, take care to select the proper wells.
7. Using the multichannel pipette, add 10 µL of the substrate into the wells.
8. Start the program, and monitor the fluorescence increase.
9. Analyze the data by following the analysis protocol outlined in section 3.1.4.

Case study: mapping substrate recognition sites on USP with effects on activity assays. Whilst the activation assay is designed for use with a minimal ubiquitin substrate (UbRho), some domains within a USP could aid specifically in the recognition or cleavage of a physiological ubiquitinated target. By omitting the domain of interest in the protein construct, one can investigate its effect in comparison to the full-length protein. We have used such a system to study the effect of the TRAF domain of USP7 on the recognition and activity of USP7 toward a ubiquitinated p53-peptide, which mimics a physiological substrate of the enzyme (Kim et al., provisionally accepted).

Quantitative USP interaction analysis

Large scale proteomic studies carried out specifically on DUBs have uncovered large protein interaction networks (Sowa, Bennett, Gygi, & Harper, 2009). These DUB interaction networks can be examined and simplified further by using *in vitro* binding assays to identify and quantify protein interactions. Most USPs are part of multiprotein complexes where the members of the complex are either substrates of the USP or regulators of USP function. Binding studies can be used to simplify these complicated interaction networks

551327-L-bw-Dharadhar
Processed on: 30-12-2020
PDF page: 61

by examining which members are responsible for direct interactions with the USP in question. Furthermore, once the binding partner has been identified, the stoichiometry of binding can also be determined using certain binding assays. Additionally, the equilibrium dissociation constant (K_D) and binding kinetics data obtained from such analyses give an indication of the lifetime of a protein interaction with its binding partner. This can then be compared with its other binding partners to obtain relative abundance of protein complexes for the protein in question. This kind of information is very useful for understanding mechanisms of USP regulation, especially when multiple regulatory factors are involved. For example, information obtained from binding studies can be used in activity assays to quantitatively analyze the effect of interactors on USP activity (refer to section 3.3.2).

Here we describe a number of *in vitro* binding assays which can be performed to study protein – protein interactions. We do not go into the details of any of these assays as they are available in the published literature. Instead, we highlight the important features and limitations of each binding assay so that an informed decision can be made by the reader before performing these assays.

In Vitro pull-down assays

In vitro pull-down assays are a fast and inexpensive way of identifying protein - protein interactions as these experiments do not require highly specialized instrumentation or a large amount of material. Pull-down assays are a type of affinity purification where one of the proteins is immobilized to a surface using a specific antibody or an affinity tag. The potential binding partner is incubated with the immobilized protein and interaction is confirmed if both proteins co-elute from the surface. Many proteins interact non-specifically with the immobilization surface which leads to false positive results. Thus, control experiments should be performed to confirm lack of non-specific interactions. Pull down assays are usually not quantitative and low affinity interactions or interactions with a fast off rate cannot be detected using this method. Additionally, if the interacting region on the immobilized protein is masked by the surface then no binding will be observed.

Analytical gel filtration

This technique is an easy way of determining if two proteins interact with each other. The biggest advantage here is that the proteins don’t have to contain any tag and also the amount of protein required is relatively low. The time required for a typical size exclusion run means that complexes with fast off-rates will be poorly detected. This technique is

551327-L-bw-Dharadhar
Processed on: 30-12-2020
PDF page: 62

primarily used for qualitative purposes, but multiple runs at varying concentrations, with sensitive read-out (e.g. western blot) would allow quantification of binding parameters.

Surface Plasmon Resonance

Surface plasmon resonance (SPR) is a spectroscopic method which is used to detect protein interactions by immobilizing the ligand on a thin metal film and measuring the change in refractive index upon binding of the analyte. SPR experiments allows quantification of the K_D, and if the binding process is well defined, also makes it possible to determine kinetic parameters (k_{ON} and k_{OFF}). High-affinity interactions of less than 1 nM (depending on the system) and low-affinity interactions upto 500 µM can both be analyzed in this label-free setup with the only requirement being that one of the proteins has to be tagged so that it can be immobilized on a complementary surface. The starting material required to carry out binding measurements is not very high unless the affinity is very low, in which case the amount of analyte required will increase considerably. The disadvantage of this system is that one of the protein partners has to be immobilized on a solid surface which can prevent binding due to steric hindrance or in some cases lead to more binding than what is actually observed in solution. Moreover, the instrument and sensors are expensive and running the instrument requires some expertise.

Fluorescence polarization

Fluorescence polarization (FP) measures protein binding based on change in polarization of emitted light upon excitation of a fluorescent molecule with plane-polarized light. Therefore, when an interacting protein binds to the fluorescently labelled protein there is a change in the polarization of emitted light due to slower tumbling of the fluorescent molecule. FP is a quantitative technique and the amount of sample required for these assays is lower compared to SPR but that again depends on the affinity of the interaction being measured. FP depends on the size of the interacting proteins; thus, it usually only works well when the size of the labelled protein is much smaller compared to the interacting protein. The other limitation of FP arises when measuring low-affinity interactions because for such cases the concentration of the unlabelled protein is very high which can lead to artificial crowding effects. Finally, the choice of label can also lead to non-specific interactions as some of the labels are very hydrophobic.

Microscale Thermophoresis

Microscale thermophoresis (MST) measures protein interactions in solution based on the diffusion of a fluorescently labelled molecule along a laser-induced local temperature gradient (Wienken, Baaske, Rothbauer, Braun, & Duhr, 2010). This technique requires labelling of one protein but unlike FP there is no limitation on the relative size of the

551327-L-bw-Dharadhar
Processed on: 30-12-2020
PDF page: 63

labelled and unlabelled proteins. Other advantages of MST are that the amount of sample required for obtaining a K_D is lower than any of the techniques described here and also the range of binding affinities that can be measured is very high. MST is a very sensitive method and because of that small changes in buffer or sample preparation can lead to changes in signal which hamper reproducibility. Additionally, kinetic parameters cannot be determined with this method and hydrophobicity of the label can lead to non-specific interactions.

Isothermal Titration Calorimetry

Isothermal Titration Calorimetry (ITC) measures the heat generated in an interaction. Upon titration of one of the partners in the interaction, it allows determination of the thermodynamic properties of protein interactions in solution and gives K_D and stoichiometry. This is a robust method which gives very solid data. It enables measuring protein interaction in a label-free environment. The biggest disadvantage of this method is the large sample quantities required, and this is particularly important in the case of USPs because many of these enzymes are not easily produced in large quantities. Other disadvantages of ITC are that measurement times are longer, it requires high concentrations, it requires stirring of the sample, and also that it does not measure kinetic parameters of binding.

Table 2: Features of commonly used binding assay for studying protein-protein interactions

	Pull down	Analytical Gel Filtration	FP	SPR	MST	ITC
K_D Quantification	–	–/+	+	+	+	+
Measurable K_D range	▮	▮	▮▮	▮▮▮	▮▮	▮▮
Quantification of kinetic parameters	–	–	–/+	+	–	–/+
Sample Size	▮	▮▮	▮	▮▮	▮	▮▮▮
Sample Labelling	+	–	+	+	+	–
Measurement time	▮▮	▮▮	▮	▮▮▮	▮▮	▮▮▮

CONCLUSIONS

The prerequisite for *in vitro* characterization of USPs is pure and stable protein. USPs are usually large proteins and often with several unstructured regions which makes their

551327-L-bw-Dharadhar
Processed on: 30-12-2020
PDF page: 64

expression and purification difficult. Purification of USPs from bacterial and insect cells presents distinct challenges which have been discussed in this chapter. The purification protocols outlined in this chapter serve as a starting point for purification of any USP but they might require modifications depending on the choice of expression construct and the USP being purified.

In vitro activity studies are a great way for studying USP function. These assays are also used to probe the role of regulatory factors in modifying USP catalytic activity. Similarly, when performing binding assays all the quality control measures mentioned above should be taken into consideration. The protocols described in this chapter in combination with several quality control measures will enable one to obtain reliable quantitative data on USP activity and regulation.

551327-L-bw-Dharadhar
Processed on: 30-12-2020
PDF page: 65

REFERENCES

Bingol, B., Tea, J. S., Phu, L., Reichelt, M., Bakalarski, C. E., Song, Q., … Sheng, M. (2014). The mitochondrial deubiquitinase USP30 opposes parkin-mediated mitophagy. *Nature*, *509*(7505), 370–5. doi:10.1038/nature13418

Cheng, J., Yang, H., Fang, J., Ma, L., Gong, R., Wang, P., … Xu, Y. (2015). Molecular mechanism for USP7-mediated DNMT1 stabilization by acetylation. *Nature Communications*, *6*, 7023. Retrieved from http://dx.doi.org/10.1038/ncomms8023

Clague, M. J., Coulson, J. M., & Urbe, S. (2012). Cellular functions of the DUBs. *J Cell Sci*, *125*(Pt 2), 277–286. doi:10.1242/jcs.090985

Clerici, M., Luna-Vargas, M. P. a, Faesen, A. C., & Sixma, T. K. (2014). The DUSP-Ubl domain of USP4 enhances its catalytic efficiency by promoting ubiquitin exchange. *Nature Communications*, *5*(May), 5399. doi:10.1038/ncomms6399

Cornelissen, T., Haddad, D., Wauters, F., Van Humbeeck, C., Mandemakers, W., Koentjoro, B., … Vandenberghe, W. (2014). The deubiquitinase USP15 antagonizes Parkin-mediated mitochondrial ubiquitination and mitophagy. *Human Molecular Genetics*, *23*(19), 5227–5242. Retrieved from http://dx.doi.org/10.1093/hmg/ddu244

Cotto-Rios, X. M., Békés, M., Chapman, J., Ueberheide, B., & Huang, T. T. (2012). Deubiquitinases as a Signaling Target of Oxidative Stress. *Cell Reports*, *2*(6), 1475–1484. doi:10.1016/j.celrep.2012.11.011

Durcan, T. M., Tang, M. Y., Perusse, J. R., Dashti, E. A., Aguileta, M. A., McLelland, G.-L., … Fon, E. A. (2014). USP8 regulates mitophagy by removing K6-linked ubiquitin conjugates from parkin. *The EMBO Journal*, *33*(21), 2473–2491. doi:10.15252/embj.201489729

Faesen, A. C., Dirac, A. M. G., Shanmugham, A., Ovaa, H., Perrakis, A., & Sixma, T. K. (2011). Mechanism of USP7/HAUSP activation by its C-Terminal ubiquitin-like domain and allosteric regulation by GMP-synthetase. *Molecular Cell*, *44*(1), 147–159. doi:10.1016/j.molcel.2011.06.034

Fernández-Montalván, A., Bouwmeester, T., Joberty, G., Mader, R., Mahnke, M., Pierrat, B., Gerhartz, B. (2007). Biochemical characterization of USP7 reveals post-translational modification sites and structural requirements for substrate processing and subcellular localization. *FEBS Journal*, *274*(16), 4256–4270. doi:10.1111/j.1742-4658.2007.05952.x

Fraile, J. M., Quesada, V., Rodríguez, D., Freije, J. M. P., & López-Otín, C. (2012). Deubiquitinases in cancer: new functions and therapeutic options. *Oncogene*, *31*(19), 2373–2388. doi:10.1038/onc.2011.443

Haahr, P., Borgermann, N., Guo, X., Typas, D., Achuthankutty, D., Hoffmann, S., … Mailand, N. (2018). ZUFSP Deubiquitylates K63-Linked Polyubiquitin Chains to Promote Genome Stability. *Molecular Cell*, *70*(1), 165–174.e6. doi:10.1016/j.molcel.2018.02.024

Hassiepen, U., Eidhoff, U., Meder, G., Bulber, J. F., Hein, A., Bodendorf, U., … Martoglio, B. (2007). A sensitive fluorescence intensity assay for deubiquitinating proteases using ubiquitin-rhodamine110-glycine as substrate. *Analytical Biochemistry*, *371*(2), 201–207. doi:10.1016/j.ab.2007.07.034

Heideker, J., & Wertz, I. E. (2015). DUBs, the regulation of cell identity and disease. *Biochemical Journal*, *465*(1), 1–26. doi:10.1042/BJ20140496

Hermanns, T., Pichlo, C., Woiwode, I., Klopffleisch, K., Witting, K. F., Ovaa, H., … Hofmann, K. (2018). A family of unconventional deubiquitinases with modular chain specificity determinants. *Nature Communications*, *9*(1). doi:10.1038/s41467-018-03148-5

Hershko, A., Heller, H., Elias, S., & Ciechanover, A. (1983). Components of Ubiquitin-Protein Ligase System. *The Journal of Biological Chemistry*, *258*(13), 8206–8214. doi:papers2://publication/uuid/C82E58FF-33C7-42BF-BC20-CDD10219EC6E

551327-L-bw-Dharadhar
Processed on: 30-12-2020
PDF page: 66

Hewings, D. S., Heideker, J., Ma, T. P., Ahyoung, A. P., El Oualid, F., Amore, A., … Wertz, I. E. (2018). Reactive-site-centric chemoproteomics identifies a distinct class of deubiquitinase enzymes. *Nature Communications*, *9*(1). doi:10.1038/s41467-018-03511-6

Holowaty, M. N., Sheng, Y., Nguyen, T., Arrowsmith, C., & Frappier, L. (2003). Protein Interaction Domains of the Ubiquitin-specific Protease, USP7/HAUSP. *Journal of Biological Chemistry*, *278*(48), 47753–47761. doi:10.1074/jbc.M307200200

Hu, M., Li, P., Li, M., Li, W., Yao, T., Wu, J. W., … Shi, Y. (2002). Crystal structure of a UBP-family deubiquitinating enzyme in isolation and in complex with ubiquitin aldehyde. *Cell*, *111*(7), 1041–1054. doi:10.1016/S0092-8674(02)01199-6

Johnson, K. A., Simpson, Z. B., & Blom, T. (2009). Global Kinetic Explorer: A new computer program for dynamic simulation and fitting of kinetic data. *Analytical Biochemistry*, *387*(1), 20–29. doi:10.1016/j.ab.2008.12.024

Kelley, L. A., Mezulis, S., Yates, C. M., Wass, M. N., & Sternberg, M. J. E. (2015). The Phyre2 web portal for protein modeling, prediction and analysis. *Nature Protocols*, *10*, 845. Retrieved from http://dx.doi.org/10.1038/nprot.2015.053

Kim, R. Q., Dijk, W. J. Van, & Sixma, T. K. (2016). Structure of USP7 catalytic domain and three Ubl-domains reveals a connector a -helix with regulatory role. *Journal of Structural Biology*, *195*(1), 11–18. doi:10.1016/j.jsb.2016.05.005

Kwasna, D., Abdul Rehman, S. A., Natarajan, J., Matthews, S., Madden, R., De Cesare, V., … Kulathu, Y. (2018). Discovery and Characterization of ZUFSP/ZUP1, a Distinct Deubiquitinase Class Important for Genome Stability. *Molecular Cell*, *70*(1), 150–164.e6. doi:10.1016/j.molcel.2018.02.023

Lee, J.-G., Baek, K., Soetandyo, N., & Ye, Y. (2013). Reversible inactivation of deubiquitinases by reactive oxygen species in vitro and in cells. *Nature Communications*, *4*, 1568. Retrieved from http://dx.doi.org/10.1038/ncomms2532

Leznicki, P., & Kulathu, Y. (2017). Mechanisms of regulation and diversification of deubiquitylating enzyme function. *Journal of Cell Science*, *130*(12), 1997–2006. doi:10.1242/jcs.201855

Luger, K., Rechsteiner, T. J., & Richmond, T. J. (1999). Preparation of nucleosome core particle from recombinant histones. *Methods in Enzymology*, *304*, 3–19. doi:10.1016/S0076-6879(99)04003-3

Luna-Vargas, M. P. A., Christodoulou, E., Alfieri, A., van Dijk, W. J., Stadnik, M., Hibbert, R. G., … Perrakis, A. (2011). Enabling high-throughput ligation-independent cloning and protein expression for the family of ubiquitin specific proteases. *Journal of Structural Biology*, *175*(2), 113–119. doi:10.1016/j.jsb.2011.03.017

Mevissen, T. E. T., & Komander, D. (2017). Mechanisms of Deubiquitinase Specificity and Regulation. *Annual Review of Biochemistry*, *86*(1), annurev-biochem-061516-044916. doi:10.1146/annurev-biochem-061516-044916

Michaelis, L., & Menten, M. L. (1913). Die Kinetik der Invertinwirkung. *Biochem Z*, *49*(February), 333–369. doi:10.1021/bi201284u

Mooij, W. T. M., Mitsiki, E., & Perrakis, A. (2009). ProteinCCD: enabling the design of protein truncation constructs for expression and crystallization experiments. *Nucleic Acids Research*, *37*(suppl_2), W402–W405. Retrieved from http://dx.doi.org/10.1093/nar/gkp256

Orcutt, S. J., Wu, J., Eddins, M. J., Leach, C. A., & Strickler, J. E. (2013). Bioluminescence Assay Platform for Selective and Sensitive Detection of Ub/Ubl Proteases. *Magn Reson Imaging*, *31*(3), 477–479. doi:10.1016/j.immuni.2010.12.017.Two-stage

Pfoh, R., Lacdao, I. K., Georges, A. A., Capar, A., Zheng, H., Frappier, L., & Saridakis, V. (2015). Crystal Structure of USP7 Ubiquitin-like Domains with an ICP0 Peptide Reveals a Novel Mechanism Used by Viral and Cellular Proteins to Target USP7. *PLOS Pathogens*, *11*(6), e1004950. Retrieved from https://doi.org/10.1371/journal.ppat.1004950

551327-L-bw-Dharadhar
Processed on: 30-12-2020
PDF page: 67

Pickart, C. M., & Rose, I. A. (1985). Ubiquitin carboxyl-terminal hydrolase acts on ubiquitin carboxyl-terminal amides. *Journal of Biological Chemistry*, *260*(13), 7903–7910.

Reddy, B. A., vanderKnaap, J. A., Bot, A. G. M., Mohd-Sarip, A., Dekkers, D. H. W., Timmermans, M. A., … Verrijzer, C. P. (2014). Nucleotide Biosynthetic Enzyme GMP Synthase Is a TRIM21-Controlled Relay of p53 Stabilization. *Molecular Cell*, *53*(3), 458–470. doi:10.1016/j.molcel.2013.12.017

Reyes-Turcu, F. E., Ventii, K. H., & Wilkinson, K. D. (2009). Regulation and cellular roles of ubiquitin-specific deubiquitinating enzymes. *Annual Review of Biochemistry*, *78*, 363–97. doi:10.1146/annurev.biochem.78.082307.091526

Sahtoe, D. D., & Sixma, T. K. (2015). Layers of DUB regulation. *Trends in Biochemical Sciences*, *40*(8), 456–67. doi:10.1016/j.tibs.2015.05.002

Senisterra, G. A., & Finerty, P. J. (2009). High throughput methods of assessing protein stability and aggregation. *Molecular BioSystems*, *5*(3), 217–223. doi:10.1039/b814377c

Sheng, Y., Saridakis, V., Sarkari, F., Duan, S., Wu, T., Arrowsmith, C. H., & Frappier, L. (2006). Molecular recognition of p53 and MDM2 by USP7/HAUSP. *Nature Structural &Amp; Molecular Biology*, *13*, 285. Retrieved from http://dx.doi.org/10.1038/nsmb1067

Sowa, M. E., Bennett, E. J., Gygi, S. P., & Harper, J. W. (2009). Defining the Human Deubiquitinating Enzyme Interaction Landscape. *Cell*, *138*(2), 389–403. doi:10.1016/j.cell.2009.04.042

Uckelmann, M., Densham, R. M., Baas, R., Winterwerp, H. H. K., Fish, A., Sixma, T. K., & Morris, J. R. (2018). USP48 restrains resection by site-specific cleavage of the BRCA1 ubiquitin mark from H2A. *Nature Communications*, *9*(1), 229. doi:10.1038/s41467-017-02653-3

Van Der Knaap, J. A., Kumar, B. R. P., Moshkin, Y. M., Langenberg, K., Krijgsveld, J., Heck, A. J. R., … Verrijzer, C. P. (2005). GMP synthetase stimulates histone H2B deubiquitylation by the epigenetic silencer USP7. *Molecular Cell*, *17*(5), 695–707. doi:10.1016/j.molcel.2005.02.013

Vasudevan, D., Chua, E. Y. D., & Davey, C. A. (2010). Crystal Structures of Nucleosome Core Particles Containing the '601' Strong Positioning Sequence. *Journal of Molecular Biology*, *403*(1), 1–10. doi:10.1016/j.jmb.2010.08.039

Wang, Y., Serricchio, M., Jauregui, M., Shanbhag, R., Stoltz, T., Di Paolo, C. T., … Angus McQuibban, G. (2015). Deubiquitinating enzymes regulate PARK2-mediated mitophagy. *Autophagy*, *11*(4), 595–606. doi:10.1080/15548627.2015.1034408

Wen, J., Arakawa, T., & Philo, J. S. (1996). Size-Exclusion Chromatography with On-Line Light-Scattering, Absorbance, and Refractive Index Detectors for Studying Proteins and Their Interactions. *Analytical Biochemistry*, *240*, 155–166. doi:10.1016/B978-0-12-805393-5.00010-5

Wienken, C. J., Baaske, P., Rothbauer, U., Braun, D., & Duhr, S. (2010). Protein-binding assays in biological liquids using microscale thermophoresis. *Nature Communications*, *1*, 100. Retrieved from http://dx.doi.org/10.1038/ncomms1093

Ye, Y., Scheel, H., Hofmann, K., & Komander, D. (2009). Dissection of USP catalytic domains reveals five common insertion points. *Molecular BioSystems*, *5*, 1797–1808. doi:10.1039/b907669g

551327-L-bw-Dharadhar
Processed on: 30-12-2020
PDF page: 68

551327-L-bw-Dharadhar
Processed on: 30-12-2020

CHAPTER 3

A Conserved Two-step Binding for the UAF1 Regulator to the USP12 Deubiquitinating Enzyme

Shreya Dharadhar[1], Marcello Clerici[1,2], Willem J. van Dijk[1], Alexander Fish[1], Titia K. Sixma[1]

[1]Division of Biochemistry and CGC.nl, Netherlands Cancer Institute, Plesmanlaan 121, 1066 CX Amsterdam, The Netherlands.
[2]Present address: Department of Biochemistry, University of Zürich, Winterthurerstrasse 190, 8057 Zürich, Switzerland.

Adapted from: J Struct Biol. 2016 Dec; 196(3):437-447

ABSTRACT

Regulation of deubiquitinating enzyme (DUB) activity is an essential step for proper function of cellular ubiquitin signals. UAF1 is a WD40 repeat protein, which binds and activates three important DUBs, USP1, USP12 and USP46. Here, we report the crystal structure of the USP12-Ub/UAF1 complex at a resolution of 2.8 Å and of UAF1 at 2.3 Å. In the complex we find two potential sites for UAF1 binding, analogous to what was seen in a USP46/UAF1 complex. In line with these observed dual binding states, we show here that USP12/UAF1 complex has 1:2 stoichiometry in solution, with a two-step binding at 4 nM and 325 nM respectively. Mutagenesis studies show that the finger sub-domain of USP12 interacts with UAF1 to form the high affinity interface. Our activation studies confirm that the high affinity binding is important for activation while the second UAF1 binding does affect activation. Nevertheless, we show that this two step binding is conserved in the well-studied USP12 paralog, USP1. Our results highlight the interfaces essential for regulation of USP12 activity and show a conserved second binding of UAF1 which could be important for regulatory functions independent of USP12 activity.

551327-L-bw-Dharadhar
Processed on: 30-12-2020
PDF page: 72

INTRODUCTION

Ubiquitination of proteins is a reversible post-translational modification that is critical for almost any cellular process. The control of these crucial pathways lies in the precise regulation of ubiquitinating and deubiquitinating enzymes (DUBs). DUBs are carefully regulated intra-cellular peptidases that cleave ubiquitin from target substrates. There are approximately 90 DUBs in the human genome, in 5 different families (Clague et al., 2013; Komander et al., 2009). The most abundant are the ubiquitin specific proteases (USPs) with 60 members that share a conserved USP catalytic domain, in which the ubiquitin core is held by the "fingers" while the catalytic centre lies between the "palm" and "thumb" subdomains. Despite this common catalytic core, the USP family members have many different modes of regulation (Sahtoe and Sixma, 2015).

Such regulation can take place in different ways and at different sites. USPs are regulated by changes in the catalytic domain, where the catalytic triad may be misarranged (Hu et al., 2002), via additional domains within the protein itself (Clerici et al., 2014; Faesen et al., 2011a), via post translational modifications (Nicassio et al., 2007), or by sub-cellular localization (Row et al., 2007). An interesting form of regulation is seen in a small sub-family of USPs, that includes USP1, USP12 and USP46. These three proteins are activated by complex formation with a WD40 repeat protein called UAF1 (USP1 associated factor, also known as WDR48) that leads to increased catalytic turnover for these enzymes (Cohn et al., 2007).

USP12 and USP46 are small proteins (370 and 366 residues respectively) with a highly conserved catalytic domain and high sequence similarity (88% identity). The related paralog USP1 (31% identity) is much larger (785 residues), due to additional inserts within its catalytic domain. The USP12/UAF1 and USP46/UAF1 complex can be further activated by binding to a second WD repeat protein, WDR20. This hyper-activation is not observed for the USP1/UAF1 complex (Kee et al., 2010). The lack of hyper-activation in USP1 could be due to the presence of the long inserts which might prevent it from interacting with WDR20. All three enzymes have low intrinsic activity in isolation and binding to UAF1 leads to activation which was shown to be due to an increase in k_{cat} with no drastic change in the K_M (Cohn et al., 2007; Faesen et al., 2011b; Villamil et al., 2012a). The exclusive k_{cat} activation is unusual for DUBs as most intermolecular activators (except GMPS) affect substrate binding (Faesen et al., 2011b).

The UAF1 regulation of this subfamily of DUBs has attracted considerable attention due to the biological importance of the enzymes involved. USP1 is important in DNA repair, where it acts on mono-ubiquitinated FANCD2 and PCNA in DNA cross-link repair and

551327-L-bw-Dharadhar
Processed on: 30-12-2020
PDF page: 73

DNA-damage avoidance pathways (Huang et al., 2006; Nijman et al., 2005). It is also found to deubiquitinate the ID family of transcriptional regulators (Williams et al., 2011). Due to these important functions, USP1 is considered a major possible drug target (Liang et al., 2014). USP46 plays important roles in neurobiology, as a small deletion mutation in USP46 leads to neurological effects in mice, including anxiety and changes in learning and memory (Imai et al., 2013; Zhang et al., 2011). The molecular basis for these effects is not yet clear. For USP12 several possible roles have been described. It is involved in stabilizing the Akt phosphatases resulting in decreased levels of pAkt (Gangula and Maddika, 2013). It has also been reported that USP12 and USP46 deubiquitinate histone H2A and H2B thereby playing a role in Xenopus development (Joo et al., 2011). Recently USP12 was shown to stabilize the T-cell receptor complex at the cell surface by deubiquitinating TCR adaptor proteins LAT and Trat1 (Jahan et al., 2016).

Several studies have tried to uncover the detailed mechanism of USP1/12/46 activation by UAF1 and also the interfaces involved in the formation of this complex. It was suggested that UAF1 binding modulates the active site conformation of USP1 resulting in a productive catalytic triad and also that phosphorylation of Ser313 is necessary for its interaction (Villamil et al., 2012a, 2012b). Other studies have shown that the regions in and around the finger domain of USP1 might be necessary for UAF1 binding (Olazabal-Herrero et al., 2015). Recently the crystal structure of the USP46-Ub and its complex with UAF1 were determined. In these structures two possible interfaces for UAF1 binding and activation were identified. The authors used mutational analysis to show that Interface 1 is critical for UAF1 binding and activation (Yin et al., 2015).

Here we present the structure of USP12-Ub/$UAF1_{580}$ complex which was solved at a resolution of 2.8 Å and compare it to the UAF1 structure alone. Intriguingly, we find that these structures resemble the USP46/UAF1 complex structure (Yin et al., 2015), including the presence of the second binding site. We then show that in solution USP12 can bind to a second molecule UAF1, but with lower affinity. We confirm for USP12 that Interface 1 at the fingers site is the high affinity interface while the second low affinity interface could be at the backside of the ubiquitin binding cleft. Moreover, mutagenesis studies suggest that the first binding event at the fingers is responsible for activation while the second binding does not influence activity.

MATERIALS AND METHODS

Plasmids and cloning

Human USP12, USP46, USP1 and UAF1 constructs were obtained from Martin Cohn. The USPs were cloned into pFastbac-HTb vector and UAF1 was cloned into pFastbac1

551327-L-bw-Dharadhar
Processed on: 30-12-2020
PDF page: 74

(N-terminal Strep tag) for insect cell expression. The sequence verified insert containing pFastbac vectors were transformed into DH10Bac cell for bacmid preparation. The recombinant bacmid was used for transfection of *Spodoptera frugiperda* (*sf*9) insect cells to produce the recombinant baculovirus. $USP12_{WT}$ (24-370) and USP46 (8-366) were also cloned into the pGEX and pET bacterial expression vectors of the NKI LIC suite, respectively (Luna-Vargas et al., 2011). All USP12 mutants were made using the QuikChange site directed mutagenesis method on pGEX USP12 bacterial construct.

Protein expression and purification

N-terminal His-tagged USP1 (21-785) and $USP12_{FL}$ were expressed using Baculovirus expression in *sf*9 insect cells. After 72 hours of infection the cells were harvested in 20 mM Tris (pH 8.0) + 200 mM NaCl + 2 mM TCEP + protease inhibitor (lysis buffer) and lysed by sonication. The lysed cells were spun down (21000 rpm for 1 hour) and the lysate was loaded on a His-affinity column (GE, USA). The column was washed with lysis buffer supplemented with 50mM Imidazole (pH 8.0) followed by elution with lysis buffer supplemented with 500 mM imidazole. The His-USP1 elution fractions were concentrated and loaded on a size exclusion chromatography column (Superdex 200, GE, USA) equilibrated in GF buffer (20 mM HEPES (pH 7.5) + 150 mM NaCl + 2 mM DTT) following which the protein fractions were concentrated upto 4.5 mg/ml and stored in -80ºC. The $USP12_{FL}$ and $USP46_{FL}$ fractions were incubated with TEV protease and dialyzed overnight in lysis buffer without imidazole. The dialysed protein sample was then loaded on a His-affinity column where the protein was obtained in the wash fractions. The protein containing fractions were then concentrated and loaded on a size exclusion chromatography column (Superdex 200, GE, USA) equilibrated in GF buffer following which protein fractions were concentrated upto 6 mg/ml and stored in -80ºC.

N-terminal GST-tagged $USP12_{WT}$ and mutants were expressed in *E. coli*. The cells were induced with 0.2 mM IPTG at 18ºC for 10-12 hours followed by which they were harvested in lysis buffer and lysed by sonication. The lysate was loaded on a GST-affinity column and washed with lysis buffer followed by elution with lysis buffer supplemented with 20 mM Glutathione. The protein containing fractions were then concentrated and loaded on a size exclusion chromatography column (Superdex 200, GE, USA) equilibrated in GF buffer following which protein fractions were concentrated upto 15 mg/ml and stored in -80ºC.

N-terminal His-tagged USP46 (8-366) was expressed in *E.coli*. The cells were induced with 0.5 mM IPTG at 20ºC for ~16hrs followed by which they were harvested in 20 mM Tris (pH 7.5), 150 mM NaCl, 10 mM Imidazole (pH 8.0) and 5 mM beta-mercaptoethanol

551327-L-bw-Dharadhar
Processed on: 30-12-2020
PDF page: 75

(lysis buffer) and lysed by sonication. The lysate was loaded on a Ni-affinity column and washed with lysis buffer supplemented with 50 mM imidazole followed by elution with lysis buffer supplemented with 500 mM imidazole. USP46 was incubated with TEV protease and dialysed overnight in lysis buffer without imidazole. The dialysed protein sample was then loaded on a His-affinity column where the protein was obtained in the wash fractions. USP46 was loaded on a size exclusion chromatography column (Superdex 200, GE, USA) equilibrated with 20 mM Tris (pH 7.5), 150 mM NaCl and 2 mM DTT.

$UAF1_{FL}$ and $UAF1_{580}$ were also purified from *sf*9 insect cells and were lysed in similar conditions as the USP purifications. The UAF1 lysates were loaded on a Strep-affinity column (IBA life sciences) and washed with 50 mM Tris (pH 8.0) + 150 mM NaCl + 2 mM TCEP (wash buffer). The strep-UAF1 protein was then eluted using wash buffer supplemented with 2.5 mM Desthiobiotin. The protein containing fractions were concentrated and loaded on a size exclusion chromatography column (Superdex 200, GE, USA) equilibrated in GF buffer. The fractions corresponding to the peak were collected. UAF1 samples were treated with 10 mM iodoacetamide to prevent background DUB activity due to minute amounts of co-purified insect cell DUBs. Following iodoacetamide treatment the protein fractions were re-purified using size exclusion chromatography (Superdex 200, GE, USA). The protein fractions were then concentrated up to 10 mg/ml and stored in -80ºC.

The USP/UAF1 complexes were co-expressed in baculovirus infected *sf*9 insect cells. USP/UAF1 complexes were purified by first carrying out a His-affinity purification followed by Strep-tag (IBA life Sciences) affinity purification as described above. The protein fractions were then concentrated and loaded on a size exclusion chromatography (Superdex S200, GE, USA) equilibrated in GF buffer. The protein containing fractions were concentrated upto 5 mg/ml and stored at -80ºC.

Covalent complexes of USP46 and $USP12_{FL}/UAF1_{580}$ with Ub-VME and Ub-PRG respectively were generated under reducing conditions at 4ºC for 12-16 hrs. The USP46 reaction was very slow and only 50% of the enzyme reacted to Ub-VME whereas approximately 80% of the $USP12_{FL}/UAF1_{580}$ complex reacted to the Ub-PRG probe. The reacted USPs were then purified from the excess probe by using a size exclusion chromatography column (Superdex 200, GE, USA) equilibrated in GF buffer. The purified USP-Ub complex was then concentrated and stored at -80ºC.

551327-L-bw-Dharadhar
Processed on: 30-12-2020
PDF page: 76

Crystallization and structure determination

USP12 and UAF1 crystals were obtained by sitting drop vapour diffusion experiment at 20°C using equal ratio of protein and mother liquor solution. $UAF1_{580}$ was setup for crystallization at 8 mg/ml and crystals were obtained in 20% PEG3350, 200 mM Tri-Sodium Citrate, Bis-Tris Propane pH 6.5. $USP12_{FL}$-Ub-PRG/$UAF1_{580}$ was setup at 5 mg/ml and crystals were obtained in 3.2% PEG4000, 0.1 mM MMT pH 6.5 and 0.1 mM TCEP. The crystals were cryo-protected by brief washing in mother liquor solution with 30% glycerol prior to flash freezing in liquid nitrogen. Diffraction data was collected at the Swiss Light Source beamline PXIII at 100K.

USP46-Ub-VME at 8 mg/ml was set up for crystallization by sitting drop vapour diffusion experiment at 20°C. Crystals were obtained in 0.96 M Sodium Citrate pH 7.5 and 0.1 mM $ZnCl_2$ with protein: precipitant ratio 1.5 : 1. The crystals were cryo-protected by brief washing in mother liquor solution with 20% glycerol prior to flash freezing in liquid nitrogen. Diffraction data was collected at the European Synchrotron Radiation Facility (ESRF) beamline ID14-1 at 100K.

Crystallographic data were processed with XDS (Kabsch, 2010) or iMOSFLM (Battye et al., 2011) and scaled using XSCALE (Kabsch, 2010) or Aimless from the CCP4 suite (Winn et al., 2011). The USP46-Ub-VME structure was solved by molecular replacement using the USP2-Ub model (PDB 2IBI) in Phaser (McCoy et al., 2007) followed by automated model building using ARP/WARP (Langer et al., 2008).The UAF1 (9-580) structure was solved by molecular replacement (PDB-1VYH) in Phaser (McCoy et al., 2007) followed by automated model building using ARP/Warp (Langer et al., 2008). The $USP12_{FL}$-Ub/$UAF1_{580}$ structure was solved by molecular replacement using the USP46, $UAF1_{580}$ and ubiquitin structures as search models in Phaser. All structures were refined by Phenix (Adams et al., 2010), autoBUSTER (Smart et al., 2012), Refmac (Murshudov et al., 1997), PDB_REDO (Joosten et al., 2014) and models were built using COOT (Emsley et al., 2010). Interface analysis was performed with PISA (Krissinel and Henrick, 2007). All structure figures were generated using PyMOL (Schrödinger, LLC).

Size exclusion chromatography Multi Angle Laser Light Scattering (SEC-MALLS)

The SEC-MALLS experiments were performed using the miniDawn Tristar light scattering detector (Wyatt technologies, USA) in line with size exclusion chromatography. After equilibration of the Superdex 200 10/300 GL and the Superose 6 increase 10/300 GL (GE, USA) in buffer containing 20 mM HEPES (pH 7.5), 150 mM NaCl, 2 mM DTT, the $USP12_{FL}$-Ub/$UAF1_{580}$ (8 µM) and the USP1/$UAF1_{FL}$ complex (6 µM) were loaded on the

551327-L-bw-Dharadhar
Processed on: 30-12-2020
PDF page: 77

Superdex 200 10/300 GL while the $USP12_{FL}$-Ub/$UAF1_{FL}$ sample (42 µM) was loaded on the Superose 6 increase 10/300 GL (GE, USA). Molecular weight estimation was done by using the refractive index signal as measure of the concentration with the Astra software (Wyatt Technologies, USA).

Size exclusion chromatography - Small Angle X-ray Scattering (SEC-SAXS)

$USP12_{FL}$-Ub/$UAF1_{FL}$ purified from insect cells was concentrated upto 38 µM. The buffer used for the size exclusion chromatography was also used for SEC-SAXS experiment on the BM29 SAXS beamline at the ESRF. Following equilibration, 30 µl of the purified $USP12_{FL}$-Ub/$UAF1_{FL}$ was loaded on the Superdex 200 5/150 GL (GE, USA) and 1500 successive 1 s frames were collected through the protein elution peak. The data were normalized to the intensity of the transmitted beam and radially averaged; the scattering of the solvent-blank (derived from the buffer run) was subtracted. Data were analysed using the ATSAS software package (Svergun et al., 2001). A moving set of 10 or 20 frames was analysed across the high-intensity peak to estimate molecular weight from various methods (DATPOROD (Konarev et al., 2006), excluded volume from DAMMIF model (Franke and Svergun, 2009) and SAXS MoW2 (Fischer et al., 2010)) and fit the data to the crystallographic structures in CRYSOL (Svergun et al., 1995). Frames prior to 670 and frames latter than 910 were considered too noisy or weak for analysis. OLIGOMER (Konarev et al., 2003) was used to perform a fit to the experimental curve from different possible models of the complex and determine volume fractions of each component. Several OLIGOMER runs were performed using the 2:1 complex, both 1:1 complexes and UAF1 alone as models in different combinations.

Ub-Rhodamine enzymatic assays

Enzymatic activity was followed as release of fluorescent rhodamine from the quenched Ub-Rho substrate, providing a direct readout for DUB activity. The fluorescent intensity was measured using Pherastar plate reader (BMG LABTECH GmbH, Germany). Activity of $USP12_{WT}$ at varying concentrations of $UAF1_{FL}$ (20-1250 nM) was tested at 100 nM of $USP12_{WT}$ and at a single substrate concentration of 1 µM. Activity was quantified by calculating the initial rates and plotted as a function of $UAF1_{FL}$ concentration. 100 nM of enzyme was used against different concentrations of the minimal substrate (32 µM to 0.25 µM) for the Michaelis Menten analysis. The initial rates were then plotted against substrate concentration and fitted with a Michaelis Menten model using non-linear regression in GraphPad Prism 6 software (GraphPad Software Inc, USA).

551327-L-bw-Dharadhar
Processed on: 30-12-2020
PDF page: 78

Binding assays

Surface Plasmon Resonance experiments were carried out to test binding of His-USP1 and Gst-USP12$_{WT}$ to UAF1$_{FL}$ in the Biacore T200 system (GE, USA). The SPR buffer for Gst-USP12$_{WT}$ and mutants consisted of 20 mM HEPES 7.5, 150 mM NaCl, 20% glycerol, 0.05% Tween-20, 2 mM TCEP (Tris (2-carboxyethyl) phosphine hydrochloride) and 1 mg/ml dextran. The SPR buffer for His-USP1 had 300 mM NaCl to neutralize any unspecific interaction with Ni on the chip surface and the rest of the components were identical. The Gst-USP12 was immobilized via goat anti-GST antibody that was pre immobilized to the CM5 chip using amine coupling. The His-USP1 was directly immobilized to the surface of NTA chip via His-tag. The binding experiments were carried out in the single cycle kinetics mode with 5 sequential injection of UAF1$_{FL}$ in each cycle. An initial experiment with 5 injections from 1 nM to 10 µM and a more detailed assay with 15 injections from 0.56 nM to 2.56 µM were carried out. Data from a reference flow cell, run in parallel with an empty chip (in case of NTA immobilization) or with GST (in case of anti-GST immobilization) were subtracted from the signal using the Biacore T200 Evaluation Software. Final analysis and the figures were done using GraphPad Prism 6 (GraphPad Software Inc, USA).

RESULTS

Crystal structures of USP46, UAF1$_{580}$ and USP12$_{FL}$-Ub/UAF1$_{580}$ complex

To study how the regulator UAF1 modulates the activity of USPs, we purified the human USP46, human USP12 and several constructs of the human UAF1. We refer to UAF1 (9-580) as UAF1$_{580}$ and to UAF1 (9-677) as UAF1$_{FL}$ (Fig.1a). By reaction of USP46 and USP12 with suicide inhibitors of ubiquitin, Ub-VME and Ub-PRG respectively, we could create covalently linked USP-Ub complexes, which were used for crystallization attempts.

We generated well diffracting crystals for USP46-Ub (1.85 Å), USP12$_{FL}$-Ub/UAF1$_{580}$ (2.8 Å) and UAF1$_{580}$ (2.3 Å). All three crystal structures were solved by molecular replacement where the covalent USP2-Ub complex model (2IBI) was used for the USP46-Ub structure and the protein PAF-AH (1VYH) was used as a model for UAF1$_{580}$. The resulting structures of USP46-Ub and UAF1$_{580}$ were used as models for the USP12$_{FL}$-Ub/UAF1$_{580}$ complex. All three structures were refined to acceptable R-factors and good geometry (Table.1).

The crystal structure of USP46-Ub reveals the canonical USP domain with a catalytic centre in the catalytically proficient state (Fig.1b). The crystallization contained only 50% of the Ub-bound form, but the crystal was fully modified, indicating a preferential crystallization of the ubiquitin-bound form. This structure is in good agreement with the

551327-L-bw-Dharadhar
Processed on: 30-12-2020
PDF page: 79

recently published structure of USP46 ((5CVM), RMSd on 308 C_α: 0.3 Å).The structure of $UAF1_{580}$ forms a 7 bladed β-propeller with an ancillary domain (Fig.1c), although

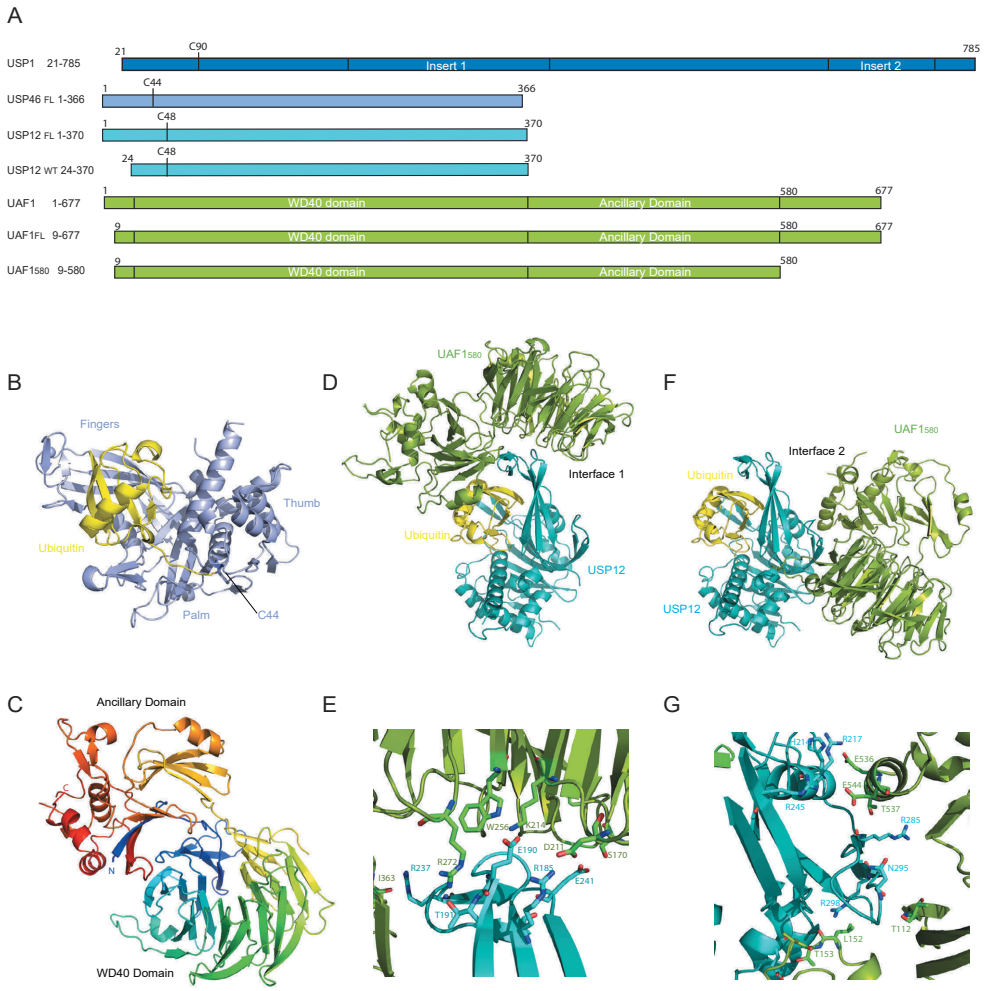

Fig.1 - Crystal structure analysis shows two possible binding options for USP12.
A) Constructs used for the present study. **B)** Crystal structure of USP46-Ub-VME in cartoon representation. **C)** Crystal structure of $UAF1_{580}$ coloured in a rainbow representation. **D)** Crystal structure of $USP12_{FL}$-Ub/$UAF1_{580}$ showing $UAF1_{580}$ bound to Interface 1.) **E)** Zoomed Interface 1 between $UAF1_{580}$ and $USP12_{FL}$-Ub showing the interface residues. **F)** Crystal structure of $USP12_{FL}$-Ub/ $UAF1_{580}$ showing $UAF1_{580}$ bound to Interface 2. **G)** Zoomed Interface 2 between $UAF1_{580}$ and $USP12_{FL}$-Ub showing the interface residues. (Colours in panel B,D-G: Ub in yellow, other proteins as in A).

WD40 domain predictions obtained from the protein sequence predicted 8 blades. The first N-terminal residues (13-24) are present in the ancillary domain and the following residues from 25-360 form the 7 bladed β-propeller. The predicted eighth blade (361-

400) forms the expected 4-stranded sheet but is located in the ancillary domain where it sits on top of a β sheet in which the N-terminal residues form an integral part. The $UAF1_{580}$ structure is very similar to the recently published structure of UAF1 ((5CVL), RMSd on 517 C_α: 1.2 Å).

In the crystal lattice of the $USP12_{FL}$-Ub/$UAF1_{580}$ complex, the asymmetric unit contains one molecule of USP12 and one molecule of UAF1. However, USP12 makes two possible interfaces with UAF1 in these crystals, one on the fingers sub-domain (Interface 1) (Fig.1d,e) and the other on the backside of the ubiquitin binding cleft (Interface 2) (Fig.1f,g). The interactions in Interface 1 are dominated by hydrophilic and charged interactions, with 794 $Å^2$ and 698 $Å^2$ buried surface area on USP12 and $UAF1_{580}$ respectively (Fig.1e). The Interface 2 is mostly hydrophobic and buries a surface area of 1030 $Å^2$ and 1111 $Å^2$ on USP12 and $UAF1_{580}$ respectively (Fig.1g). Intriguingly the same crystal packing was seen for the USP46/UAF1 complex (PDB code: 5CVN) that was published during the refinement of our structures (Yin et al., 2015). In that publication the authors confirmed by mutational analysis that Interface 1 is the relevant interface for activation. USP46/UAF1 was crystallized in the same space group, with similar cell dimensions, which is not surprising since USP12 and USP46 have 88% sequence similarity, although neither interface is fully conserved. A second crystal form for USP46/$UAF1_{FL}$ was determined in a different crystal lattice (C2), with different packing, but even in this crystal lattice, the USP still has maintained both interfaces (PDB code: 5CVO). The striking similarity and conservation of these two USP/UAF1 interfaces among three different crystal structures suggested that this was not due to a crystal packing artefact and further analysis of the second interface would be worthwhile (Supp.Fig.1a).

A superposition of our USP46 structure on USP12 in complex with $UAF1_{580}$ revealed no significant conformational change in the USP moiety (RMSd on 309 C_α: 0.9 Å). When the UAF1 moieties are compared by superposition of the $UAF1_{580}$ onto the $USP12_{FL}$-Ub/$UAF1_{580}$ complex, no conformational change is observed in $UAF1_{580}$ close to Interface 1 (Supp.Fig.1b), whereas a large shift is observed in the extended loop of blade 3, the region where $UAF1_{580}$ forms Interface 2 (Supp.Fig.1c). This conformational change due to interaction of $UAF1_{580}$ at Interface 2 is also observed in the USP46/UAF1 structure upon UAF1 binding (Yin et al., 2015). Since the conformational change as well as the presence of two UAF1 interfaces seems to be conserved between USP46 and USP12, we wondered what stoichiometry the USP12/UAF1 complex has in solution.

551327-L-bw-Dharadhar
Processed on: 30-12-2020
PDF page: 81

Table 1. Crystallography Details

Data Collection			
	USP46-UbVME	$UAF1_{580}$	USP12-UbPRG/$UAF1_{580}$
Wavelength (Å)	0.93	0.92	1.00
Resolution (Å)	28.41-1.85 (1.90-1.85)	48.97-2.30 (2.35-2.30)	47.41-2.79 (2.92-2.79)
Space Group	C 2 2 21	P 2 21 21	I 2 2 2
Unit Cell a, b , c (Å)	91.95 104.66 135.31	73.30 131.60 148.67	103.68 152.82 182.93
$CC_{1/2}$	0.999 (0.720)*	0.999 (0.585)	0.995 (0.638)
R_{merge}	0.12 (0.84)	0.05 (1.0)	0.08 (0.72)
R_{pim}		0.04 (0.84)	0.06 (0.57)
I/σI	17.68 (2.0)	16.1 (1.4)	10.4 (1.6)
Completeness (%)	98.8 (99.7)	99.6 (95.9)	99.3 (94.8)
Redundancy	3.56 (3.3)	4.5 (4.1)	4.5 (4.3)
Refinement			
Unique Reflections (nr)	55291	64580	36148
Atoms total (nr)	3442	8586	7290
Protein atoms (nr)	3192	8195	7266
Solvent atoms (nr)	250	391	24
B-factors	31.9	58.3	72.4
TLS groups	4	4	4
R_{work}/R_{free} (%)	16.6/19.4	18.5/22.4	20.8/25.9
Rmsd bond lengths (Å)	0.017	0.007	0.014
Rmsd bond angles (º)	1.758	1.235	1.642
Ramachandran (%) Preferred/ outliers	97.89/0	97.27/0.30	95.5/0.34
Molprobity score	1.01	0.82	1.77
PDB code	5L8H	5L8E	5L8W

High Resolution shell in parentheses; (*- Reprocessed with aimless)

551327-L-bw-Dharadhar
Processed on: 30-12-2020
PDF page: 82

The USP12/UAF1 complex has 1:2 stoichiometry

To study relative amounts of USP12 and UAF1 in solution we carried out size exclusion chromatography coupled with multi-angle laser scattering (SEC-MALLS) of the purified $USP12_{FL}$-Ub/$UAF1_{580}$ complex which was used for obtaining the crystal structure. The molecular weight obtained from the MALLS experiment was approximately 166 KDa which is much closer to the calculated mass for 1:2 complex (180 KDa) than for a 1:1 complex (115 KDa). The calculated molecular weight was not constant within the peak, which suggests a dynamic equilibrium between the 1:2 and 1:1 complexes (Fig.2a).

Next, we carried out small angle X-ray scattering (SAXS) experiments coupled to size exclusion chromatography. At the high concentration necessary for SAXS experiments higher order species are observed (Fig.2b). The purified complex of $USP12_{FL}$ with covalently bound Ub-PRG and $UAF1_{FL}$ was used for these experiments. Frames corresponding to the different parts of the peak were averaged and analysed separately (Supp.Fig.1d). Molecular weight estimation of the data (898-909) from the latter half of the peak was consistent, when carried out using different methods (Porod volume (Konarev et al., 2006), excluded volume from DAMMIF model (Franke and Svergun, 2009), and SAXS MoW2 (Fischer et al., 2010)), where we observed that $USP12_{FL}$-Ub/$UAF1_{FL}$ has a molecular weight of 190 KDa corresponding to a 1:2 stoichiometry of the complex. Additionally, Porod analysis of the frames in the early half of the peak corresponded to a molecular weight of 390 KDa indicating formation of high molecular weight species which fits well with the MALLS data (Fig.2b).

Moreover, we compared the experimental SAXS profile of frames (898-909) with calculated scattering curves based on the crystal structure either with one $UAF1_{FL}$ bound (in either of the two sites), or with two $UAF1_{FL}$ molecules bound. We obtained a much worse fit with the 1:1 profile (Fig.2c,e) compared to the possible 1:2 profile (Fig.2d). To further analyze these data, we tested whether the OLIGOMER algorithm would change the fit. Other possible options did not improve the fit, but when testing for the 1:2 profile, we found an improved fit (Fig.2f) with volume fractions of 81% for the 1:2 complex (81%) and a smaller fraction for $UAF1_{FL}$ (19%). In principle such a fraction was expected to be a mixture of the 1:1 complex and $UAF1_{FL}$. It is possible that the computational analysis selects against this complex mixture when fractions are small.

551327-L-bw-Dharadhar
Processed on: 30-12-2020
PDF page: 83

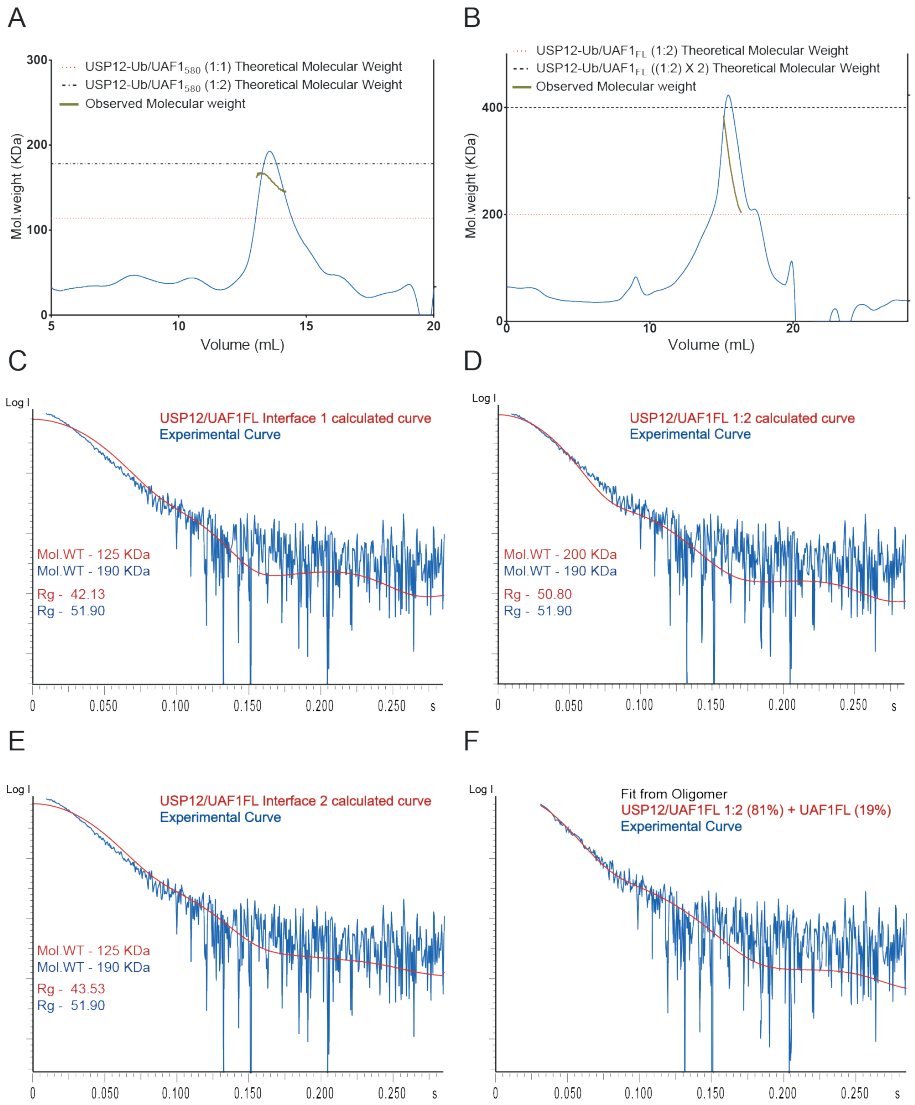

Fig.2 - USP12/UAF1 has 1:2 stoichiometry.
A) SEC-MALLS analysis of $USP12_{FL}$-Ub/$UAF1_{580}$ (8 µM) shows a molecular weight corresponding to a 1:2 complex. **B)** SEC-MALLS analysis of $USP12_{FL}$-Ub/$UAF1_{FL}$ at high concentration (42 µM) shows a dynamic equilibrium between high molecular weight species and the 1:2 complex in agreement with the SAXS data. **C,D,E)** Experimental SEC-SAXS curve of $USP12_{FL}$-Ub/$UAF1_{FL}$ fits better with the scattering curve based on the structure of the 1:2 complex as compared to the 1:1 complex at either of the two interfaces. **F)** OLIGOMER fit of the Experimental SEC-SAXS curve of $USP12_{FL}$-Ub/$UAF1_{FL}$.

551327-L-bw-Dharadhar
Processed on: 30-12-2020
PDF page: 84

UAF1 binds USP12 in two distinct steps with different affinities

We investigated if the two binding events indicative of the 1:2 stoichiometry could be observed in an *in-vitro* binding experiment. Therefore, we analysed the binding of $UAF1_{FL}$ to GST-$USP12_{WT}$ by surface plasmon resonance (SPR) and indeed observed two distinct binding events (Fig.3a). We found a high-affinity binding (K_d = 4 nM) with an extremely low off-rate, which saturated at 100 nM. Moreover, when we added higher concentrations of $UAF1_{FL}$, a second binding event could be observed (K_d =325 nM) (Fig.3b) with faster binding and dissociation. In conclusion, we observed two binding events for $UAF1_{FL}$ binding to $USP12_{WT}$ with different binding characteristics.

Table 2. Michaelis Menten analysis of $USP12_{WT}$ with UAF1

Protein	K_{cat} (x $10^{-2} s^{-1}$)	K_M (µM)	K_{cat}/K_M ($M^{-1} s^{-1}$)
$USP12_{WT}$(100 nM)	0.076	50	0.15 x 10^2
$USP12_{WT}$+UAF1(100 nM)	2.6	50	5.20 x 10^2
$USP12_{WT}$+UAF1(1250 nM)	3.3	64	5.15 x 10^2

We tested which of these events contributed to activation. We performed an enzymatic assay against the minimal substrate ubiquitin rhodamine (Ub-Rho), as a function of activator concentration. We could see a clear activation that correlates with the high-affinity binding site. In contrast, the second binding event does not affect the activation status, as no further activation is observed when the $UAF1_{FL}$ binds the second site (Fig.3c,d). We then performed a kinetic analysis of USP12 activity, either at equal concentration to UAF1 (1:1) or when an excess of UAF1 is present (Fig.3e). The Michaelis Menten parameters K_{cat} and K_M did not change with higher UAF1 concentration, confirming that only Interface 1 is important for UAF1 mediated USP12 activation (Table 2).

The Finger sub-domain in USP12 is crucial for binding and activation by UAF1

We validated the role of Interface 1 by making a series of mutations. In line with their role in the USP46/ UAF1 interface (Yin et al., 2015), a triple mutant made on UAF1 ($UAF1_{3X}$ =K214E+W256A+R272D) and a reciprocal mutant (E190K) on USP12 interfered with high affinity binding (Fig.4a,b). The high affinity binding could be partially rescued by combining the $USP12_{E190K}$ with the $UAF1_{3X}$ mutant, in a similar fashion to what was observed for USP46 and UAF1 binding (Fig.4c)(Yin et al., 2015). Additionally, the binding of the $USP12_{E190K}$ to the low affinity site remained unchanged. On comparing the binding characteristics of these mutants with $USP12_{WT}$, we noted that the $UAF1_{3X}$ mutant only

551327-L-bw-Dharadhar
Processed on: 30-12-2020
PDF page: 85

binds at very high concentrations and does not release easily, while the $USP12_{E190K}$ mutant binds with a fast release (Fig.4a). We also made a series of mutations at Interface 2 on $USP12_{WT}$, by either reversing charges (R217D or R285E) or changing the hydrophobic interface (F287A) but none of them could disrupt binding of UAF1 to this site (Fig.4g,h).

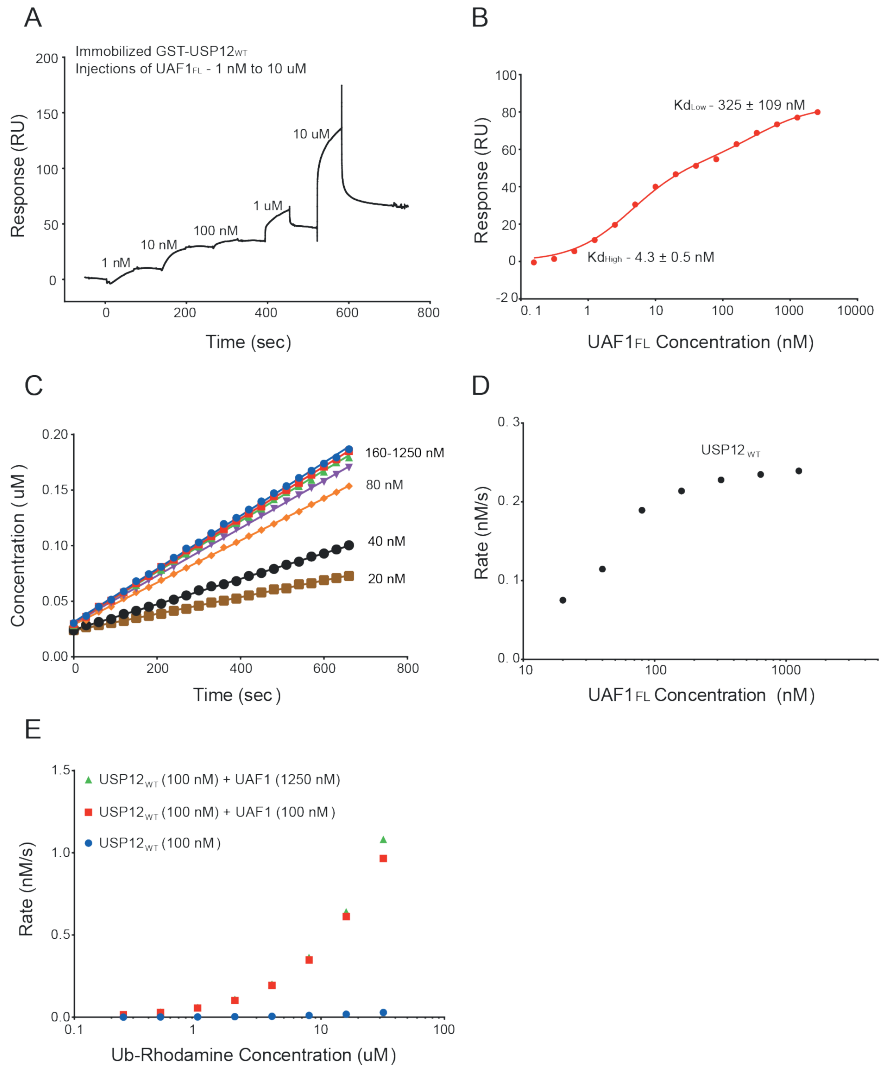

Fig.3 - UAF1 binds USP12 in two steps with different affinities.
A) Qualitative SPR analysis of five successive injections of $UAF1_{FL}$ on immobilized $USP12_{WT}$, raw data show how initial injections show slow kinetics, and binding at higher concentrations displays fast off-rates. **B)** Fitting quantitative SPR analysis of $UAF1_{FL}$ to $USP12_{WT}$, obtained from 15 successive injections of $UAF1_{FL}$. Curve is fit to a two-step binding model with K_D as indicated. **C)** Cleavage of Ub-Rhodamine by $USP12_{WT}$ at different concentrations of $UAF1_{FL}$(10 nM-1250 nM). **D)** Initial rates of $USP12_{WT}$ plotted as a function of $UAF1_{FL}$ concentration shows the importance of high affinity site for activation. **E)** Michaelis Menten analysis of $USP12_{WT}$ (100 nM) alone and in two different concentrations of $UAF1_{FL}$ (100 nM, 1250 nM) shows that the second binding of UAF1 leads to no further activation.

551327-L-bw-Dharadhar
Processed on: 30-12-2020
PDF page: 86

We then carried out an *in-vitro* Ub-Rho assay to analyse the effects of these mutations on USP12 activation and compare it with previously published findings for USP46 (Yin et al., 2015). Wild type UAF1 was unable to activate $USP12_{E190K}$ to similar levels as compared to $USP12_{WT}$ (Fig.4d,e) and similarly, the $UAF1_{3X}$ mutant did no longer activate. However, as shown previously for USP46/UAF1 (Yin et al., 2015), the combination of these complementary mutants rescues the activation (Fig.4f), highlighting the importance of the finger sub domain in USP12 and USP46 (Yin et al., 2015) activation by UAF1.

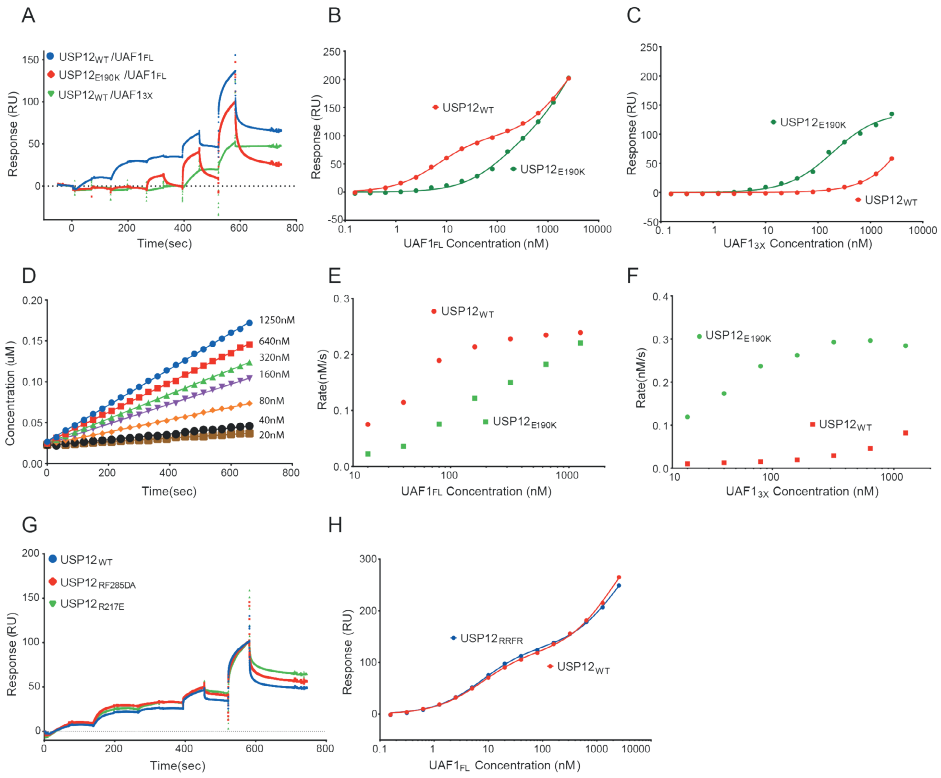

Fig.4 - Interface 1 is the high affinity site and is responsible for activation by UAF1
A) Comparing Qualitative SPR analysis of five successive injections of $UAF1_{FL}$ and $UAF1_{3X}$ on immobilized US-$P12_{WT}$ and $USP12_{E190K}$ shows differences in binding characteristics. **B)** Semi-quantitative SPR analysis of $UAF1_{FL}$ to $USP12_{WT}$ and $USP12_{E190K}$ mutant highlights weaker binding of the mutant to the high affinity interface. **C)** Semi-quantitative SPR analysis of $UAF1_{3X}$ to $USP12_{WT}$ and $USP12_{E190K}$, curves show disruption of binding in $USP12_{WT}$ which is rescued by the $USP12_{E190K}$ mutant. **D)** Cleavage of Ub-Rhodamine by $USP12_{E190K}$ at different concentrations of $UAF1_{FL}$ shows loss in activation by $UAF1_{FL}$. **E)** Comparison of initial rates of $USP12_{WT}$ and $USP12_{E190K}$ at different $UAF1_{FL}$ concentrations shows that when high affinity interaction is lost the activity is impaired. **F)** Comparison of initial rates of $USP12_{WT}$ and $USP12_{E190K}$ at different concentrations of $UAF1_{3X}$ shows the rescue of activation by the $USP12_{E190K}$ mutant. **G)** Comparing Qualitative SPR analysis of five successive injections of $UAF1_{FL}$ on immobilized $USP12_{WT}$ and USP12 interface 2 mutants shows no significant change in binding characteristics. **H)** Semi-quantitative SPR analysis of $UAF1_{FL}$ to Interface 2 mutant $USP12_{RRFR}$ and $USP12_{WT}$ shows identical binding.

551327-L-bw-Dharadhar
Processed on: 30-12-2020

The two-step binding is conserved in USP1

Some aspects of USP1 regulation are different from the USP12 and USP46, as USP1 is a much larger enzyme, and it cannot be hyper-activated by WDR20. We therefore wondered whether the 1:2 stoichiometry is also conserved in this important DNA repair enzyme. We carried out SEC-MALLS of the purified USP1/UAF1 complex and the molecular weight obtained was approximately 220 KDa which closely corresponds to the 1:2 complex (235 KDa) rather than a 1:1 complex (160 KDa). Similar to the USP12/UAF1 MALLS data (Fig.2a), the molecular weight was not constant within the peak suggesting a dynamic equilibrium between the two states of the complex (Fig.5a). We then performed the UAF1 binding assay with His-USP1 on the SPR chip (Fig.5b, c). Again, we observed a two-step binding, and although the high RU values for the second step suggests an additional unexplained background process, the fitting identified similar affinities for USP1 to those observed for USP12. Thus from our SPR result in addition to the MALLS data, we could confirm the presence of this unusual regulatory step in USP1.

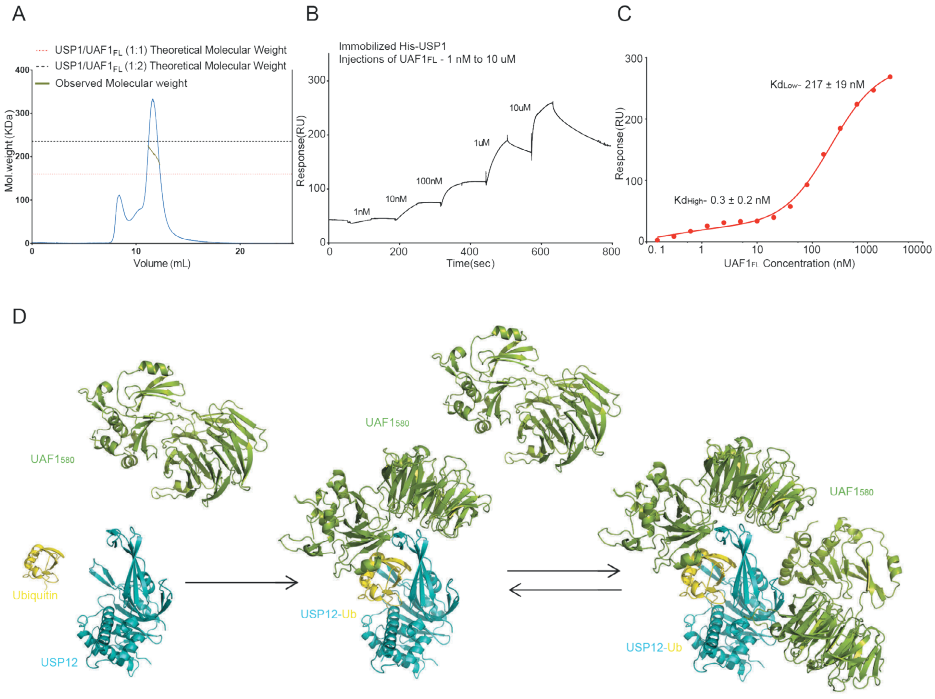

Fig.5 - The two step UAF1 binding is conserved in USP1.
A) SEC-MALLS analysis of USP1/UAF1$_{FL}$ (6 μM) shows a molecular weight corresponding to the 1:2 complex. **B)** Qualitative SPR analysis shows that USP1 has conserved the two-step binding to UAF1$_{FL}$, with similar kinetics. **C)** Fitting of quantitative SPR analysis of UAF1$_{FL}$ to USP1 obtained from 15 successive injections of UAF1$_{FL}$ to quantify the K_D values. Curve is fit to a two-step binding model with affinities as indicated. **D)** UAF1 binds USP12 at the fingers sub-domain which activates USP12 and then UAF1 also binds on the backside of the ubiquitin binding cleft.

551327-L-bw-Dharadhar
Processed on: 30-12-2020
PDF page: 88

DISCUSSION AND CONCLUSIONS

Here we present a series of structures that contribute to the understanding of regulation of DUBs by non-substrate partners. In our analysis we identified two possible binding sites for UAF1 on USP12-Ub (Fig.5d), that are conserved from USP46. The two UAF1 binding sites are distant from the catalytic centre and binding of UAF1 did not induce significant rearrangements in the USP structure. Thus it is very hard to envision from these structures how USP12 is activated by UAF1, especially when the activation is due to an increase in k_{cat} and not K_M. It is possible that UAF1 binding stabilizes the flexible USP12 "finger", transforming it into a catalytically proficient state and this may not be visible since we compare it to a ubiquitin-bound USP structure. Therefore an apo-structure of USP12 could shed more light on this issue.

The binding analysis shows that Interface 1 provides the high affinity interaction that is responsible for the activation of the USP. We measure a binding affinity in the order of 4 nM with extremely slow dissociation. The affinity is less tight than the 0.1 nM observed for USP46 by Yin et al, 2015, most likely due to differences in the experimental setup. Their lowest concentration of UAF1 used was far above the reported K_D (7-fold), and the K_D was estimated based on very slow dissociation constant derived from the global kinetic fit. Overall, the structure of USP12-Ub/$UAF1_{580}$ and the UAF1 mediated activation through Interface 1 bears close resemblance to the published data on USP46 (Yin et al., 2015), again highlighting the high degree of conservation between these USPs. The Interface 1 has a relatively small surface area, with a predominance of charged interactions. For such a small interface, even the observed affinity of 4 nM is rather surprising since such strong binding between two proteins is rarely mediated by interfaces having less than 1000 $Å^2$ buried surface area (Chen et al., 2013). However, previous reports have suggested the importance of the finger domain for UAF1 binding and activation (Olazabal-Herrero et al., 2015). It is still unclear how S313 phosphorylation which is present in the long insert of USP1 could play a role in UAF1 binding (Villamil et al., 2012b), as the (shorter) corresponding region on USP12 is not involved in UAF1 binding for either of the interfaces.

In the USP12/$UAF1_{580}$ complex we observe a conserved second interface (Interface 2) at the backside of the ubiquitin binding cleft. The buried surface area of this interface is larger than for Interface 1, and the contact is more hydrophobic, indicating that its properties are very different. Our binding data confirm the presence of a secondary interaction, with an affinity of ~300 nM and fast kinetics. Unfortunately we were unable to validate this interface by mutational analysis. It is possible that this is due to the large surface area involved in this binding. Additionally the surface shape complementarity

551327-L-bw-Dharadhar
Processed on: 30-12-2020
PDF page: 89

between the extended loop in USP12 and the relatively concave architecture of ancillary domain and β-propeller in the UAF1 molecule could contribute to the interaction primarily by backbone interactions.

The two binding interfaces on UAF1 seem independent of each other as they reside in distant parts of the protein. Thus mutating residues on Interface 1 is unlikely to affect binding to Interface 2 or vice-versa. Our binding studies with the $UAF1_{3X}$ mutant showed binding to the high affinity site at very high concentrations and no binding to the low affinity site. This could mean that UAF1 can only bind the low affinity site once the high affinity site has been fully occupied. It is possible that high overall flexibility in USP12 in the unbound state prevents binding to the low affinity site, thereby making the high affinity binding mandatory for binding the second UAF1.

During revision of this manuscript, a structure for the USP12/UAF1/WDR20 complex was published (Li et al., 2016). In this structure WDR20 binds to a number of structural elements at the palm domain of USP12 with an affinity of 7 nM. Interestingly, the binding interface for WDR20 partially overlaps with the second binding site of UAF1 on USP12 (Supp.Fig.1d), but the contacts are very different, explaining how a F287A/V279D mutation can disrupt WDR20 binding whereas F287A does not affect the UAF1 interface, which is dominated by backbone interactions in this area. The partial overlap of the binding interfaces and the high affinity of WDR20 suggests that WDR20 binding to USP12/UAF1 can either prevent binding of the second UAF1 molecule or it can actively compete out UAF1 if it is bound to the USP12/UAF1 complex. The partial overlap of this interface could hint towards a possible regulatory role for the second UAF1 binding.

The second binding of UAF1 to USP12 does not seem to play a role in the activation of USP12 on a minimal substrate. Meanwhile the effect of the second UAF1 binding on the catalytic activity of USP12 against one of its natural substrates remains to be tested and this could yield more insight on the possible function of this regulatory event. In any case, the conservation of the 1:2 stoichiometry and the two step binding of UAF1 in this small family of USPs highlights the importance of the second binding and implies that the binding could be important for functions which are independent of activation on a minimal substrate.

All available data (Cohn et al., 2009; Sowa et al., 2009) and the high affinity with slow off-rates indicate that USP12/UAF1 form a constitutive complex in cells. In contrast, the fast kinetics of the second binding site indicates that it could play a role in regulation. This is in line with the recent quantitative analysis of protein abundance in HeLa cells

551327-L-bw-Dharadhar
Processed on: 30-12-2020
PDF page: 90

that place the concentration of USP12 and UAF1 at 2 and 77 nM, respectively (Hein et al., 2015). At that concentration the first interface would be fully saturated, and a significant fraction of the USPs would start to bind a second molecule. This means that the second binding could potentially play an important regulatory role.

Acknowledgements

We thank Michael Uckelmann and Robbert Kim for critical reading of the manuscript and other members in the lab for their helpful suggestions. We thank Martin Cohn for the USP1, USP12, USP46 and UAF1 constructs, Huib Ovaa and Farid El Oualid for providing us with the Ub-PRG, Ub-VME and Ub-Rhodamine. We thank Tassos Perrakis for discussion of SAXS data and Tatjana Heidebrecht for technical assistance. We thank beamline scientists at beam lines SLS PXIII, ESRF ID14-1 and ESRF BM29 where diffraction and SAXS data were collected. The authors acknowledge funding from the Dutch Cancer Society KWF, projects NKI-2014-6858 and NKI 2008-4014, ERC advanced grant, Ubiquitin Balance (249997) and CGC.nl.

Conflict of Interest

The authors declare that there is no actual or perceived conflict of interest on the part of any author.

Author Contributions

SD designed, performed and analyzed biochemical experiments, expressed UAF1 constructs, performed UAF1 and USP12/UAF1 structural analysis and wrote the paper. MC set up expression and purification protocols and determined the USP46 structure. AF designed, performed and analyzed the SPR experiments. WJvD provided technical assistance. TKS conceived and coordinated the study and wrote the paper. All authors reviewed the results and approved the final version of the manuscript.

551327-L-bw-Dharadhar
Processed on: 30-12-2020
PDF page: 91

REFERENCES

Adams, P.D., Afonine, P. V., Bunkóczi, G., Chen, V.B., Davis, I.W., Echols, N., Headd, J.J., Hung, L.W., Kapral, G.J., Grosse-Kunstleve, R.W., McCoy, A.J., Moriarty, N.W., Oeffner, R., Read, R.J., Richardson, D.C., Richardson, J.S., Terwilliger, T.C., Zwart, P.H., 2010. PHENIX: A comprehensive Python-based system for macromolecular structure solution. Acta Crystallogr. Sect. D Biol. Crystallogr. 66, 213–221. doi:10.1107/S0907444909052925

Battye, T.G.G., Kontogiannis, L., Johnson, O., Powell, H.R., Leslie, A.G.W., 2011. iMOSFLM: A new graphical interface for diffraction-image processing with MOSFLM. Acta Crystallogr. Sect. D Biol. Crystallogr. 67, 271–281. doi:10.1107/S0907444910048675

Chen, J., Sawyer, N., Regan, L., 2013. Protein-protein interactions: General trends in the relationship between binding affinity and interfacial buried surface area. Protein Sci. 22, 510–515. doi:10.1002/pro.2230

Clague, M.J., Barsukov, I., Coulson, J.M., Liu, H., Rigden, D.J., Urbé, S., 2013. Deubiquitylases from genes to organism. Physiol. Rev. 93, 1289–315. doi:10.1152/physrev.00002.2013

Clerici, M., Luna-Vargas, M.P. a, Faesen, A.C., Sixma, T.K., 2014. The DUSP-Ubl domain of USP4 enhances its catalytic efficiency by promoting ubiquitin exchange. Nat. Commun. 5, 5399. doi:10.1038/ncomms6399

Cohn, M.A., Kee, Y., Haas, W., Gygi, S.P., D'Andrea, A.D., 2009. UAF1 is a subunit of multiple deubiquitinating enzyme complexes. J. Biol. Chem. 284, 5343–5351. doi:10.1074/jbc.M808430200

Cohn, M.A., Kowal, P., Yang, K., Haas, W., Huang, T.T., Gygi, S.P., D'Andrea, A.D., 2007. A UAF1-Containing Multisubunit Protein Complex Regulates the Fanconi Anemia Pathway. Mol. Cell 28, 786–797. doi:10.1016/j.molcel.2007.09.031

Emsley, P., Lohkamp, B., Scott, W.G., Cowtan, K., 2010. Features and development of Coot. Acta Crystallogr. Sect. D Biol. Crystallogr. 66, 486–501. doi:10.1107/S0907444910007493

Faesen, A.C., Dirac, A.M.G., Shanmugham, A., Ovaa, H., Perrakis, A., Sixma, T.K., 2011a. Mechanism of USP7/HAUSP activation by its C-Terminal ubiquitin-like domain and allosteric regulation by GMP-synthetase. Mol. Cell 44, 147–159. doi:10.1016/j.molcel.2011.06.034

Faesen, A.C., Luna-Vargas, M.P.A., Geurink, P.P., Clerici, M., Merkx, R., Van Dijk, W.J., Hameed, D.S., El Oualid, F., Ovaa, H., Sixma, T.K., 2011b. The differential modulation of USP activity by internal regulatory domains, interactors and eight ubiquitin chain types. Chem. Biol. 18, 1550–1561. doi:10.1016/j.chembiol.2011.10.017

Fischer, H., De Oliveira Neto, M., Napolitano, H.B., Polikarpov, I., Craievich, A.F., 2010. Determination of the molecular weight of proteins in solution from a single small-angle X-ray scattering measurement on a relative scale. J. Appl. Crystallogr. 43, 101–109. doi:10.1107/S0021889809043076

Franke, D., Svergun, D.I., 2009. DAMMIF, a program for rapid ab-initio shape determination in small-angle scattering. J. Appl. Crystallogr. 42, 342–346. doi:10.1107/S0021889809000338

Gangula, N.R., Maddika, S., 2013. WD repeat protein WDR48 in complex with deubiquitinase USP12 suppresses akt-dependent cell survival signaling by stabilizing ph domain leucine-rich repeat protein phosphatase 1 (PHLPP1). J. Biol. Chem. 288, 34545–34554. doi:10.1074/jbc.M113.503383

Hein, M.Y., Hubner, N.C., Poser, I., Cox, J., Nagaraj, N., Toyoda, Y., Gak, I.A., Weisswange, I., Mansfeld, J., Buchholz, F., Hyman, A.A., Mann, M., 2015. A Human Interactome in Three Quantitative Dimensions Organized by Stoichiometries and Abundances. Cell 163, 712–723. doi:10.1016/j.cell.2015.09.053

551327-L-bw-Dharadhar
Processed on: 30-12-2020
PDF page: 92

Hu, M., Li, P., Li, M., Li, W., Yao, T., Wu, J.W., Gu, W., Cohen, R.E., Shi, Y., 2002. Crystal structure of a UBP-family deubiquitinating enzyme in isolation and in complex with ubiquitin aldehyde. Cell 111, 1041–1054. doi:10.1016/S0092-8674(02)01199-6

Huang, T.T., Nijman, S.M.B., Mirchandani, K.D., Galardy, P.J., Cohn, M. a, Haas, W., Gygi, S.P., Ploegh, H.L., Bernards, R., D'Andrea, A.D., 2006. Regulation of monoubiquitinated PCNA by DUB autocleavage. Nat. Cell Biol. 8, 339–347. doi:10.1038/ncb1378

Imai, S., Kano, M., Nonoyama, K., Ebihara, S., 2013. Behavioral Characteristics of Ubiquitin-Specific Peptidase 46-Deficient Mice. PLoS One 8, 0–8. doi:10.1371/journal.pone.0058566

Jahan, A.S., Lestra, M., Swee, L.K., Fan, Y., Lamers, M.M., Tafesse, F.G., Theile, C.S., Spooner, E., Bruzzone, R., Ploegh, H.L., Sanyal, S., 2016. Usp12 stabilizes the T-cell receptor complex at the cell surface during signaling. Proc. Natl. Acad. Sci. 113, 201521763. doi:10.1073/pnas.1521763113

Joo, H.Y., Jones, A., Yang, C., Zhai, L., Smith IV, A.D., Zhang, Z., Chandrasekharan, M.B., Sun, Z.W., Renfrow, M.B., Wang, Y., Chang, C., Wang, H., 2011. Regulation of histone H2A and H2B deubiquitination and xenopus development by USP12 and USP46. J. Biol. Chem. 286, 7190–7201. doi:10.1074/jbc.M110.158311

Joosten, R.P., Long, F., Murshudov, G.N., Perrakis, A., 2014. The *PDB_REDO* server for macromolecular structure model optimization. IUCrJ 1, 213–220. doi:10.1107/S2052252514009324

Kabsch, W., 2010. Xds. Acta Crystallogr. Sect. D Biol. Crystallogr. 66, 125–132. doi:10.1107/S0907444909047337

Kee, Y., Yang, K., Cohn, M.A., Haas, W., Gygi, S.P., D'Andrea, A.D., 2010. WDR20 regulates activity of the USP12.UAF1 deubiquitinating enzyme complex. J. Biol. Chem. 285, 11252–11257. doi:10.1074/jbc.M109.095141

Komander, D., Clague, M.J., Urbé, S., 2009. Breaking the chains: structure and function of the deubiquitinases. Nat. Rev. Mol. Cell Biol. 10, 550–563. doi:10.1038/nrm2731

Konarev, P. V., Petoukhov, M. V., Volkov, V. V., Svergun, D.I., 2006. ATSAS 2.1, a program package for small-angle scattering data analysis. J. Appl. Crystallogr. 39, 277–286. doi:10.1107/S0021889806004699

Konarev, P. V., Volkov, V. V., Sokolova, A. V., Koch, M.H.J., Svergun, D.I., 2003. PRIMUS: A Windows PC-based system for small-angle scattering data analysis. J. Appl. Crystallogr. 36, 1277–1282. doi:10.1107/S0021889803012779

Krissinel, E., Henrick, K., 2007. Inference of Macromolecular Assemblies from Crystalline State. J. Mol. Biol. 372, 774–797. doi:10.1016/j.jmb.2007.05.022

Langer, G., Cohen, S.X., Lamzin, V.S., Perrakis, A., 2008. Automated macromolecular model building for X-ray crystallography using ARP/wARP version 7. Nat. Protoc. 3, 1171–9. doi:10.1038/nprot.2008.91

Li, H., Lim, K.S., Kim, H., Hinds, T.R., Jo, U., Mao, H., Weller, C.E., Sun, J., Chatterjee, C., D'Andrea, A.D., Zheng, N., 2016. Allosteric Activation of Ubiquitin-Specific Proteases by β-Propeller Proteins UAF1 and WDR20. Mol. Cell 1–12. doi:10.1016/j.molcel.2016.05.031

Liang, Q., Dexheimer, T.S., Zhang, P., Rosenthal, A.S., Villamil, M. a, You, C., Zhang, Q., Chen, J., Ott, C. a, Sun, H., Luci, D.K., Yuan, B., Simeonov, A., Jadhav, A., Xiao, H., Wang, Y., Maloney, D.J., Zhuang, Z., 2014. A selective USP1-UAF1 inhibitor links deubiquitination to DNA damage responses. Nat. Chem. Biol. 10, 298–304. doi:10.1038/nchembio.1455

Luna-Vargas, M.P.A., Christodoulou, E., Alfieri, A., van Dijk, W.J., Stadnik, M., Hibbert, R.G., Sahtoe, D.D., Clerici, M., Marco, V. De, Littler, D., Celie, P.H.N., Sixma, T.K., Perrakis, A., 2011. Enabling high-throughput ligation-independent cloning and protein expression for the family of ubiquitin specific proteases. J. Struct. Biol. 175, 113–119. doi:10.1016/j.jsb.2011.03.017

551327-L-bw-Dharadhar
Processed on: 30-12-2020
PDF page: 93

McCoy, A.J., Grosse-Kunstleve, R.W., Adams, P.D., Winn, M.D., Storoni, L.C., Read, R.J., 2007. Phaser crystallographic software. J. Appl. Crystallogr. 40, 658–674. doi:10.1107/S0021889807021206

Murshudov, G.N., Vagin, A.A., Dodson, E.J., 1997. Refinement of macromolecular structures by the maximum-likelihood method. Acta Crystallogr. Sect. D Biol. Crystallogr. doi:10.1107/S0907444996012255

Nicassio, F., Corrado, N., Vissers, J.H.A., Areces, L.B., Bergink, S., Marteijn, J.A., Geverts, B., Houtsmuller, A.B., Vermeulen, W., Di Fiore, P.P., Citterio, E., 2007. Human USP3 Is a Chromatin Modifier Required for S Phase Progression and Genome Stability. Curr. Biol. 17, 1972–1977. doi:10.1016/j.cub.2007.10.034

Nijman, S.M.B., Huang, T.T., Dirac, A.M.G., Brummelkamp, T.R., Kerkhoven, R.M., D'Andrea, A.D., Bernards, R., 2005. The deubiquitinating enzyme USP1 regulates the fanconi anemia pathway. Mol. Cell 17, 331–339. doi:10.1016/j.molcel.2005.01.008

Olazabal-Herrero, A., García-Santisteban, I., Rodríguez, J.A., 2015. Structure-function analysis of USP1: insights into the role of Ser313 phosphorylation site and the effect of cancer-associated mutations on autocleavage. Mol. Cancer 14, 33. doi:10.1186/s12943-015-0311-7

Row, P.E., Liu, H., Hayes, S., Welchman, R., Charalabous, P., Hofmann, K., Clague, M.J., Sanderson, C.M., Urbé, S., 2007. The MIT domain of UBPY constitutes a CHMP binding and endosomal localization signal required for efficient epidermal growth factor receptor degradation. J. Biol. Chem. 282, 30929–30937. doi:10.1074/jbc.M704009200

Sahtoe, D.D., Sixma, T.K., 2015. Layers of DUB regulation. Trends Biochem. Sci. 40, 456–67. doi:10.1016/j.tibs.2015.05.002

Smart, O.S., Womack, T.O., Flensburg, C., Keller, P., Paciorek, W., Sharff, A., Vonrhein, C., Bricogne, G., 2012. Exploiting structure similarity in refinement: Automated NCS and target-structure restraints in BUSTER. Acta Crystallogr. Sect. D Biol. Crystallogr. 68, 368–380. doi:10.1107/S0907444911056058

Sowa, M.E., Bennett, E.J., Gygi, S.P., Harper, J.W., 2009. Defining the Human Deubiquitinating Enzyme Interaction Landscape. Cell 138, 389–403. doi:10.1016/j.cell.2009.04.042

Svergun, D., Barberato, C., Koch, M.H., 1995. CRYSOL - A program to evaluate X-ray solution scattering of biological macromolecules from atomic coordinates. J. Appl. Crystallogr. 28, 768–773. doi:10.1107/S0021889895007047

Svergun, D.I., Petoukhov, M. V, Koch, M.H., 2001. Determination of domain structure of proteins from X-ray solution scattering. Biophys. J. 80, 2946–2953. doi:10.1016/S0006-3495(01)76260-1

Villamil, M.A., Chen, J., Liang, Q., Zhuang, Z., 2012a. A noncanonical cysteine protease USP1 is activated through active site modulation by USP1-associated factor 1. Biochemistry 51, 2829–2839. doi:10.1021/bi3000512

Villamil, M.A., Liang, Q., Chen, J., Choi, Y.S., Hou, S., Lee, K.H., Zhuang, Z., 2012b. Serine phosphorylation is critical for the activation of ubiquitin-specific protease 1 and its interaction with WD40-repeat protein UAF1. Biochemistry 51, 9112–9113. doi:10.1021/bi300845s

Williams, S.A., Maecker, H.L., French, D.M., Liu, J., Gregg, A., Silverstein, L.B., Cao, T.C., Carano, R.A.D., Dixit, V.M., 2011. USP1 deubiquitinates ID proteins to preserve a mesenchymal stem cell program in osteosarcoma. Cell 146, 918–930. doi:10.1016/j.cell.2011.07.040

Winn, M.D., Ballard, C.C., Cowtan, K.D., Dodson, E.J., Emsley, P., Evans, P.R., Keegan, R.M., Krissinel, E.B., Leslie, A.G.W., McCoy, A., McNicholas, S.J., Murshudov, G.N., Pannu, N.S., Potterton, E.A., Powell, H.R., Read, R.J., Vagin, A., Wilson, K.S., 2011. Overview of the CCP4 suite and current developments. Acta Crystallogr. Sect. D Biol. Crystallogr. 67, 235–242. doi:10.1107/S0907444910045749

Yin, J., Schoeffler, A.J., Wickliffe, K., Newton, K., Starovasnik, M.A., Dueber, E.C., Harris, S.F., 2015. Structural Insights into WD-Repeat 48 Activation of Ubiquitin-Specific Protease 46. Structure 23, 2043–2054. doi:10.1016/j.str.2015.08.010

551327-L-bw-Dharadhar
Processed on: 30-12-2020
PDF page: 94

Zhang, W., Tian, Q.B., Li, Q.K., Wang, J.M., Wang, C.N., Liu, T., Liu, D.W., Wang, M.W., 2011. Lysine 92 amino acid residue of USP46, a gene associated with “behavioral despair” in mice, influences the deubiquitinating enzyme activity. PLoS One 6, 2–7. doi:10.1371/journal.pone.0026297

551327-L-bw-Dharadhar
Processed on: 30-12-2020
PDF page: 95

SUPPLEMENTAL DATA

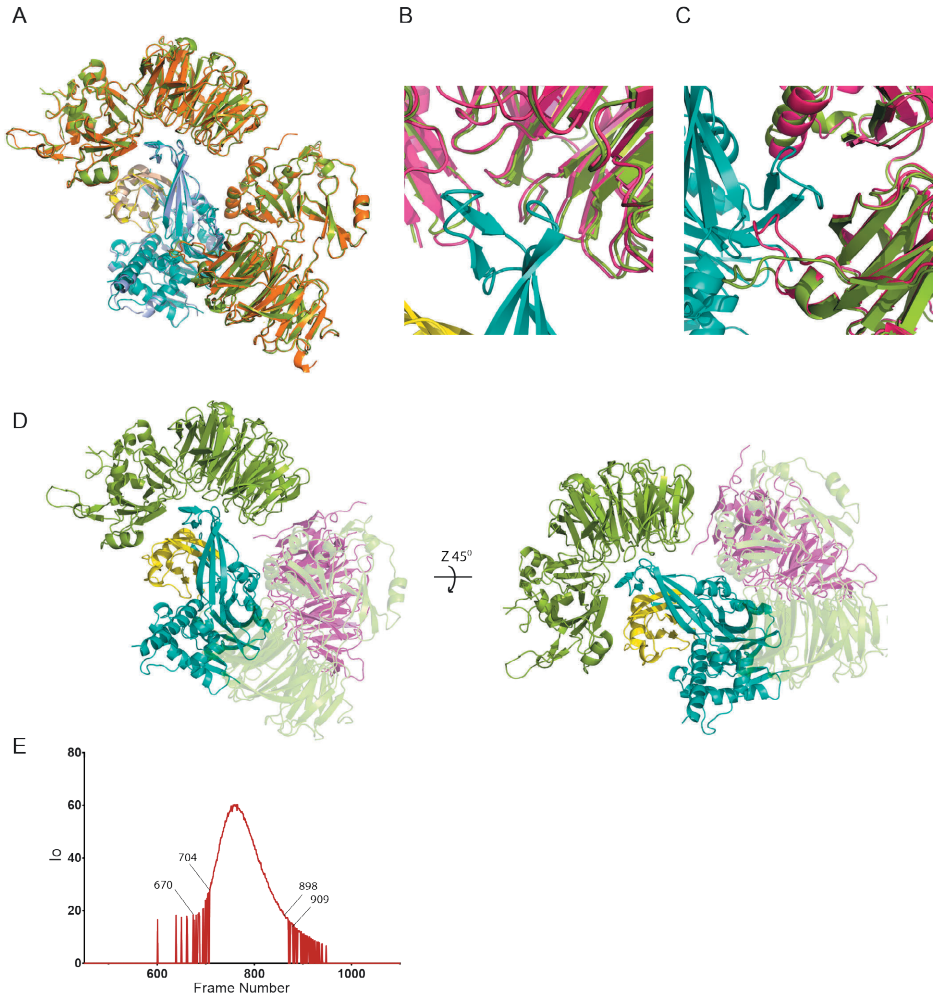

A) Superposition of USP12-Ub/UAF1 (colours as indicated earlier) with USP46-Ub/UAF1 (Colours; USP46 – as in Fig 1b, Ubiquitin – Light Brown, UAF1 – Orange) (PDB code – 5CVN).
B, C) Superposition of free $UAF1_{580}$ (Dark Pink) on $USP12_{FL}$-Ub/$UAF1_{580}$ ($UAF1_{580}$ in green) structure at Interface 1 and 2 respectively.
D) Superposition of WDR20 (Dark Pink) with $UAF1_{580}$ (light green) bound at Interface 2 on USP12-Ub/$UAF1_{580}$ (colours as indicated earlier).
E) Io is plotted on the y-axis against the corresponding frame number on the x-axis, frames 670-704 and 898-909 were analysed separately for the high molecular weight species and the 1:2 complex respectively.

551327-L-bw-Dharadhar
Processed on: 30-12-2020
PDF page: 96

551327-L-bw-Dharadhar
Processed on: 30-12-2020

CHAPTER 4

Insert L1 is a central hub for allosteric regulation of USP1 activity

Shreya Dharadhar[1], Willem J. van Dijk[1], Serge Scheffers[1], Alexander Fish[1], Titia K. Sixma[1]

[1]Division of Biochemistry and Oncode Institute, Netherlands Cancer Institute, Plesmanlaan 121, 1066 CX Amsterdam, The Netherlands

Accepted in EMBO Reports

ABSTRACT

During DNA replication, the deubiquitinating enzyme USP1 limits the recruitment of translesion polymerases by removing ubiquitin marks from PCNA to allow specific regulation of the Translesion synthesis (TLS) pathway. USP1 activity depends on an allosteric activator, UAF1 and this is tightly controlled. In comparison to paralogs USP12 and USP46, USP1 contains three defined inserts and lacks the second WDR20 mediated activation step. Here we show how insert L1 and L3 together limit intrinsic USP1 activity and how this is relieved by UAF1. Intriguingly, insert L1 also conveys substrate-dependent increase in USP1 activity through DNA and PCNA interactions, in a process that is independent of UAF1-mediated activation. This study establishes insert L1 as an important regulatory hub within USP1 necessary for both substrate mediated activity enhancement and allosteric activation upon UAF1 binding.

551327-L-bw-Dharadhar
Processed on: 30-12-2020
PDF page: 100

INTRODUCTION

Dynamic regulation of ubiquitination on proteins involved in DNA repair pathways is essential for proper functioning of these pathways. (De)-Ubiquitination enzymes that control these processes have gained a lot of attention, as these are attractive targets to attenuate DNA repair pathways. USP1 is a deubiquitinase (DUB) that acts on mono-ubiquitinated PCNA and FANCD2, making it crucial for the regulation of translesion synthesis and the Fanconi anaemia pathway respectively (Nijman *et al*, 2005; Huang *et al*, 2006). Recently, it was also shown that USP1 inhibition resulted in replication fork destabilization and decreased viability of BRCA1-deficient cells indicating a synthetic lethal relationship (Lim *et al*, 2018). To target USP1 effectively it would be important to know how its catalytic activity is regulated.

USP1 belongs to the ubiquitin specific protease (USP) family of DUBs and it forms a small sub-family with two other USPs, USP12 and USP46 (Mevissen & Komander, 2017). These USPs bind a common co-factor called UAF1 (also known as WDR48), which leads to activation of these enzymes by an increase in the catalytic turnover (k_{cat}) (Cohn *et al*, 2007, 2009). Relative to these paralogs, USP1 is much larger, primarily due to the presence of three inserts within its well conserved USP catalytic domain (Fig 1a, Fig EV1a). It also lacks the binding site for another activator, WDR20, which binds USP12 and USP46, leading to further activation (Kee *et al*, 2010). In contrast, it was reported recently that USP1 activity is further enhanced upon binding DNA and this interaction is mediated by insert L1 of USP1 (Lim *et al*, 2018). Insert L1 was also shown to be the site of multiple phosphorylations (Villamil *et al*, 2012; Olazabal-Herrero *et al*, 2015) and it has been reported to carry two nuclear localization signals that are important for its translocation to the nucleus (Garcia-Santisteban *et al*, 2012).

So far there is no structural information available for USP1 alone or the USP1-UAF1 complex, but crystal structures of the paralogs with and without the activators have been solved (Yin *et al*, 2015; Li *et al*, 2016; Dharadhar *et al*, 2016). Based on these USP12 and USP46 structures it is clear that UAF1 binds USP1 on the 'finger' sub-domain of the catalytic domain (Yin *et al*, 2015). It has also been shown that UAF1 activation of USP12 is mainly caused by a series of subtle structural rearrangements in various parts of the enzyme. One such region is the proximal knuckle (PK) helix and its preceding loop called the PK loop which also form a part of the WDR20 interface (Li *et al*, 2016). Interestingly, USP1 has a small insertion of 20 amino acids in the PK loop and this insert is located in the WDR20 binding interface of USP12 and USP46 (Insert L3, Fig EV1b). Whether this small insert of USP1 plays any role in its activation by UAF1 and if there are other

551327-L-bw-Dharadhar
Processed on: 30-12-2020

unique elements within USP1 which compensate for the lack of WDR20 activation are not known.

USP1 activity on FANCD2-Ub is well studied and the N-terminal extension of USP1 is important for activity on FANCD2 (Arkinson *et al*, 2018). DNA binding was shown to promote USP1-UAF1 activity on FANCD2-Ub, but in this case activation is dependent on a DNA binding role of UAF1 (Liang *et al*, 2019). Additionally, the C-terminal SUMO-like domains (SLD) of UAF1 also play a role in the recruitment of USP1 to ubiquitinated substrates (Yang *et al*, 2011; Lee *et al*, 2010). In contrast, how USP1 acts on PCNA is not clear. Moreover, whether its activity is affected by DNA loading of PCNA-Ub has not been studied. This may be important for USP1 activity as it is thought to travel along the replicating fork where it carries out its deubiquitinating activity in crucial DNA repair pathways (Dungrawala *et al*, 2015).

In this study we demonstrate the molecular details of USP1 allosteric regulation by UAF1 and its natural substrate i.e. DNA-loaded PCNA-Ub. We study the role of USP1 inserts on enzymatic activity towards substrates of increasing complexity. This reveals that the combined action of insert L1 and L3 inhibits USP1 catalytic activity and that this auto-inhibition is relieved by UAF1-dependent activation on a minimal substrate (Ub-Rho). On PCNA-Ub we find that a PIP motif in insert L1 is crucial for activity. Finally, we developed a protocol to load PCNA-Ub on DNA. On this substrate, we identify a secondary enhancement in USP1 activity, that is only triggered upon interaction with DNA-loaded PCNA-Ub. Furthermore, we demonstrate that both DNA and PCNA interaction with USP1 are important for this substrate-mediated increase in activity.

RESULTS

USP1 catalytic activity is inhibited by its inserts

To address the role of the inserts in USP1 catalytic activity, we made deletion mutants of USP1 that either lack each insert individually or in combinations (Fig 1a). These deletion mutants were successfully purified and their catalytic activities were tested against the minimal substrate ubiquitin-rhodamine (Ub-Rho). None of the variants lacking a single insert ($USP1^{\Delta L1}$, $USP1^{\Delta L2}$, $USP1^{\Delta L3}$) showed any change in activity compared to wild type USP1 ($USP1^{WT}$), but when both insert L1 and L3 were removed ($USP1^{\Delta L1L3}$) a significant hyper-activation was observed (Fig 1b).

This hyper-activation was unique to this combination, as deletion of insert L1 and L2 ($USP1^{\Delta L1L2}$) or insert L2 and L3 ($USP1^{\Delta L2L3}$) did not affect USP1 catalytic activity (Fig 1b). The insert L3 in USP1 is located in the PK loop. In USP12 this loop is important

551327-L-bw-Dharadhar
Processed on: 30-12-2020
PDF page: 102

for activation, as mutation of a stretch of glycine residues within the loop leads to loss in activation of USP12 by either UAF1 or WDR20. In USP1, deletion of insert L3 alone does not affect USP1 activity but the deletion of both insert L3 and insert L1 leads to an increased activity of USP1.

We tested whether phosphorylation of serine 313 in insert L1 had a direct effect on USP1 catalytic activity, since Ser313 phosphorylation was previously reported as necessary for UAF1 binding and its ability to activate (Villamil *et al*, 2012; Olazabal-Herrero *et al*, 2015). We tested both the phospho-dead (Ser to Ala) and phospho-mimic (Ser to Asp) mutations, but neither showed an effect on activity of USP1 alone or upon binding with UAF1, relative to $USP1^{WT}$ (Fig EV2a).

We performed Michaelis-Menten kinetic analysis under increasing concentrations of Ub-Rho substrate (Fig 1d, Table 1) and fitted $USP1^{WT}$ and all the deletion mutants. As the reaction velocity curves for $USP1^{\Delta L1L3}$ did not reach saturation, the estimation of Vmax and subsequently K_M was not reliable. To validate our findings we fitted $USP1^{WT}$ and $USP1^{\Delta L1L3}$ activity data using *KinTek Explorer* (Johnson *et al*, 2009a) simultaneously, using all the data rather than initial rates only. Similar to our standard Michaelis-Menten analysis, this improved analysis again showed that the activation in $USP1^{\Delta L1L3}$ was mostly due to an increase in k_{cat} (Fig EV2b). We conclude that insert L1 and L3 together inhibit the intrinsic catalytic activity of USP1.

UAF1 binding relieves insert L1 and L3 mediated auto-inhibition of USP1 activity

UAF1 mediated activation of USP1 is primarily due to an increase in k_{cat} (Cohn *et al*, 2007) which is similar to what we observe in $USP1^{\Delta L1L3}$. To test whether insert L1 and L3 mediated auto-inhibition of USP1 can be relieved by UAF1, we performed kinetic analysis in the presence of UAF1 on Ub-Rho (Fig 1e). We observed that the hyper-activation of USP1 that deletion of insert L1 and L3 had caused was lost in the presence of UAF1, as the catalytic activity of $USP1^{\Delta L1L3}$ no longer differed significantly from $USP1^{WT}$, nor from any of the other deletion mutants. (Fig 1c, e, Table 1). These experiments also show that the deletion of insert L1 and insert L3 is not sufficient to completely recapitulate UAF1 mediated activation as UAF1 binding can still activate $USP1^{\Delta L1L3}$. However, our data suggests that one of the primary mechanisms by which USP1 is activated by UAF1 is through relieving the auto-inhibition caused by the joint action of insert L1 and L3.

551327-L-bw-Dharadhar
Processed on: 30-12-2020
PDF page: 103

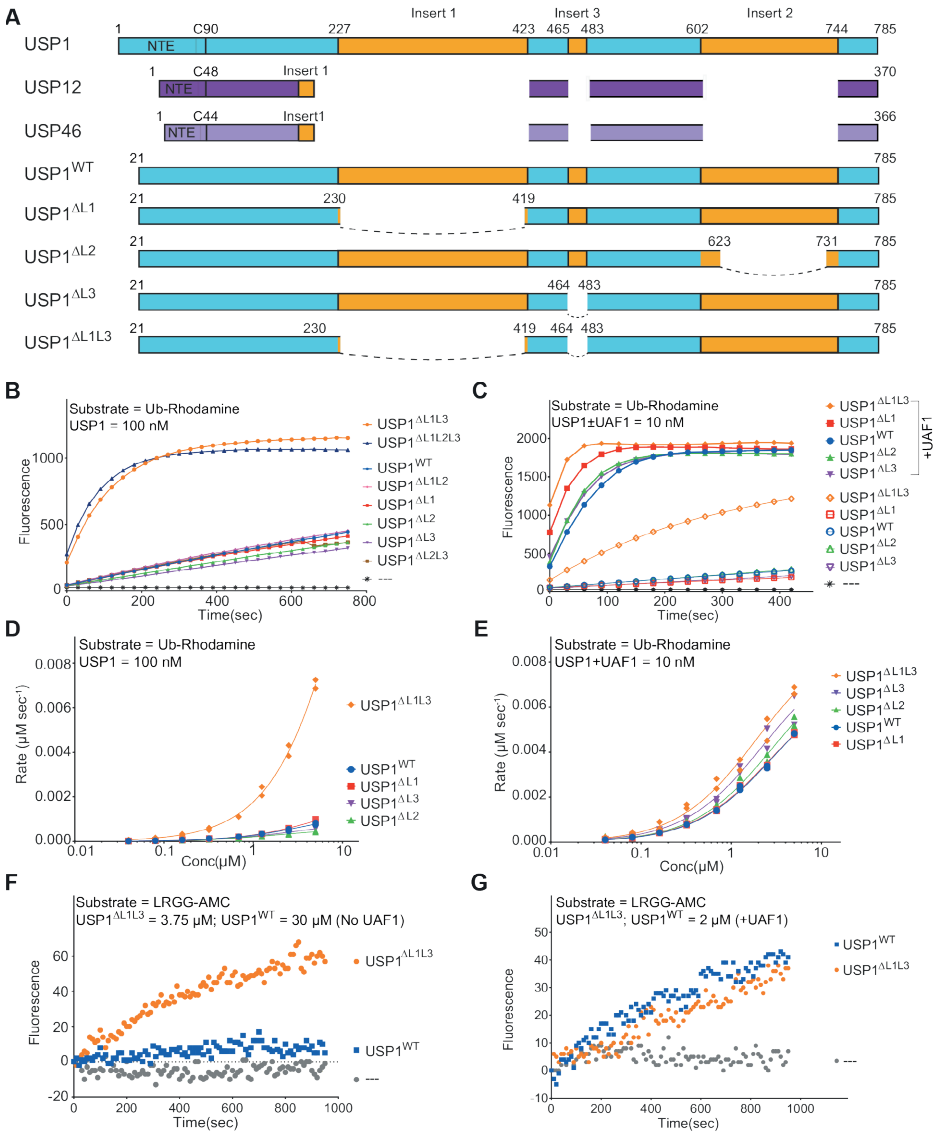

Fig.1) UAF1 activates USP1 allosterically by relieving the insert 1 and 3 mediated auto-inhibition of USP1 catalytic activity.
A) Schematic diagram of the USP1 subfamily and the USP1 deletion mutants tested in this study.
B) Single point activity assays of $USP1^{WT}$ and deletion mutants on Ub-Rho show significantly increased activity in mutants where insert L1 and L3 are both deleted.
C) Single point activity assays of $USP1^{WT}$ and deletion mutants (± UAF1) on Ub-Rho show the loss in hyper-activation of $USP1^{\Delta L1L3}$ upon addition of UAF1.
D) Michaelis-Menten analysis of USP1 deletion mutants against ubiquitin-rhodamine (Ub-Rho) shows that $USP1^{\Delta L1L3}$ has significantly higher activity compared to WT and other mutants (n=2).
E) Michaelis-Menten analysis of USP1 deletion mutants (+UAF1) against Ub-Rho shows that all deletions mutants have similar catalytic activity (n=2).

551327-L-bw-Dharadhar
Processed on: 30-12-2020

F) Comparing activity of $USP1^{WT}$ and $USP1^{\Delta L1L3}$ on a peptide substrate i.e. LRGG-AMC (100μM). $USP1^{\Delta L1L3}$ cleaves the peptide substrate more efficiently compared to $USP1^{WT}$ (n=2).
G) Comparing activity of $USP1^{WT}$ and $USP1^{\Delta L1L3}$ (+UAF1) on a peptide substrate i.e. LRGG-AMC (100μM). Addition of UAF1 allows cleavage of LRGG-AMC by both $USP1^{WT}$ and $USP1^{\Delta L1L3}$ (n=2).

Table 1 Kinetic analysis of $USP1^{WT}$ and deletion mutants using the Michaelis-Menten equation.

	(- UAF1)			(+ UAF1)		
	k_{cat} (sec^{-1})	**K_M (μM)**	**k_{cat}/K_M (sec^{-1} μM^{-1})**	**k_{cat} (sec^{-1})**	**K_M (μM)**	**k_{cat}/K_M (sec^{-1} μM^{-1})**
$USP1^{WT}$	0.014 (± 0.001)	3.80 (± 0.52)	0.0036	0.73 (± 0.03)	2.68 (± 0.25)	0.272
$USP1^{\Delta L1}$	0.018 (± 0.0007)	4.50 (± 0.33)	0.0039	0.71 (± 0.03)	2.53 (± 0.23)	0.283
$USP1^{\Delta L2}$	0.004 (± 0.0001)	1.03 (± 0.11)	0.0043	0.80 (± 0.03)	2.63 (± 0.22)	0.306
$USP1^{\Delta L3}$	0.007 (± 0.0003)	1.8 (± 0.19)	0.0040	0.82 (± 0.01)	2.03 (± 0.09)	0.406
$USP1^{\Delta L1L3}$	0.26 (± 0.01)	13.7 (± 0.79)	0.019	1.01 (± 0.07)	2.37 (± 0.37)	0.425

Based on the published structures of USP12+UAF1 and USP12+UAF1+WDR20 (Li *et al*, 2016; Dharadhar *et al*, 2016) we generated a homology model of USP1, that shows the location of the inserts of USP1 (Fig EV1b). Interestingly, Insert L3 of USP1 overlaps with the binding site of WDR20 in USP12 suggesting that the effect of WDR20 could be mimicked by a joint mechanism which involves rearrangement of both insert L1 and L3.

A defining feature of WDR20-dependent activation, is that it is necessary for the ability of USP12 to cleave a peptide substrate, Leu-Arg-Gly-Gly (LRGG)-AMC, since USP12-UAF1 alone cannot cleave such a substrate (Li *et al*, 2016). Therefore, we analysed whether USP1 could process this substrate. First, we compared $USP1^{WT}$ in the presence and absence of UAF1. Like USP12, USP1 alone cannot cleave the peptide substrate. However, addition of UAF1 is sufficient to activate $USP1^{WT}$ such that it can now process this substrate (Fig 1f, g), whereas USP12 requires WDR20 to make this happen (Fig EV2c) (Li *et al*, 2016). Unlike $USP1^{WT}$, the $USP1^{\Delta L1L3}$ alone can cleave the peptide substrate which is in line with the idea that rearrangement of insert L1 brings about conformational changes in insert L3 which are necessary for activation of USP1 by bringing it to a WDR20 like state.

551327-L-bw-Dharadhar
Processed on: 30-12-2020
PDF page: 105

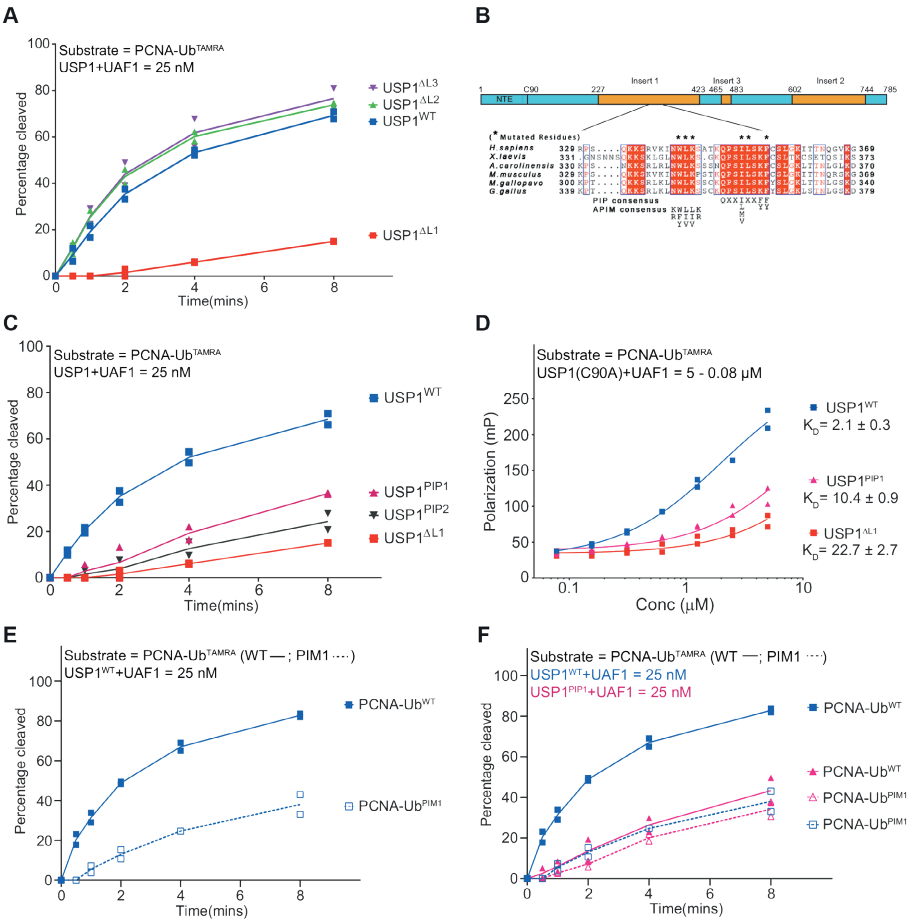

Fig.2) Insert L1 of USP1 contains a PIP motif which is essential for activity of USP1 on PCNA-Ub.
A) Quantification of gel-based activity assays where the activity of USP1^{WT} and deletion mutants (+UAF1) on PCNA-Ub^{TAMRA} is compared. The USP1$^{\Delta L1}$ mutant has reduced activity on PCNA-Ub^{TAMRA} compared to the other USP1 variants tested (n=2).
B) Multiple sequence alignment of USP1 insert L1 which highlights the conservation of the PIP and APIM motif in USP1 across species, the residues mutated in this region are indicated with an asterisk.
C) Quantification of gel-based activity assays where the activity of USP1 PIP mutants (+UAF1) on PCNA-Ub^{TAMRA} is compared. Both the PIP mutants have reduced activity on PCNA-Ub compared to USP1^{WT} (n=2).
D) FP based binding assays of USP1 mutants (+ UAF1) with PCNA-Ub^{TAMRA} show reduced binding of USP1$^{\Delta L1}$ and USP1^{PIP1} compared to USP1^{WT} (n=2).
E) Quantification of gel-based activity assays where the activity of USP1^{WT}+UAF1 on PCNA-Ub^{WT} is compared with PCNA-Ub^{PIM1} shows that PCNA-Ub^{WT} is cleaved much faster compared to PCNA-Ub^{PIM1} (n=2)
F) Comparing activity of USP1^{WT} and USP1^{PIP1} (+UAF1) on PCNA-Ub^{WT} and PCNA-Ub^{PIM1} in gel-based assays shows that the activity of USP1^{WT} is severely reduced by the PIM1 mutation in PCNA, whereas USP1^{PIP1} activity is not further affected indicating that PIP1 and PIM mutation affect the same interaction (n=2).

551327-L-bw-Dharadhar
Processed on: 30-12-2020
PDF page: 106

These results show on one hand that removal of insert L1 and L3 mediated auto-inhibition of USP1 brings it to a WDR20-bound-like state, and on the other hand that for USP1, the activation by UAF1 already achieves a state that requires WDR20 in the USP12/46 paralogs. It seems likely that this activation is mediated by some form of UAF1-induced conformational change in Insert L1 and L3. When UAF1 binds, at the tip of the finger sub-domain, this induces a cascade of rearrangements, as it does in USP12. We speculate that this brings about changes in insert L3, located at the base of the fingers and results in the removal of auto-inhibition by insert L1 and L3 (Fig EV1b). To understand how L1 and L3 mediate their inhibition structural information will be important.

Insert L1 is necessary for USP1 activity on PCNA-Ub

To test whether the inserts of USP1 play any role in the deubiquitination of its natural substrate i.e. monoubiquitinated PCNA (PCNA-Ub), we carried out activity assays on reconstituted PCNA-Ub (Hibbert & Sixma, 2012). In these assays we used a TAMRA label at the N-terminus of ubiquitin for ease of quantitation (Dharadhar et al., 2019), as this has no effect on the rates (Fig EV2d). Comparing WT and deletion mutants, we observed that loss of insert L1 in USP1 severely impairs its ability to deubiquitinate PCNA-Ub^{TAMRA} (Fig 2a), whereas this deletion does not affect activity on a minimal substrate.

We analysed the sequence of insert L1 in a multi-sequence alignment with different species (Fig 2b). We identified a degenerate PCNA-interacting-peptide (PIP) box, which is highly conserved across vertebrates (Fig 2b). Compared to traditional PIP motifs, there is one phenylalanine missing in the final FF, replaced by KF. Additionally, there was a possible APIM-like motif just upstream of the PIP site. We made two mutants, a triple mutant in the PIP (PIP1: I351A, L352A and F355A) and one with additional changes in the APIM (PIP2: I351A, L352A and F355A; W341A, L342A and K343A). These mutants were co-purified with UAF1 and tested for activity on PCNA-Ub^{TAMRA}. Both USP1^{PIP1} and USP1^{PIP2} had reduced activity on PCNA-Ub^{TAMRA} compared to USP1^{WT} but were not affected in their activity on a minimal substrate (Fig 2c; Fig EV2e).

Importantly, we then analysed binding of USP1 to PCNA-Ub in a fluorescence polarization (FP) assay. Here we found that deletion of insert L1 (USP1$^{\Delta L1}$) or mutation of the PIP motif (PIP1) leads to a 10- and 5-fold reduction in binding to PCNA-Ub^{TAMRA} respectively (Fig 2d).

To validate the role of the PIP interaction between USP1 and PCNA, we made mutations in PCNA (PIM1: L126A and I128A; PIM2: D232A and P234A; PIM3: P253A and K254A), in the PIP interaction site (Eissenberg *et al*, 1997). USP1^{WT} activity was substantially

551327-L-bw-Dharadhar
Processed on: 30-12-2020
PDF page: 107

reduced on the PCNA-Ub PIM1 and PIM2 mutant while the activity on the PIM3 mutant was the same when compared to PCNA-Ub (WT) (Fig EV3a). We then compared the activity of $USP1^{WT}$ and $USP1^{PIP1}$ on both $PCNA\text{-}Ub^{PIM1}$ and $PCNA\text{-}Ub^{WT}$. The activity of $USP1^{WT}$ was reduced on $PCNA\text{-}Ub^{PIM1}$ but activity of $USP1^{PIP1}$ was not further depleted on $PCNA\text{-}Ub^{PIM1}$ relative to $PCNA\text{-}Ub^{WT}$, indicating that both mutations affect the same interaction (Fig 2e, f). These binding and mutant data together confirm that insert L1 of USP1 contains a well conserved PIP motif which is important for USP1 interaction and activity on PCNA-Ub.

Purification of PCNA-Ub loaded on circular DNA

USP1-UAF1 is known to play a role in PCNA-Ub mediated translesion synthesis (Huang *et al*, 2006). Moreover, it has been suggested that USP1-UAF1 travels with elongating replication forks where it deubiquitinates its substrates. Removal of USP1 from this environment was shown to generate increased ubiquitination of proteins residing at the fork (Dungrawala *et al*, 2015). Other studies have shown that both USP1 and UAF1 have DNA binding properties (Liang *et al*, 2016; Lim *et al*, 2018). We could confirm that USP1 binds DNA, and the fact that this interaction is dependent on insert L1 (Fig EV3b). However, we did not observe the (very small) effect on catalytic activity against a minimal substrate, Ub-Rhodamine (Lim *et al*, 2018) (Fig 3b). Nevertheless, we wondered if the observed interaction with DNA could affect the activity on a more natural substrate, PCNA-Ub loaded on DNA.

To enable analysis of USP1 activity on DNA-loaded substrate, we established efficient DNA loading procedures for human PCNA-Ub on circular DNA using the RFC clamp loader complex from yeast (Yoder & Burgers, 1991). First, we successfully purified PCNA-Ub where each monomer of the clamp was mono-ubiquitinated using previously published protocols (Hibbert & Sixma, 2012) and then we performed *in vitro* loading assays on nicked circular DNA (Fig 3a). Our results show that PCNA and PCNA-Ub are loaded with similar efficiency onto nicked circular DNA (Fig EV3c). We then used size exclusion chromatography to obtain large amounts of purified PCNA-Ub loaded on nicked circular DNA (Fig 3a). Due to the presence of a TAMRA label on each ubiquitin molecule we could measure the exact concentrations of DNA-loaded PCNA-Ub which allowed us to perform quantitative *in vitro* deubiquitination assays.

The loading and purification of DNA-loaded PCNA-Ub is technically complex since many factors are involved in this reaction. Moreover, the half-life of PCNA on DNA is approximately 25 minutes which makes downstream experiments challenging due to the time constraints (Zhao *et al*, 2017). We circumvented this problem by carrying out the activity assays within 20 minutes after elution from a size exclusion column.

551327-L-bw-Dharadhar
Processed on: 30-12-2020
PDF page: 108

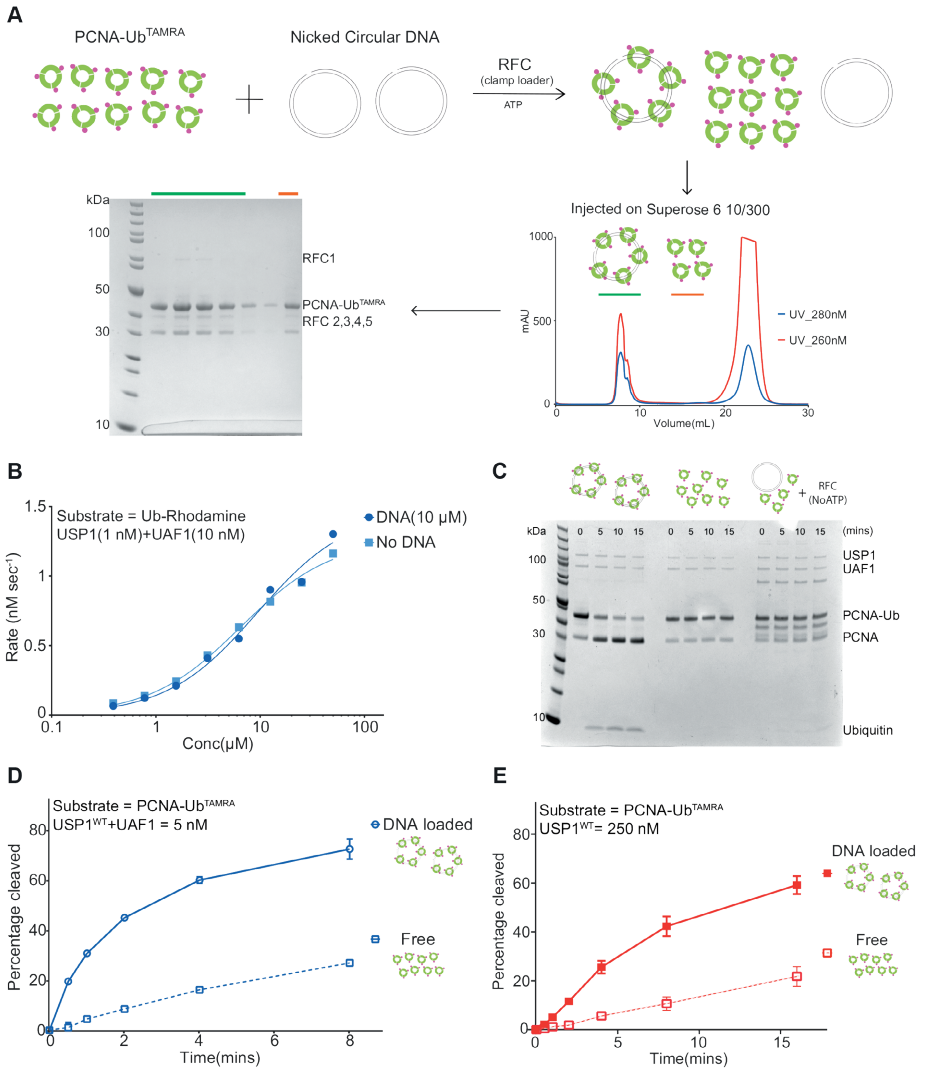

Fig.3) USP1 (±UAF1) has higher catalytic activity on PCNA-Ub when it is loaded on DNA.
A) Schematic representation of loading and purification of PCNA-Ub on nicked circular DNA. The DNA-loaded PCNA-Ub elutes in the void of the SEC column and this sample is collected and used for studying activity of USP1 on DNA-loaded PCNA-Ub.
B) Michaelis-Menten analysis of USP1+UAF1 with and without DNA (65bp dsDNA) shows that DNA binding alone has no effect on USP1 activity (n=2).
C) Coomassie stained gel of *in vitro* activity assay showing increased activity of USP1-UAF1 on DNA-loaded PCNA-Ub compared to PCNA-Ub (-DNA) and PCNA-Ub (+DNA, +RFC and not ATP).
D) Quantification of gel-based activity assays showing enhanced activity of USP1+UAF1 on DNA-loaded PCNA-Ub compared to free PCNA-Ub (n=3).
E) Quantification of gel-based activity assays showing enhanced activity of USP1 on DNA-loaded PCNA-Ub compared to free PCNA-Ub (n=3).

551327-L-bw-Dharadhar
Processed on: 30-12-2020
PDF page: 109

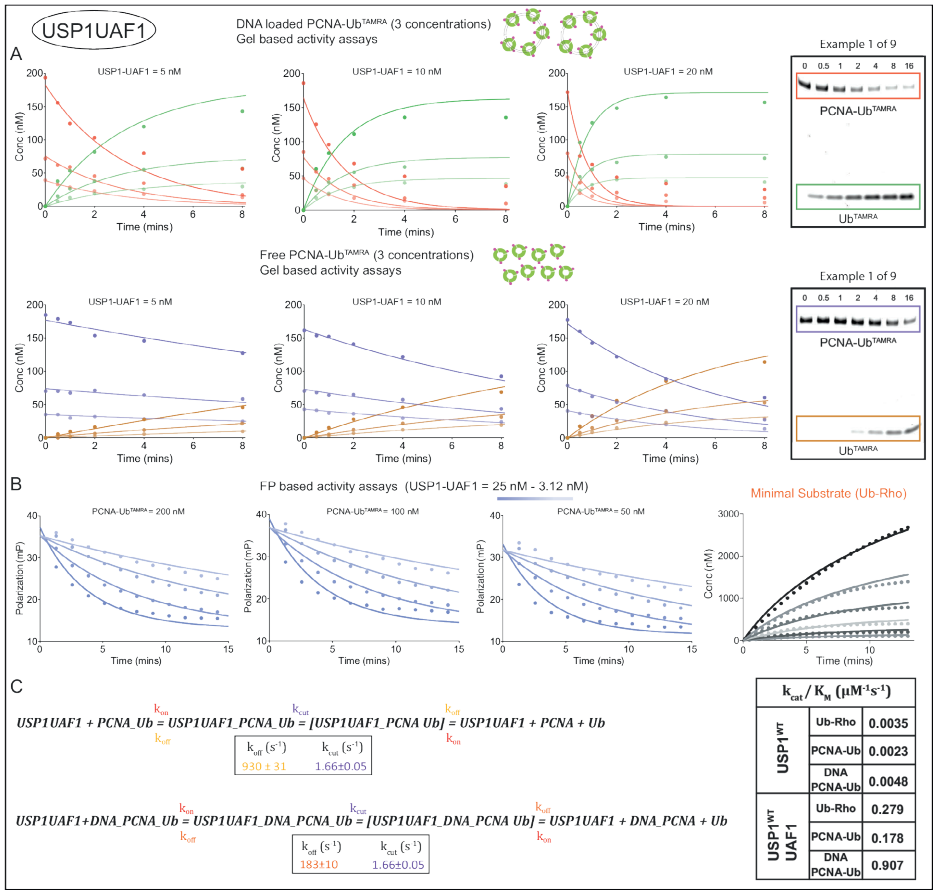

Fig.4) Modelling the enhanced USP1 activity on DNA-loaded PCNA-Ub.
A) Gel based quantification of USP1-UAF1 activity on PCNA-Ub (DNA loaded and free) for three different concentration of enzyme and substrate.
B) FP based activity assays on free PCNA-Ub (three concentrations of USP1 and PCNA-Ub) and activity of USP1 on increasing concentrations of Ub-Rho.
C) Kinetic model of USP1-UAF1 activity on PCNA-Ub and DNA-loaded PCNA-Ub (Ub-Rho not shown here, see EV 4c for full model), constants with the same colour were linked during the fitting and they share same values.

USP1 deubiquitinates PCNA-Ub more efficiently when it is loaded on DNA

We compared the deubiquitination activity of USP1 (±UAF1) on DNA-loaded PCNA-Ub with free PCNA-Ub in a gel-based activity assay. This showed that USP1-mediated ubiquitin hydrolysis is much faster when PCNA-Ub is loaded on DNA (Fig 3c, d, e). In these experiments a minor fraction of the RFC co-eluted with DNA-loaded PCNA-Ub which allowed reloading of PCNA-Ub. However, this is not critical for the enhanced activity that we observe, as our control experiments with RFC and DNA in the absence of ATP do not show similar activity of USP1 (Fig 3c).

To obtain a detailed mechanism of USP1 activity, we performed kinetic analysis and modelling using the *KinTek explorer* software (Johnson *et al*, 2009a). We quantified USP1 (±UAF1) activity data under either different enzyme concentrations or different substrate concentrations against three different substrates, Ub-Rho, PCNA-Ub and DNA-loaded PCNA-Ub. We used SDS PAGE-based setup for DNA-loaded PCNA-Ub and free PCNA-Ub (Fig.4a, Fig EV4a). For PCNA-Ub we additionally performed fluorescence polarization (FP) based activity assays. Additionally, activity data of USP1 (±UAF1) on increasing concentrations of Ub-Rhodamine was also included (Fig 4b, Fig EV4b). The resulting data only fits in a model where the enhanced activity on DNA-loaded PCNA-Ub is mediated by an increase in affinity of USP1 (± UAF1) for the substrate with no change in catalytic activity. The *KinTek* analysis allowed us to quantify the magnitude of enhanced USP1 activity both in the presence and absence of UAF1. We observed that loading of PCNA increases USP1 activity ~2-fold, but in the presence of UAF1 the increase is 5-fold (Fig 4c). The extra increase in USP1 activity given by UAF1 was caused by an increase in affinity for DNA-loaded PCNA-Ub of USP1+UAF1, as the change is limited to K_M. This observation corresponds well with previously published data which show that UAF1 itself has DNA binding properties in the range of 400nM (Liang *et al*, 2019). To validate our kinetic modelling, we performed EMSA based binding analysis for USP1 (±UAF1) on DNA which confirmed that USP1-UAF1 has stronger binding compared to USP1 alone (Fig EV4d). Altogether, our quantitative kinetic analysis shows that USP1 alone has enhanced activity on the natural substrate which is further strengthened when in complex with UAF1.

Table 2 KinTek modelling of USP1 (±UAF1) activity on three substrates i.e. Ub-Rho, PCNA-Ub and DNA-loaded PCNA-Ub

	Units	- UAF1			+UAF1		
		Ub-Rho	**PCNA-Ub**	**DNA-PCNA-Ub**	**Ub-Rho**	**PCNA-Ub**	**DNA-PCNA-Ub**
k_{on} *	$\mu M^{-1}s^{-1}$	100	100	100	100	100	100
k_{off} *	s^{-1}	594 ± 24	930 ± 31	433±8	594 ± 24	930 ± 31	183±10
k_{cat} (k_{cut})*#	s^{-1}	0.021±0.001	0.021±0.001	0.021±0.001	1.66±0.05	1.66±0.05	1.66±0.05
K_M	µM	5.94 ± 0.24	9.3 ± 0.31	4.33 ± 0.08	5.94 ± 0.24	9.3 ± 0.31	1.83 ± 0.01
k_{cat}/K_M	$\mu M^{-1}s^{-1}$	0.0035 ± 0.0002	0.0023 ± 0.0001	0.0048 ± 0.0002	0.279 ± 0.014	0.178 ± 0.008	0.907 ± 0.027

(* Constants with the same colour were linked during the fitting and they share same values)
(# Although k_{cut} mathematically is not equivalent to Michaelis-Menten catalytic rate constant k_{cat} the difference in the values between them in this model is neglectable in comparison to measurement and fitting errors)

551327-L-bw-Dharadhar
Processed on: 30-12-2020

Insert L1 is critical for enhanced activity of USP1 on DNA-loaded PCNA-Ub

To dissect how USP1 has higher activity on DNA-loaded PCNA-Ub, we compared how insert deletions affected the activity on DNA-loaded PCNA-Ub relative to free (unloaded) PCNA-Ub. The USP1$^{\Delta L2}$ and USP1$^{\Delta L3}$ showed similar activity to USP1^{WT} in cleaving PCNA-Ub by loading on DNA, but the USP1$^{\Delta L1}$ mutant showed no increase in activity on the loaded substrate (Fig 5a). The activity of USP1$^{\Delta L1}$ on PCNA-Ub is weak, and upon DNA loading its activity is not enhanced, in fact the activity is slightly lowered. These experiments show that the insert L2 and L3 within USP1 are not involved in enhancing USP1 activity while insert L1 is solely responsible for achieving this substrate dependent increase in USP1 activity.

Since insert L1 has been previously shown to possess both PCNA and DNA binding properties, we tested if both these functions could be responsible for increased USP1 activity on DNA loaded PCNA-Ub, relative to PCNA-Ub alone. To test how DNA binding could alter USP1 activity, we had to first identify residues involved in DNA binding so that we could separate the DNA and PCNA binding roles of insert L1. We analysed the insert L1 sequence using multiple sequence alignment and identified a region within insert L1 with several positively charged residues, which are well conserved across vertebrates (Fig 5b). Insert L1 WT and three sets of triple mutants containing charge swaps were cloned and then purified for DNA binding studies using SPR. Our binding experiments showed that insert L1 can bind DNA whereas all the triple mutants almost completely lost DNA binding (Fig 5c), thereby highlighting the role of electrostatic interaction in USP1 binding to DNA.

Insert L1 mediated DNA and PCNA interactions are crucial for increasing USP1 activity on DNA loaded PCNA-Ub

Insert L1 of USP1 is a large insert of 200 amino acids with two distinct well conserved regions for which we show interaction with DNA and PCNA respectively. To gain further mechanistic insight into the insert L1 mediated increase of USP1 activity, we compared the activity of a USP1 DNA binding mutant (USP1^{DM1}; KKK281EEE) and a USP1 PCNA interaction mutant (USP1^{PIP1}) on DNA loaded PCNA-Ub with free PCNA-Ub. In both mutants, the increase in activity on the DNA-loaded substrate was substantially reduced relative to USP1^{WT} (Fig 5d).

551327-L-bw-Dharadhar
Processed on: 30-12-2020
PDF page: 112

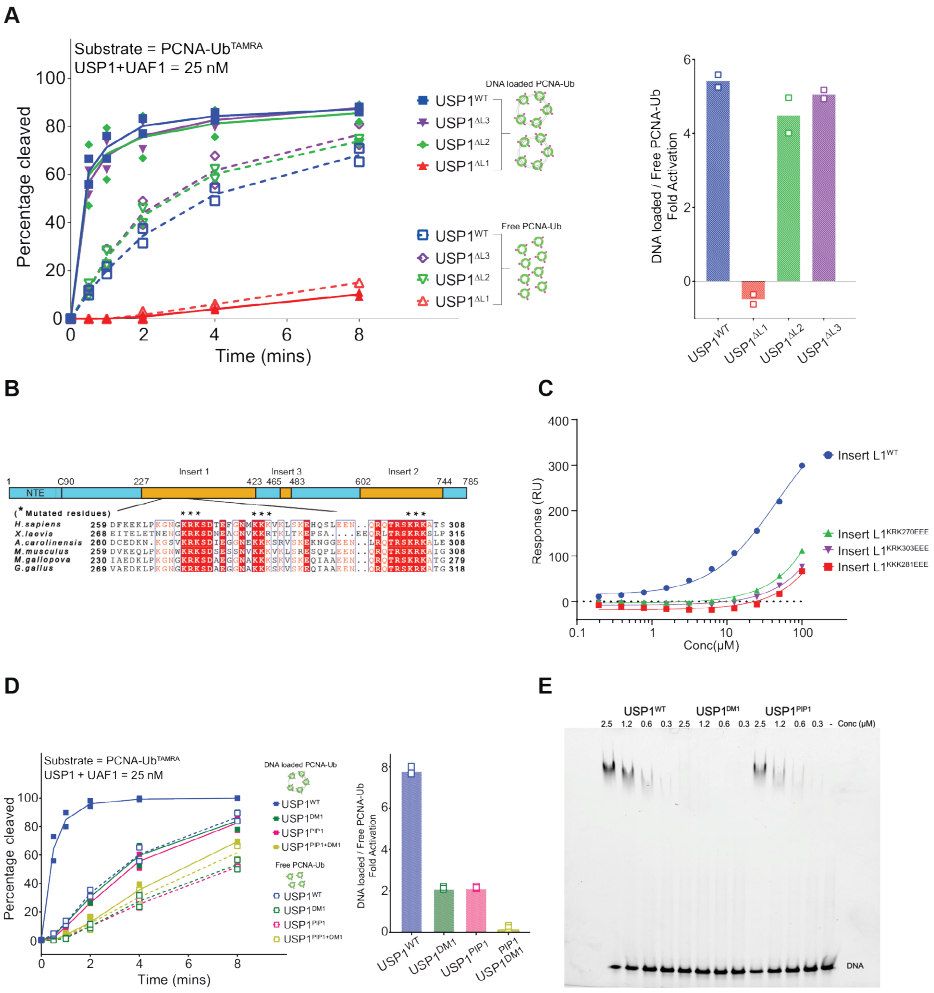

Fig.5) Insert L1 mediated DNA and PCNA interactions are crucial for increase in USP1 activity on DNA loaded PCNA-Ub

A) Comparison of USP1^{WT} and deletion mutants (+UAF1) for activity on DNA-loaded PCNA-Ub (solid lines) and free PCNA-Ub (dashed lines) shows no increase in USP1$^{\Delta L1}$ activity on the loaded substrate. Left panel: Quantification of gel-based activity assays showing percentage of cleaved PCNA-Ub at the mentioned time points (n=2), Right panel: Quantification of the activation fold observed in USP1^{WT} and mutants on DNA-loaded PCNA-Ub versus free PCNA-Ub (n=2).

B) Multiple sequence alignment of USP1 insert L1 which highlights the DNA binding region and the conservation of the positively charged residues across species, the residues mutated in this region are indicated with an asterisk.

C) SPR based binding experiments show binding of insert L1 (WT) to double stranded DNA (65bp) and the importance of the positively charged residues (see Fig 5b) of insert L1 in DNA binding.

D) Comparison of USP1^{DM1}, USP1^{PIP1} and USP1$^{PIP1+DM1}$ (+UAF1) activity on DNA-loaded PCNA-Ub (solid lines) and free PCNA-Ub (dashed lines) shows reduced increase in activity of these mutants compared to USP1^{WT}. Left panel: Quantification of gel based activity assays showing percentage of cleaved PCNA-Ub at the mentioned time points (n=2), Right panel: Quantification of the activation fold observed in USP1^{WT}, USP1^{PIP1}, USP1^{DM1} and USP1$^{PIP1+DM1}$ on DNA-loaded PCNA-Ub versus free PCNA-Ub (n=2).

E) EMSA based DNA binding experiment shows that USP1^{PIP1} and USP1^{WT} has similar DNA binding capability while USP1^{DM1} has lost its ability to bind DNA.

The USP1^{DM1} mutant also has reduced activity on free PCNA-Ub compared to USP1^{WT}. This means that we cannot fully confirm whether its loss in activity on the DNA-loaded substrate is due to loss of DNA interaction. To delineate this further we made a milder version (USP1^{DM2}, KKK281AEA) of the original DNA binding mutant (USP1^{DM1}). The USP1^{DM2} has similar activity on free PCNA-Ub as USP1^{WT} but still lost DNA binding ability when compared with USP1^{WT} (Fig EV5a, b). When USP1^{DM2} was tested on DNA loaded PCNA we found that it was poorly able to activate on this substrate, similar to USP1^{DM1} (Fig EV5c). Taken together these mutants confirm that DNA interaction through insert 1 is important for enhanced USP1 activity on DNA loaded PCNA-Ub.

In contrast, the PCNA-interaction mutant USP1^{PIP1}, had retained the ability to bind DNA, in an electrophoretic mobility shift assay on a 65bp dsDNA (Fig 5e). This indicates that USP1^{PIP1} is only affected in PCNA interaction and the loss of activity on DNA-loaded PCNA-Ub in this mutant is due to the defect in PCNA interaction.

Both the USP1^{DM1} and USP1^{PIP1} mutant still show considerable increase in activity on DNA-loaded PCNA-Ub, although to a lesser degree than USP1^{WT}. Therefore, we generated a USP1 double mutant lacking both DNA and PCNA interactions (USP1$^{PIP1+DM1}$) and compared its activity on DNA loaded PCNA-Ub and free PCNA-Ub. This double mutant has a very slightly enhanced activity on both substrates, but no significant difference between the two, indicating that it has completely lost the ability to enhance USP1 activity on DNA-loaded PCNA-Ub. The complete loss of substrate-mediated activity increase in this USP1 mutant shows that PCNA interaction and DNA interaction together are necessary and sufficient for the increase in USP1 activity.

Altogether, these experiments establish insert L1 as a central regulatory hub for USP1 activity and highlight the role of various elements which play a role in allosteric regulation of USP1 activity. These mutations could be used for validation in vivo, but unfortunately the DNA-binding site overlaps with the previously assigned NLS, suggesting some difficulties in separating these functions out, Nevertheless, these newly identified USP1 hotspots are important as they may serve as novel starting points for development of specific allosteric modulators of USP1 function.

USP1 is activated by two distinct mechanisms involving UAF1 and DNA-loaded PCNA-Ub

The activation of USP1 by UAF1 takes place through an allosteric mechanism where the catalytic turnover (k_{cat}) of the enzyme is increased several fold (Cohn *et al*, 2007). We have shown here that this activation requires the rearrangement of insert L1 and L3

551327-L-bw-Dharadhar
Processed on: 30-12-2020
PDF page: 114

which auto-inhibit USP1 in the absence of UAF1 (Fig 1d, e; Table 1). In this study we also uncover a secondary step that enhances USP1 activity which is caused upon interaction with DNA-loaded PCNA-Ub.

Based on our preliminary biochemical analysis we assumed that the increase in USP1 activity on DNA-loaded PCNA-Ub takes place solely through a change in the affinity of the enzyme for the loaded substrate versus the unloaded substrate, as cleavage rate values remained similar in individual runs. Therefore, they were linked in the final analysis accordingly (Fig EV4, Table 2).

Interestingly we note that not only USP1-UAF1 is activated by DNA-loading of PCNA, but also USP1 alone, which shows an increase in catalytic efficiency of from 2.3 mM^{-1} s^{-1} to 4.8 mM^{-1} s^{-1}. This confirms that also in the absence of UAF1 USP1 has higher activity on the DNA-loaded substrate. The PCNA and DNA interaction regions of Insert L1 are likely to play a key role in this since we have shown that mutating these two regions leads to no increase in activity.

Nevertheless, the increase in activity is larger in the presence of UAF1, increasing from 178 mM^{-1} s^{-1} on PCNA-Ub to 907 mM^{-1} s^{-1} on DNA-loaded PCNA-Ub (Table 2, Fig 4c), primarily due to a difference in K_{off}. In both USP1 and USP1-UAF1, the enzyme is faster on DNA-loaded PCNA-Ub, but the increase in activity due to DNA-loading is higher in the presence of UAF1: 5-fold increase in USP1-UAF1 and a 2-fold increase in USP1 alone (Table 2, Fig 4c).

Recently, it has been shown that USP1 activity on Ub-FANCD2 is higher in the presence of DNA and this is dependent on UAF1 binding (Liang *et al*, 2019). This suggests that the DNA interaction of UAF1 may help to increase the affinity of USP1 for DNA-loaded PCNA-Ub (Fig 4, Fig EV4). Apparently USP1 activity is regulated by two separate mechanisms, one which involves the change in catalytic turnover upon UAF1 binding while the other involves a change in affinity towards its natural substrate i.e. DNA-loaded PCNA-Ub (Fig 6). Therefore, we propose that UAF1 activation and DNA-loaded Ub-PCNA mediated enhancement of USP1 activity are mechanistically independent of each other.

551327-L-bw-Dharadhar
Processed on: 30-12-2020
PDF page: 115

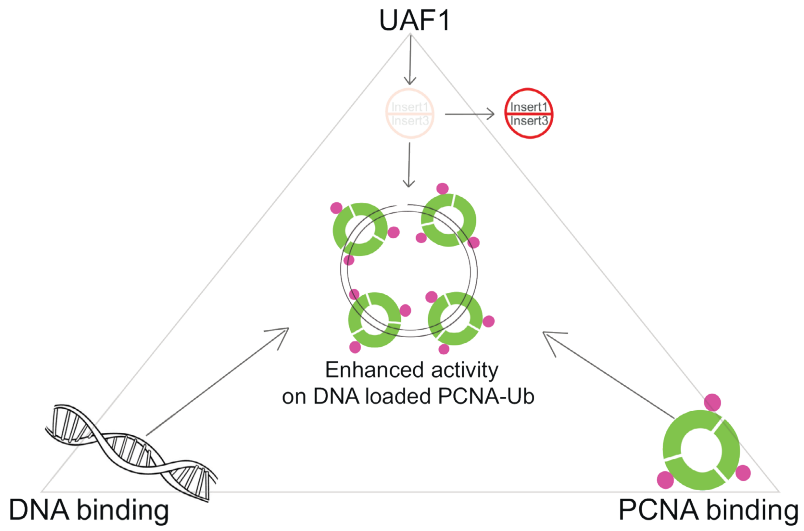

Fig.6) Schematic model for USP1 activity regulation by UAF1 and DNA loaded PCNA-Ub

MATERIALS AND METHODS

Plasmids and cloning

Human USP1 and UAF1 (WDR48) constructs were obtained from Martin Cohn (University of Oxford). Human WDR20 (isoform 5) was subcloned from the HAP1 cell line (Essletzbichler *et al*, 2014) into pGEXNKI-GST3C-LIC vector (Luna-Vargas *et al*, 2011) for expression in *Escherichia Coli*. Plasmid pBL481 for overexpression of the entire RFC complex was a gift from Peter Burgers (Washington University, St. Louis). A 1.7Kb circular plasmid (RC1766) used for PCNA-Ub loading was a gift from Rafael Fernández Leiro (CNIO, Madrid). The USP1 constructs were all cloned in the pFastbac-HTb vector (N-terminal His tag) while the UAF1 construct was cloned into the pFastbac1 vector (N-terminal Strep tag) for expression in *Spodoptera frugiperda* (*sf*9) cells. USP1 point mutants were generated using QuikChange site directed mutagenesis and mutants were confirmed by sequencing. USP1 insert 1 (230-420) was cloned into the pGEXNKI-GST3C-LIC vector and the ^{Cys}Ubiquitin construct was cloned into the pETNKI-His-SUMO2-kan vector for expression in *Escherichia Coli* (Luna-Vargas *et al*, 2011). Plasmids used for PCNA, Uba1 (E1), UbCH5C (S22R), ubiquitin and have been described previously (Hibbert & Sixma, 2012).

Protein expression and purification

Complexes of recombinant UAF1 with USP1 wild type and mutant proteins (USP1^{KKK281EEE}, USP1^{PIP1,2},USP1 insert deletions) were co-expressed and co-purified from *sf*9 cells as described previously (Dharadhar *et al*, 2019). Complex of USP12-UAF1 protein was co-

551327-L-bw-Dharadhar
Processed on: 30-12-2020
PDF page: 116

expressed and co-purified from *sf*9 cells as described previously (Dharadhar *et al*, 2016). PCNA, UBA1, ubiquitin and UbCH5c (S22R) (UBE2D3) were expressed and purified from *Escherichia Coli* as described previously (Hibbert & Sixma, 2012).

Purification of USP1

In experiments where USP1 was used without UAF1, both USP1 wild type and deletion mutants were expressed by Baculovirus expression in *sf*9 cells for 72 hours by infecting cells at a density of 1 $X10^6$ cells/ml. Cells were harvested in lysis buffer (50mM Tris pH 8.0, 200mM NaCl, 5mM TCEP) with complete EDTA-free protease inhibitor (Sigma) and lysed by sonication. The lysed cells were spun down (53000 x *g* for 30 minutes) in a high-speed centrifuge at 4°C and the supernatant was loaded on a column of Ni^{2+}-Sepharose beads pre-equilibrated in lysis buffer. Once the supernatant had passed through the column, it was washed with 30 column volumes (CV) of wash buffer (lysis buffer + 20mM Imidazole pH 8.0) and then USP1 was eluted with 5CV of elution buffer (lysis buffer + 500mM Imidazole pH 8.0). The elution fraction was diluted two-fold with 50mM Tris pH 8.0 and loaded on an anion exchange column (Resource Q, GE Healthcare) pre-equilibrated with 50mM Tris pH 8.0, 100mM NaCl, 2mM DTT (IEX buffer). The column was washed with 3CV of IEX buffer and elution was carried out by applying a salt gradient of 20CV from 100mM - 1M NaCl. Fractions containing USP1 were combined and concentrated at 4°C in an Amicon Ultra-15 centrifugal filter unit (30 kDa cut-off; Merck) and then loaded on a size exclusion column (Superdex 200 10/300; GE) equilibrated in 20mM HEPES pH 7.5, 150mM NaCl, 2mM DTT (SEC buffer). Pure USP1 fractions were concentrated at 4°C and stored at -80°C.

Purification of USP1 insert L1

Insert L1 wild type and mutant proteins were expressed in BL21 (*E. coli)* cells by inducing cells at an OD of 0.8 with 0.2mM IPTG followed by overnight expression at 18°C. Cells were harvested in lysis buffer (50mM Tris pH 8.0, 200mM NaCl, 2mM DTT) with complete EDTA-free protease inhibitor (Sigma) and lysed by sonication. The lysed cells were spun down (53000 x *g* for 30 minutes) in a high-speed centrifuge at 4°C and the lysate was loaded on a column of Glutathione Sepharose 4B beads (GE Healthcare) pre-equilibrated in lysis buffer. Once the lysate had passed through the column, it was washed with 30CV of lysis buffer following which insert 1 was eluted with 5CV of elution buffer (lysis buffer + 50mM reduced glutathione). GST-tag was cleaved in 2 hours with 3C protease while dialysing against 20mM Tris pH 8.0, 100mM NaCl, 2mM DTT (Heparin buffer). The sample was collected from the dialysis bag and loaded on a Heparin column (GE Healthcare) pre-equilibrated in Heparin buffer. After sample application, the column was washed with 3CV of Heparin buffer and protein was eluted using a salt gradient of

551327-L-bw-Dharadhar
Processed on: 30-12-2020
PDF page: 117

20CV from 100mM - 1M NaCl. Fractions containing pure insert 1 were combined and concentrated at 4°C in an Amicon Ultra-15 centrifugal filter unit (10 kDa cut-off; Merck) and then loaded on a size exclusion column (Superdex 200 10/300; GE) equilibrated in SEC buffer. Pure insert 1 fractions were concentrated at 4°C and stored at -80°C.

Purification of GST-WDR20

GST-WDR20 was expressed in BL21 (*E. coli*) cells by inducing at an OD of 0.8 with 0.2mM IPTG followed by overnight expression at 18°C. Cells were harvested in lysis buffer (50mM Tris pH 7.5, 200mM NaCl, 2mM DTT) with complete EDTA-free protease inhibitor (Sigma) and lysed by sonication. The lysed cells were spun down (53000 x *g* for 30 minutes) and the clarified lysate was loaded on a column of Glutathione Sepharose 4B beads (GE Healthcare) pre-equilibrated in lysis buffer. The beads were incubated with the lysate for 30 mins at 4C and then the lysate was allowed to pass through the column. The beads were washed with 30CV of lysis buffer and GST-WDR20 was eluted in 5CV of lysis buffer with 20mM reduced glutathione. The eluted sample was then loaded on a cation exchange column (POROS S, GE Healthcare) pre-equilibrated with 20mM Tris pH 7.5, 200mM NaCl, 2mM DTT (IEX buffer). GST-WDR20 eluted upon applying a salt gradient of 10CV from 200-1000mM NaCl. Fractions containing GST-WDR20 were combined and concentrated at 4°C in an Amicon Ultra-15 centrifugal filter unit (30 kDa cut-off; Merck).

Purification of PCNA-Ub^{TAMRA}

Ubiquitin with a cysteine residue introduced at the N terminus after the methionine at position 1 (^{Cys}Ubiquitin) was labelled using maleimide linked TAMRA dye (Setareh Biotech). The purification of ^{Cys}Ubiquitin and its labelling with maleimide linked TAMRA has been described previously (Dharadhar et al., 2019).

The components required for the *in vitro* mono-ubiquitination of PCNA are Ub^{TAMRA}, Uba1, PCNA and UbCH5c (S22R) (UBE2D3). Once all the components were purified, the reaction was setup as described previously to a final reaction volume of 20 ml (Hibbert & Sixma, 2012). Upon completion of the reaction, the PCNA-Ub^{TAMRA} was purified from the rest of the components using anion exchange chromatography followed by size exclusion chromatography in GF buffer. The purified sample was concentrated at 4°C in an Amicon Ultra-15 centrifugal filter unit (10 kDa cut-off; Merck) and stored at -80°C.

Purification of RFC

The procedure for the purification of the RFC complex was adapted from a previously described protocol by the Burgers lab (Gomes *et al*, 2000). Protein was expressed in *E. coli* grown in Terrific broth (TB) medium. Cells were induced at an OD of 1.6 with 0.2mM

551327-L-bw-Dharadhar
Processed on: 30-12-2020
PDF page: 118

IPTG followed by overnight expression at 16°C. The cells were harvested in lysis buffer (30mM HEPES 7.5, 200mM NaCl, 1mM DTT, 0.5mM EDTA, 10% Glycerol, 0.5mM PMSF, complete protease inhibitor) and lysed by sonication. The lysed cells were kept stirring on ice and 0.5% Polymin P was added followed by incubation for 5 minutes. The lysed cells were spun down at 53000 x *g* for 40 mins at 4°C and the supernatant was collected. Ammonium sulphate (0.28 g/ml) was added to the supernatant while stirring on ice for 30 minutes and then the precipitated proteins were collected by spinning at 12000 x *g* for 60 minutes. The proteins were resuspended in 30mM HEPES 7.5, 1mM DTT, 0.5mM EDTA, 10% Glycerol, 0.5mM PMSF, complete protease inhibitor followed by dialysis for 2 hours against 30mM HEPES 7.5, 100mM NaCl, 1mM DTT, 0.5mM EDTA, 10% Glycerol. The dialysed sample was loaded on a cation exchange column (POROS S 6ml, GE Healthcare) pre-equilibrated in 30mM HEPES 7.5, 100mM NaCl, 1mM TCEP, 10% Glycerol (PorosS buffer). Subsequently, the column was washed with 5CV of PorosS buffer and the protein was eluted by applying a salt gradient from 100mM – 1M NaCl. The fractions containing all 5 subunits of RFC are collected and loaded on Ni^{2+}-Sepharose beads pre-equilibrated in 20mM HEPES 7.5, 200mM NaCl, 10% Glycerol, 1 mM TCEP (His buffer). The column is then washed with 30CV of wash buffer (His buffer + 20mM Imidazole pH 8.0) and the protein is eluted with 5CV of elution buffer (20mM HEPES pH 7.5, 300mM NaCl, 300mM Imidazole pH 8.0, 10% Glycerol, 1 mM TCEP, 0.05% Ampholytes). Sample was concentrated at 4°C in an Amicon Ultra-15 centrifugal filter unit (10 kDa cut-off; Merck) and then loaded on a size exclusion column (Superdex 200 10/300; GE) equilibrated in 20mM HEPES pH 7.5, 200mM NaCl, 10% Glycerol, 1mM DTT, 0.05% Ampholytes. Fractions containing the RFC complex were concentrated at 4°C and stored at -80°C.

Production of Nicked Circular DNA

The RC1766 plasmid was nicked using a nicking endonuclease, Nt.BbvCI. The nicked circular DNA was then loaded on a size exclusion column (Superose 6 10/300; GE) equilibrated in 20mM HEPES pH 7.5, 150mM NaCl, 2mM DTT. The fractions containing the nicked circular DNA were collected and concentrated in an Amicon Ultra-15 centrifugal filter unit (10 kDa cut-off; Merck) up to a final concentration of 1µM.

Purification of DNA-loaded PCNA-Ub

To load PCNA-Ub on DNA, we added 10µM PCNA-Ub, 0.2µM nicked circular DNA and 1µM RFC in 20mM HEPES pH 7.5, 150mM NaCl, 10mM $MgCl_2$, 2mM ATP, 1mM DTT at a final volume of 500µl. The reaction was incubated at 4°C for 2 hours and then it was injected on a size exclusion column (Superose 6 10/300; GE) pre-equilibrated in 20mM HEPES pH 7.5, 100mM NaCl, 10mM $MgCl_2$, 0.5mM ATP, 1mM DTT. DNA-loaded PCNA-

551327-L-bw-Dharadhar
Processed on: 30-12-2020
PDF page: 119

Ub elutes at the void volume of the column and is ready to be used for downstream applications.

Ub-Rhodamine activity assays

Enzymatic activity was followed as release of fluorescent rhodamine from the quenched Ub-Rhodamine substrate (UbiQ; The Netherlands), providing a direct readout for DUB activity. The fluorescence intensity at 590 nm was measured using the Pherastar plate reader (BMG LABTECH GmbH, Germany). The assays were carried out in 384 well plates (Corning, flat bottom, low flange) at 25°C in a reaction buffer of 20mM HEPES pH 7.5, 150mM NaCl, 5mM DTT, 0.05% Tween-20. Single point assays were carried out at 1μM substrate concentration and different enzyme concentrations. The enzyme concentrations used are indicated in the figure. For the Michaelis Menten analysis, 100nM of USP1 and 10nM of USP1-UAF1 was used against different substrate concentration starting from 5μM to 0.1μM. The initial velocity rates were obtained from the slopes of the linear phase of the curve. These rates were plotted against substrate concentration and fitted with a Michaelis Menten model using non-linear regression in GraphPad Prism 7 software (GraphPad Software Inc., USA). Since the reaction velocity of $USP1^{L1L3}$ has not reached saturation, the K_M values obtained by this approach are unreliable. Therefore, the $USP1^{\Delta L1L3}$ activity curves were fitted in addition using Kintek Explorer version 8.0 (Kintek Corporation (Johnson *et al*, 2009a)) alongside $USP1^{WT}$ to establish if there is indeed a real change in the K_M values between the two enzymes.

Peptide substrate LRGG-AMC activity studies

Enzymatic activity was followed as a release of fluorescent AMC from the quenched LRGG-AMC substrate (Boston Biochem), providing a direct readout for DUB activity on a minimal peptide. The fluorescence intensity at 440 nm was measured using the Pherastar plate reader (BMG LABTECH GmbH, Germany). The assays were carried out in 384 well plates (Corning, flat bottom, low flange) at 25°C in a reaction buffer of 20mM HEPES pH 7.5, 150mM NaCl, 5mM DTT, 0.05% Tween-20. USP1 WT and mutants were tested at different concentrations against 100μM of LRGG-AMC, enzymes concentrations used are indicated in the figures.

Fluorescence Polarization based binding assay

The FP assays were carried out in 384 well plates at 25°C in a reaction buffer of 20mM HEPES pH 7.5, 100mM NaCl, 2mM DTT, 0.05% Tween-20. All USP1-UAF1 mutants tested also had their active site cysteine mutated to alanine which resulted in catalytically dead USP1-UAF1. These mutants were tested for binding to PCNA-Ub^{TAMRA} by measuring FP at varying concentrations of USP1-UAF1 (5μM-80nM) while keeping the PCNA-Ub^{TAMRA} at

551327-L-bw-Dharadhar
Processed on: 30-12-2020
PDF page: 120

a constant concentration of 25nM. The FP measurements were taken in the Pherastar plate reader (BMG LABTECH GmbH, Germany), using excitation wavelength of 540nm (±20) and the polarization was detected at 590nm (±20). The initial polarization of PCNA-Ub^{TAMRA} was set at 30 mp and any increase in polarization upon binding of USP1-UAF1 was plotted using GraphPad Prism 7 (GraphPad software Inc.,USA).

SPR based binding assay

SPR binding experiments were carried out in the Biacore T200 system (GE, USA) to test the binding of USP1 WT and mutants with double stranded DNA. The running buffer used for the SPR experiment was 20mM HEPES pH 7.5, 150mM NaCl, 2mM DTT, 0.05% Tween 20, 1mg/ml BSA and the DNA was immobilized on a Streptavidin chip (Sensor chip SA, GE) using the biotin present on the 5' end of the DNA. The binding experiments were carried out in the single cycle kinetics mode with 10 sequential injections of USP1 and $USP1^{\Delta L1}$ from 25μM to 0.05μM, while the insert 1 and mutants were injected from 100μM to 0.2μM. Data from a reference flow cell (- DNA) which was run in parallel to the experiment was subtracted from the signal using the Biacore T200 evaluation software. The final analysis and figures were done in GraphPad Prism 7 software (GraphPad Software Inc, USA).

Electrophoretic mobility shift assays (EMSA)

USP1 binding to DNA was also tested by performing EMSA's with native 4-12% pre-cast Tris-Glycine gels at 4ºC (Life Technologies). The gels were equilibrated by running them in Tris Glycine buffer at 125 V for 90 mins at 4ºC prior to the start of the actual experiment. USP1 and mutants were serially diluted to make a two-fold dilution series from 2.5μM to 0.3μM and the DNA was added to a final concentration of 0.2μM. The USP1-DNA samples were incubated at 4ºC for 15 mins prior to loading in the pre-equilibrated gel which was then run at 125 V for 90 mins at 4ºC. DNA bands were visualized by GelRed staining followed by imaging in a ChemiDoc XRS instrument (BioRad).

Gel based activity assays

PCNA-Ub^{TAMRA} cleavage assays were performed in a reaction buffer composed of 20mM HEPES pH 7.5, 100mM NaCl, 5mM $MgCl_2$, 0.25mM ATP, 2mM DTT. The cleavage reaction was started by addition of USP1 (±UAF1) followed by incubation at room temperature for the specified time course. The concentration of DUB used for the kinetic modelling experiments was 1μM, 0.5μM, 0.25μM for USP1 and 20nM, 10nM, 5nM for USP1-UAF1. All the mutants tested for activity on PCNA-Ub^{TAMRA} were in complex with UAF1 and they were run in parallel with wild type USP1 at a concentration of 25 nM. Samples were collected at the indicated time points and the reaction was stopped by adding SDS loading buffer.

551327-L-bw-Dharadhar
Processed on: 30-12-2020
PDF page: 121

Samples were loaded on NuPAGE 4-12% Bis-Tris SDS gel (Invitrogen) and separated by running them at 180 V for 30 mins. The TAMRA fluorescence signal was visualized using a Typhoon FLA-9500 gel scanner (GE Healthcare) and the concentration of PCNA-Ub^{TAMRA} and ubiquitin was quantified by comparing the TAMRA fluorescence of the individual bands with a calibration curve of TAMRA fluorescence in the same experimental setting.

Kinetic modelling of USP1 activity on DNA-loaded and free PCNA-Ub

Kintek Explorer version 8.0 (Kintek Corporation (Johnson *et al*, 2009a)) was used to fit the reaction mechanism. Cleavage data from three different substrates i.e Ub-Rhodamine, PCNA-Ub and DNA-loaded PCNA (Fig.4 and Sup. Fig.4) was used for the fitting simultaneously. The fitting presented here is based on all the data, but the model was built in stages. At first step, enzymatic activity assays data of USP1 and USP1-UAF1 on minimal substrate Ub-Rhodamine was fitted to a product inhibition model. Which includes three steps: substrate binding, substrate cleavage and product release. The associations rate constants of substrate and product binding (k_{on}) were set to diffusion limit approximation (100 $\mu M^{-1}s^{-1}$) and dissociation rate constants substrate and product (k_{off}) share the same value in both reactions. The results of the fitting (k_{cat}, K_M and k_{cat}/K_M) were compared with the results of Michalis-Menten calculations (Table 1).

$$k_{cat} = \frac{k_{cut} * k_{off}}{k_{cut} + k_{off}}$$

$$K_M = \frac{k_{off}}{k_{on}}$$

$$k_{cat}/K_M = \frac{k_{cut} * k_{on}}{k_{cut} + k_{off}}$$

k_{cut} – cleavage rate constant
k_{on} – substrate and product binding rate constant
k_{off} – substrate and product dissociation rate constant

Next, the enzymatic activity FP assays data on PCNA-Ub^{TAMRA} substrate was added to the analysis. Same model was used and in addition to previous constrains cleavage rate constant (k_{cut}) was shared same value for each enzyme, and k_{off} shared same value in the reactions with same substrate. In additions concentrations of enzymes and substrates were allowed to vary up to 5% from the theoretical value in order to compensate for experimental pipetting error. At the last step of model building the data from gel base enzymatic activity assays on PCNA-Ub^{TAMRA} and DNA-loaded PCNA-Ub^{TAMRA} substrates was added to the analysis. Same model and rate constraints were used for the fitting.

551327-L-bw-Dharadhar
Processed on: 30-12-2020
PDF page: 122

However, it was not possible to achieve good global fit of the date unless the value of k_{off} for USP1 in reaction with DNA-loaded PCNA-Ub^{TAMRA} was different from the value of k_{off} for USP1-UAF1 in reaction with DNA-loaded PCNA-Ub^{TAMRA}. Solution landscape analysis of the fitted parameters was done using FitSpace Editor (Johnson *et al*, 2009b). It showed correlation between values of k_{off} and k_{cut}. Thus, only their ratios and magnitude are directly defined within the model, meaning that the values of kinetic efficiency (k_{cat}/K_M) are giving the best representation of the modelling results.

ACKNOWLEDGEMENTS

We thank Niels Keizer and Andrea Murachelli for critical reading of the manuscript and other group members for their helpful suggestions. We thank Peter Burgers for the RFC construct and Martin Cohn for USP1 and UAF1 constructs. We thank Athanassios Adamopoulos for help with mutant cloning. We thank Farid El Oualid for providing us with Ub-Rhodamine. The authors acknowledge funding from the Dutch Cancer Society (KWF 2014-6858) and Oncode Institute.

Author Contributions

SD designed, performed and analysed biochemical experiments with assistance from TKS and AF. SD and SS performed mutant design and cloning. SD, SS and WJvD performed protein purification. Kinetic modelling using the KinTek software was done by AF. SPR experiments were done by SD and AF. TKS conceived and coordinated the study and SD wrote the paper with assistance from TKS. All authors reviewed the results and approved the final version of the manuscript.

Conflict of Interest

The authors declare that there is no actual or perceived conflict of interest on the part of any author.

Data Availability

This study includes no data deposited in external repositories.

551327-L-bw-Dharadhar
Processed on: 30-12-2020
PDF page: 123

REFERENCES

Arkinson C, Chaugule VK, Toth R & Walden H (2018) Specificity for deubiquitination of monoubiquitinated FANCD2 is driven by the N-terminus of USP1. *Life Sci Alliance* 1: 1–15

Cohn MA, Kee Y, Haas W, Gygi SP & D'Andrea AD (2009) UAF1 is a subunit of multiple deubiquitinating enzyme complexes. *J Biol Chem* 284: 5343–5351

Cohn MA, Kowal P, Yang K, Haas W, Huang TT, Gygi SP & D'Andrea AD (2007) A UAF1-Containing Multisubunit Protein Complex Regulates the Fanconi Anemia Pathway. *Mol Cell* 28: 786–797

Dharadhar S, Clerici M, Dijk WJ Van, Fish A & Sixma TK (2016) A conserved two-step binding for the UAF1 regulator to the USP12 deubiquitinating enzyme. *J Struct Biol*

Dharadhar S, Kim RQ, Uckelmann M & Sixma TK (2019) Quantitative analysis of USP activity in vitro 1st ed. Elsevier Inc.

Dungrawala H, Rose KL, Bhat KP, Mohni KN, Glick GG, Couch FB & Cortez D (2015) The Replication Checkpoint Prevents Two Types of Fork Collapse without Regulating Replisome Stability. *Mol Cell*

Eissenberg JC, Ayyagari R, Gomes X V & Burgers PM (1997) Mutations in yeast proliferating cell nuclear antigen define distinct sites for interaction with DNA polymerase delta and DNA polymerase epsilon. *Mol Cell Biol* 17: 6367–6378

Essletzbichler P, Konopka T, Santoro F, Chen D, Gapp B V., Kralovics R, Brummelkamp TR, Nijman SMB & Bürckstümmer T (2014) Megabase-scale deletion using CRISPR/Cas9 to generate a fully haploid human cell line. *Genome Res* 24: 2059–2065

Garcia-Santisteban I, Zorroza K & Rodriguez JA (2012) Two nuclear localization signals in USP1 mediate nuclear import of the USP1/UAF1 complex. *PLoS One* 7

Gomes X V., Gary SL & Burgers PMJ (2000) Overproduction in Escherichia coli and characterization of yeast replication factor C lacking the ligase homology domain. *J Biol Chem* 275: 14541–14549

Hibbert RG & Sixma TK (2012) Intrinsic flexibility of ubiquitin on proliferating cell nuclear antigen (PCNA) in translesion synthesis. *J Biol Chem* 287: 39216–39223

Huang TT, Nijman SMB, Mirchandani KD, Galardy PJ, Cohn M a, Haas W, Gygi SP, Ploegh HL, Bernards R & D'Andrea AD (2006) Regulation of monoubiquitinated PCNA by DUB autocleavage. *Nat Cell Biol* 8: 339–347

Johnson KA, Simpson ZB & Blom T (2009a) Global Kinetic Explorer: A new computer program for dynamic simulation and fitting of kinetic data. *Anal Biochem* 387: 20–29

Johnson KA, Simpson ZB & Blom T (2009b) FitSpace Explorer: An algorithm to evaluate multidimensional parameter space in fitting kinetic data. *Anal Biochem* 387: 30–41

Kee Y, Yang K, Cohn MA, Haas W, Gygi SP & D'Andrea AD (2010) WDR20 regulates activity of the USP12.UAF1 deubiquitinating enzyme complex. *J Biol Chem* 285: 11252–11257

Lee KY, Yang K, Cohn MA, Sikdar N, D'Andrea AD & Myung K (2010) Human ELG1 regulates the level of ubiquitinated proliferating cell nuclear antigen (PCNA) through its interactions with PCNA and USP1. *J Biol Chem* 285: 10362–10369

Li H, Lim KS, Kim H, Hinds TR, Jo U, Mao H, Weller CE, Sun J, Chatterjee C, D'Andrea AD, *et al* (2016) Allosteric Activation of Ubiquitin-Specific Proteases by ??-Propeller Proteins UAF1 and WDR20. *Mol Cell* 63: 249–260

Liang F, Longerich S, Miller AS, Tang C, Buzovetsky O, Xiong Y, Maranon DG, Wiese C, Kupfer GM & Sung P (2016) Promotion of RAD51-Mediated Homologous DNA Pairing by the RAD51AP1-UAF1 Complex. *Cell Rep* 15: 2118–2126

551327-L-bw-Dharadhar
Processed on: 30-12-2020
PDF page: 124

Liang F, Miller AS, Longerich S, Tang C, Maranon D, Williamson EA, Hromas R, Wiese C, Kupfer GM & Sung P (2019) DNA requirement in FANCD2 deubiquitination by USP1-UAF1-RAD51AP1 in the Fanconi anemia DNA damage response. *Nat Commun* 10: 1–8

Lim KS, Li H, Roberts EA, Gaudiano EF, Clairmont C, Sambel LA, Ponnienselvan K, Liu JC, Yang C, Kozono D, *et al* (2018) USP1 Is Required for Replication Fork Protection in BRCA1-Deficient Tumors. *Mol Cell* 72: 925-941.e4

Luna-Vargas MPA, Christodoulou E, Alfieri A, van Dijk WJ, Stadnik M, Hibbert RG, Sahtoe DD, Clerici M, Marco V De, Littler D, *et al* (2011) Enabling high-throughput ligation-independent cloning and protein expression for the family of ubiquitin specific proteases. *J Struct Biol* 175: 113–119

Mevissen TET & Komander D (2017) Mechanisms of Deubiquitinase Specificity and Regulation. *Annu Rev Biochem* 86: annurev-biochem-061516-044916

Nijman SMB, Huang TT, Dirac AMG, Brummelkamp TR, Kerkhoven RM, D'Andrea AD & Bernards R (2005) The deubiquitinating enzyme USP1 regulates the fanconi anemia pathway. *Mol Cell* 17: 331–339

Olazabal-Herrero A, García-Santisteban I & Rodríguez JA (2015) Structure-function analysis of USP1: insights into the role of Ser313 phosphorylation site and the effect of cancer-associated mutations on autocleavage. *Mol Cancer* 14: 33

Villamil MA, Liang Q, Chen J, Choi YS, Hou S, Lee KH & Zhuang Z (2012) Serine phosphorylation is critical for the activation of ubiquitin-specific protease 1 and its interaction with WD40-repeat protein UAF1. *Biochemistry* 51: 9112–9113

Yang K, Moldovan GL, Vinciguerra P, Murai J, Takeda S & D'Andrea AD (2011) Regulation of the Fanconi anemia pathway by a SUMO-like delivery network. *Genes Dev* 25: 1847–1858

Yin J, Schoeffler AJ, Wickliffe K, Newton K, Starovasnik MA, Dueber EC & Harris SF (2015) Structural Insights into WD-Repeat 48 Activation of Ubiquitin-Specific Protease 46. *Structure* 23: 2043–2054

Yoder BL & Burgers PMJ (1991) Saccharomyces cerevisiae replication factor C: I. purification and characterization of its atpase activity. *J Biol Chem* 266: 22689–22697

Zhao G, Gleave ES & Lamers MH (2017) Single-molecule studies contrast ordered DNA replication with stochastics translesion synthesis. *Elife* 6: e32177

551327-L-bw-Dharadhar
Processed on: 30-12-2020
PDF page: 125

SUPPLEMENTAL DATA

A

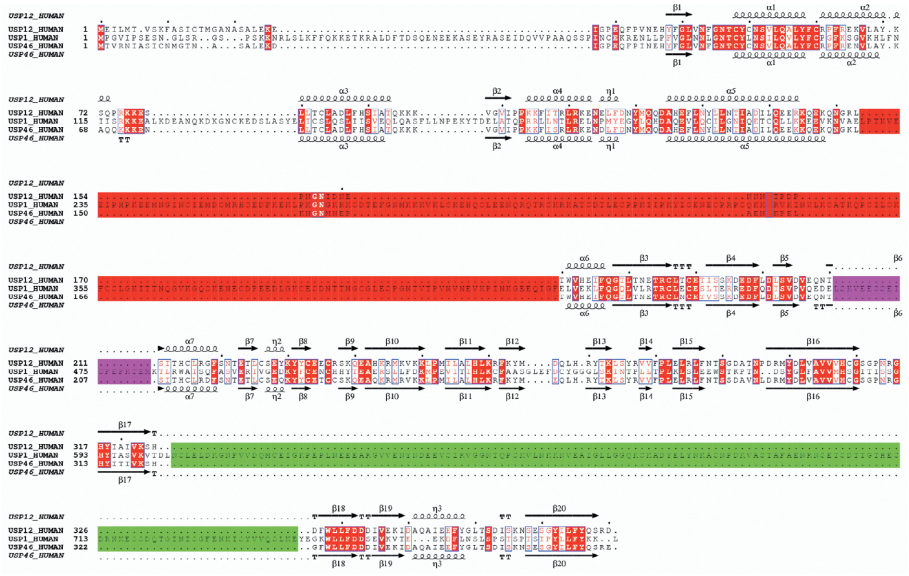

B

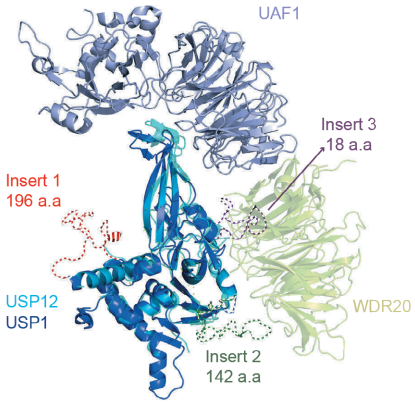

Fig EV1a) Structure based sequence alignment of USP1, USP12 and USP46 shows the relative positioning of inserts within USP1 which are highlighted as following, Insert 1 (red), Insert 2 (green) and Insert 3 (violet).
Fig EV1b) Homology model of USP1 (dark blue) based on the structure of USP12 (light blue) bound to UAF1 and WDR20 (green) highlights the positioning of USP1 inserts relative to its catalytic domain.

551327-L-bw-Dharadhar
Processed on: 30-12-2020
PDF page: 126

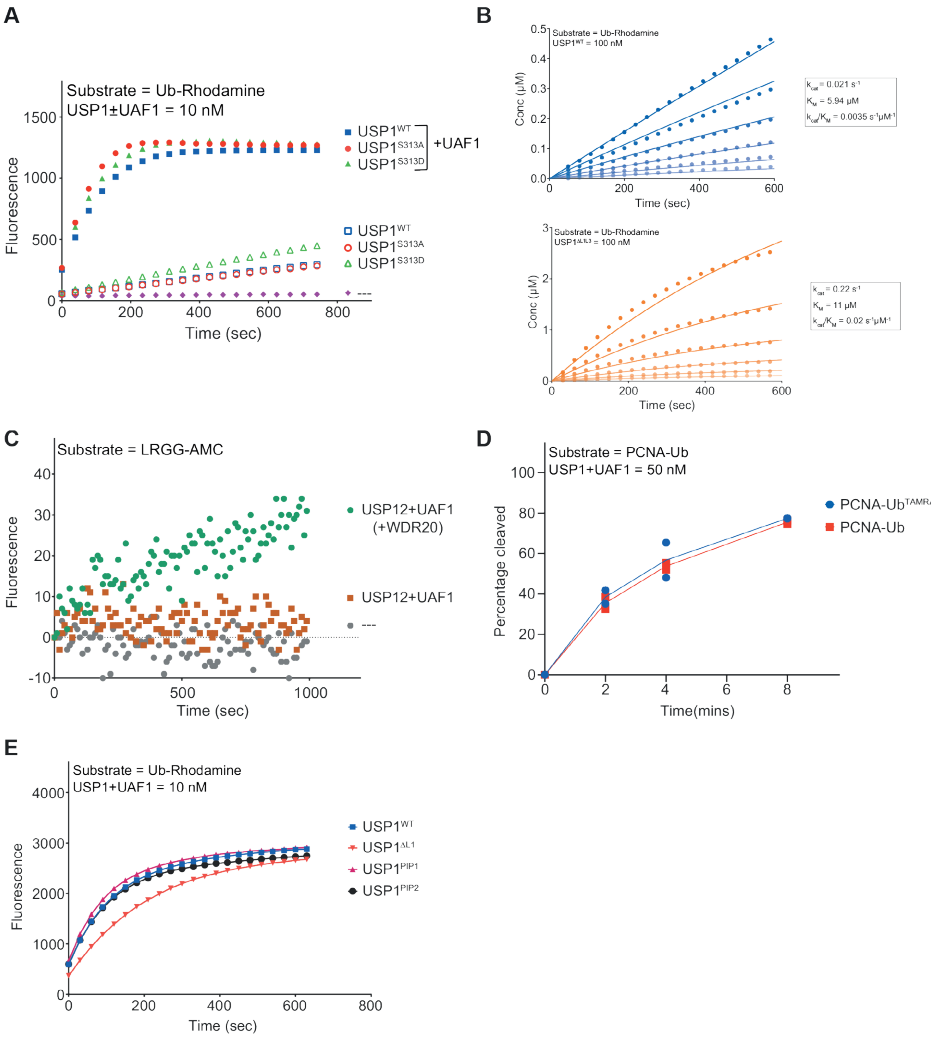

Fig EV2a) Single point activity assays of USP1^{WT}, USP1^{S313A}, USP1^{S313D} (+UAF1) shows no effect of these mutations on USP1 activity against the minimal substrate (Ub-Rho).
Fig EV2b) KinTek analysis of USP1$^{\Delta L1L3}$ and USP1^{WT} activity on Ub-Rhodamine reveals that activation of USP1$^{\Delta L1L3}$ is due to an increase in k_{cat}.
Fig EV2c) Comparison of USP1-UAF1 activity on PCNA-Ub and PCNA-Ub^{TAMRA} shows that the TAMRA label does not affect the rate of ubiquitin cleavage (n=2).
Fig EV2d) Single point activity assays of USP1^{WT}, USP1$^{\Delta L1}$ and USP1^{PIP} mutants (+UAF1) on Ub-Rho shows similar activity of all mutants compared to USP1^{WT}.

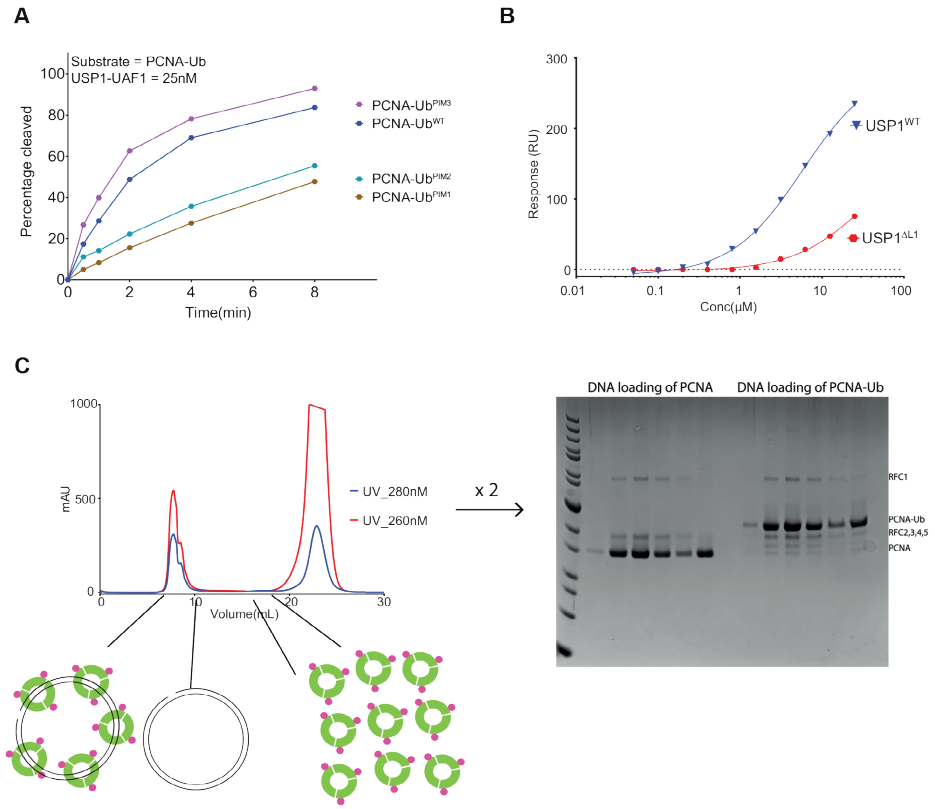

Fig EV3a) Comparison of USP1+UAF1 activity on PCNA-Ub^{WT} and PCNA-Ub^{PIM} mutants shows lower USP1 activity on PIM1 and PIM2 mutants.
Fig EV3b) SPR based binding experiments show that USP1$^{\Delta L1}$ has a reduced affinity for double stranded DNA (65bp) compared to USP1^{WT}.
Fig EV3c) RFC mediated PCNA-Ub loading on nicked circular DNA has the same efficiency as loading of PCNA. Left Panel: Schematic representation of the purification of DNA loaded PCNA-Ub, Right panel: Coomassie stained gel of fractions corresponding to the first (green) and second (orange) peak from SEC of the PCNA and PCNA-Ub loading reactions respectively.

551327-L-bw-Dharadhar
Processed on: 30-12-2020
PDF page: 128

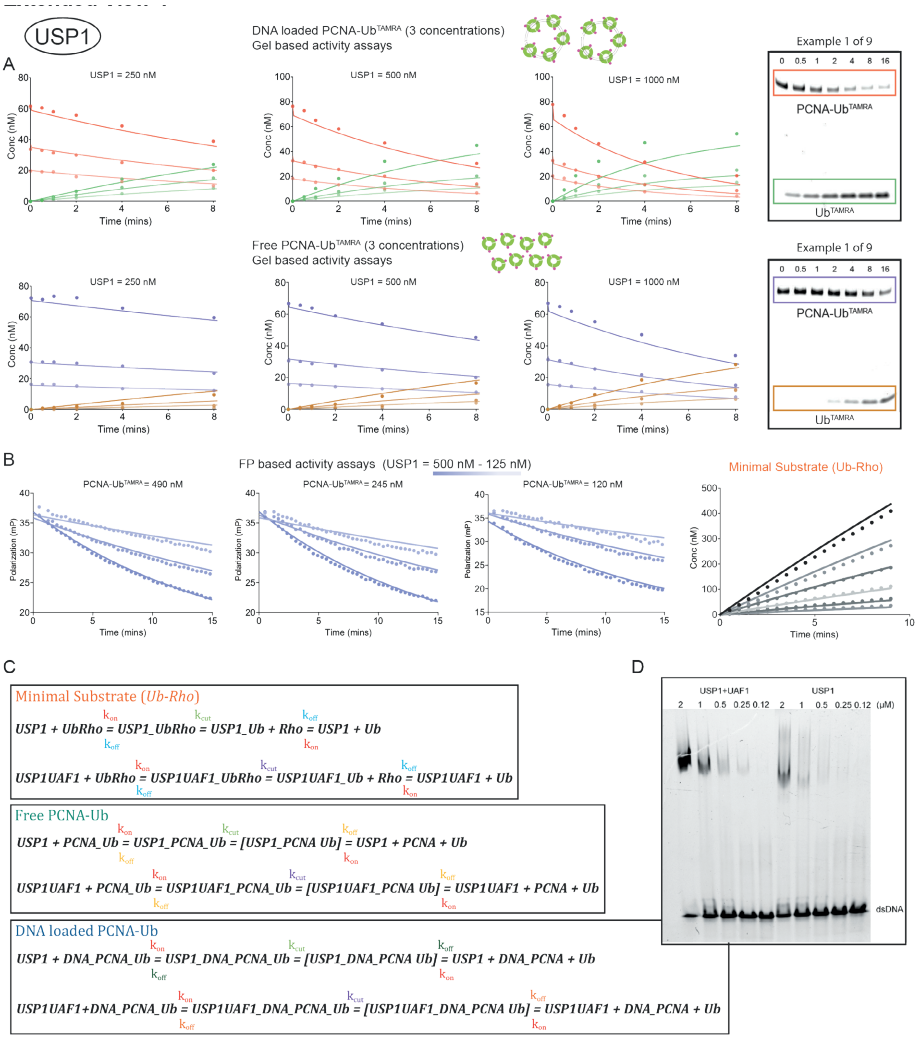

Fig EV4) USP1 activity data used for KinTek analysis of USP1 on Ub-Rho, free PCNA-Ub and DNA loaded PCNA-Ub.

Fig EV4a) Gel based quantification of USP1 activity on PCNA-Ub (DNA loaded and free) for three different concentration of enzyme and substrate.

Fig EV4b) FP based activity assays on free PCNA-Ub (three concentrations of USP1 and PCNA-Ub) and activity of USP1 on increasing concentrations of Ub-Rho.

Fig EV4c) Full kinetic model of USP1 activity on three different substrates, constants with the same colour were linked during the fitting and they share same values.

Fig EV4d) EMSA based DNA binding experiment validates our KinTek modelling as it shows that USP1-UAF1 has a higher DNA binding capacity compared to USP1 alone.

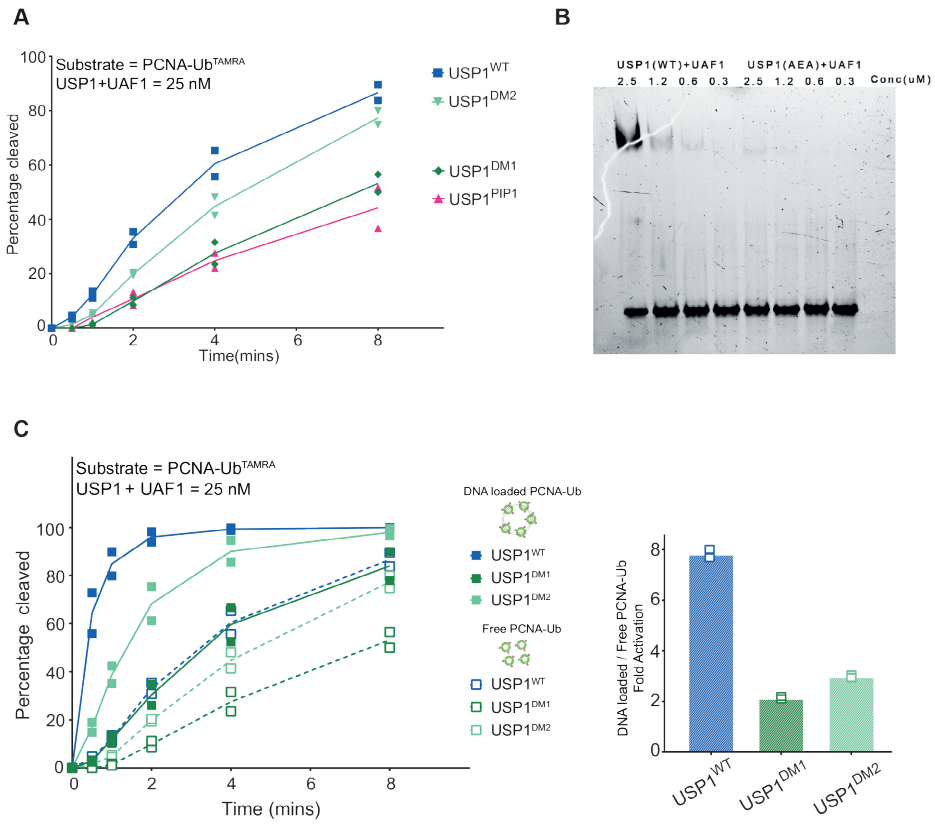

Fig EV5a) Comparing activity of USP1 mutants on free PCNA-Ub substrate (n=2).
Fig EV5b) EMSA based DNA binding experiment shows that USP1^{DM2} (AEA) has reduced binding compared to USP1^{WT}.
Fig EV5c) Comparing USP1 activity of DNA binding mutants and USP1^{WT} on DNA-loaded PCNA-Ub (solid lines) and free PCNA-Ub (dashed lines) shows reduced activation of the DNA binding mutants compared to USP1^{WT}. Left panel: Quantification of gel based activity assays showing percentage of cleaved PCNA-Ub at the mentioned time points (n=2), Right panel: Quantification of the activation fold observed in USP1^{WT}, USP1^{DM1} and USP1^{DM2} on DNA-loaded PCNA-Ub versus free PCNA-Ub (n=2).

551327-L-bw-Dharadhar
Processed on: 30-12-2020

551327-L-bw-Dharadhar
Processed on: 30-12-2020

CHAPTER 5

Studying the mechanism of RAD6-RAD18 mediated PCNA mono-ubiquitination.

Shreya Dharadhar[1], Serge Scheffers[1], Willem J. van Dijk[1], Titia K. Sixma[1]

[1]Division of Biochemistry and Oncode Institute, Netherlands Cancer Institute, Plesmanlaan 121, 1066 CX Amsterdam, The Netherlands

Manuscript in Preparation

ABSTRACT

During S phase, replication of damaged DNA relies on translesion DNA synthesis (TLS), a process where a special set of polymerases are recruited that can bypass the lesion. TLS polymerases get recruited to the damage site upon RAD6-RAD18 mediated mono-ubiquitination of PCNA. This is therefore an essential step for regulation of the TLS pathway. The E3 ligase RAD18 is a DNA binding protein and its ability to activate RAD6 (E2) is enhanced once PCNA is loaded on DNA. Here, we study this activation of RAD18 biochemically on DNA-loaded PCNA and this leads to novel mechanistic insights. Testing a series of mutants gives insight into a unique method of ubiquitin stabilization during PCNA modification. We identify a PIP motif within the RAD18 SAP domain which is essential for activity on free PCNA and obtain a mutant that separates DNA and PCNA interactions of the SAP domain. This helps to show that RAD18 DNA binding is sufficient for RAD18 activation on DNA-loaded PCNA unlike the PIP interaction which has no effect. The application of quantitative activity assays on DNA-loaded PCNA allows us to gain new insights into RAD18 mediated auto-ubiquitination as well as the role of the SAP domain in its activity on PCNA.

551327-L-bw-Dharadhar
Processed on: 30-12-2020
PDF page: 134

INTRODUCTION

In replication, DNA lesions can block the replicative polymerases, leading to fork stalling that could cause toxic double stranded breaks. To ensure genome duplication and continuation of the cell cycle, cells employ the DNA damage tolerance (DDT) pathways which promote damage bypass without removal of the lesion from the template strand. Translesion synthesis (TLS) is a DDT pathway where low fidelity translesion polymerases incorporate stable yet potentially faulty nucleotides opposite the damaged strand, thereby allowing the continuation of normal replication (Hedglin & Benkovic, 2017). Although, this pathway often leads to mutations, the cell is prepared to allow this as a trade-off to blocked replication which would lead to more toxic DNA damage.

The error prone TLS pathway is tightly regulated by (de)-ubiquitination of PCNA at a specific lysine residue (i.e.K164) (Choe & Moldovan, 2017). Upon fork stalling, PCNA is mono-ubiquitinated by the E2/E3 pair RAD6-RAD18 at K164. This ubiquitination leads to the recruitment of translesion polymerases at the replication fork (Hoege *et al*, 2002). RAD18 is the sole E3 ligase involved in this pathway as inactivation of RAD18 leads to loss of PCNA mono-ubiquitination and downstream recruitment of Polη (Tateishi *et al*, 2003; Watanabe *et al*, 2004). In vitro reconstitution of the ubiquitination reaction for yeast proteins, showed that RAD6-RAD18 mediated mono-ubiquitination of PCNA is greatly enhanced upon loading of PCNA on DNA by the replication factor complex (RFC) (Garg & Burgers, 2005; Haracska *et al*, 2006a). In this study we reconstitute the ubiquitination reaction using human PCNA and shed light on the mechanism of this activation.

RAD18 is a multi-domain RING E3 ligase that is active upon homodimerization mediated by its N-terminal RING domain. It belongs to the type 1 RING ligase class which are characterised by helical interactions between protomers (Huang *et al*, 2011). RAD18 binds RAD6 through a specialized RAD6 binding domain (R6BD) at the C-terminal and also through the canonical RING domain interaction (Watanabe *et al*, 2004; Huang *et al*, 2011). Other domains in RAD18 are a zinc-finger (ZnF) and a SAP domain, both of which have been shown to be essential for RAD18 activity on PCNA. How they relate to RAD18 activity is controversial, due to conflicting reports implicating them together or individually (Nakajima *et al*, 2006; Tsuji *et al*, 2008; Tateishi *et al*, 2000; Miyase *et al*, 2005; Notenboom *et al*, 2007a). Moreover, the function of these individual domains in RAD18 mediated mono-ubiquitination of DNA-loaded PCNA has not been studied biochemically.

The Zinc-Finger (ZnF) domain of RAD18 may be important for recruitment of RAD18 at damaged DNA and also for its auto-ubiquitination capability (Nakajima *et al*, 2006; Miyase *et al*, 2005). It was observed that a RAD18 construct containing residues 84-282 was

551327-L-bw-Dharadhar
Processed on: 30-12-2020
PDF page: 135

sufficient for RAD18 recruitment to damage sites and this could be disturbed by a single point mutation in the ZnF domain (C207F) (Nakajima *et al*, 2006). In another study, this same RAD18 C207F mutation resulted in lack of self-association of RAD18 resulting in loss of RAD18 auto-ubiquitination but did not affect PCNA mono-ubiquitination (Miyase *et al*, 2005). However, in vitro reconstitution showed that this mutant had identical activity on both PCNA and itself as $RAD18^{WT}$ (Notenboom *et al*, 2007a). Here, we have tried to bring some clarity on the role of the ZnF domain in RAD18 activity by studying the activity of a ZnF deletion construct on itself and PCNA.

RAD18 has been reported to bind DNA through its SAP domain, with a preference for single-stranded DNA when compared with double-stranded DNA (Bailly et al., 1997; Notenboom et al., 2007). Additionally, it has been demonstrated that RAD18 lacking the SAP domain is unable to carry out PCNA mono-ubiquitination in vitro. Mutations within the SAP domain that affect DNA binding have been identified but they also have an effect on PCNA mono-ubiquitination (Notenboom *et al*, 2007b; Tsuji *et al*, 2008). Collectively, these data indicate that the SAP domain contains both the DNA and PCNA interaction regions within RAD18. But the region within the SAP domain responsible for PCNA recognition remains to be identified. Since these two functions of the SAP domain have not been delineated, it is unclear if both these functions have a role in the activation of the ubiquitination reaction when PCNA is loaded on DNA.

The mechanism of RING-mediated ubiquitination is thought to be conserved between all members of the RING E3 ligases (Plechanovová *et al*, 2011; Dou *et al*, 2012; Pruneda *et al*, 2012). In dimeric RING ligases, ubiquitin is stabilized by a second, inactive monomer. In type 1 RING ligases this stabilization was shown to be mediated by a charged residue which is essential for engaging the thioester linked ubiquitin and promoting its transfer from the ubiquitin-loaded E2 (Densham *et al*, 2016). In the RAD18 RING domain, Arg 76 was identified as the crucial residue and upon mutation to alanine the levels of PCNA mono-ubiquitination upon UV damage were severely reduced. The mono-ubiquitination of PCNA by the R76A mutant was reduced but not completely lost which is unlike similar mutations of BRCA1-BARD1 and RING1B-BMI1, where the point mutant caused complete loss of activity.

In this study, we uncover novel mechanistic insights in the DNA mediated activation of PCNA mono-ubiquitination by RAD6-RAD18. We develop a quantitative in vitro ubiquitination assay with purified DNA-loaded PCNA and RAD6-RAD18 proteins. This allows us to demonstrate that the ZnF domain is not required for the ubiquitination activity of RAD18 on both free and DNA-loaded PCNA. We also study the role of the

551327-L-bw-Dharadhar
Processed on: 30-12-2020
PDF page: 136

SAP domain in DNA binding and PCNA function by mutagenesis which leads to the identification of a putative PCNA interaction motif (PIP). We obtain a mutant within the SAP domain that uncouples DNA binding and PCNA function. This allows us to highlight the importance of DNA binding in activation of PCNA mono-ubiquitination. Finally, we investigate the role of the R76A mutant in our activity assays and show that R76 is not the primary interface in RAD18 for ubiquitin transfer when PCNA is loaded on DNA.

RESULTS

Purification of PCNA loaded on circular DNA

RAD6-RAD18 mediated PCNA mono-ubiquitination is enhanced ~70-fold when PCNA is loaded on DNA (Garg & Burgers, 2005). To uncover mechanistic details of this activation we decide to set up a quantifiable ubiquitination assay on DNA-loaded PCNA. This requires purified DNA-loaded PCNA in sufficient amounts for biochemical studies. We use yeast RFC, as this was shown to be capable of loading human PCNA on DNA (Yoder & Burgers, 1991). We first purified all the components necessary for the loading reaction, i.e. PCNA, nicked circular DNA and RFC. Then, we optimized the PCNA loading reaction by varying RFC concentrations and incubation conditions. DNA-loaded PCNA was separated from free PCNA by size exclusion chromatography which resulted in large amounts of purified DNA-loaded PCNA (Fig.1b).

A gel-based ubiquitination assay was then set up to compare the activity of RAD6-RAD18 on DNA-loaded PCNA versus free PCNA. We confirmed that RAD6/RAD18 activity is increased significantly when its substrate PCNA is loaded on DNA (Garg & Burgers, 2005; Haracska *et al*, 2006b). We also analysed Rad18 auto-ubiquitination under these conditions, and found that this is not affected by the presence of DNA (Fig.1c). Together, these data suggest that the activation we observe upon PCNA loading on DNA is an effect that specifically activates the RAD6/RAD18 combination for ubiquitin transfer to K164 on PCNA, rather than a general activation, and conclude that DNA binding to Rad18 does not alter its intrinsic activity.

The RAD18 SAP domain is essential for its activity on PCNA

The SAP domain in RAD18 is important for its DNA binding function (Notenboom *et al*, 2007b; Tsuji *et al*, 2008; Davies *et al*, 2008). In a single study the SAP domain was shown to be critical for PCNA mono-ubiquitination (Tsuji *et al*, 2008). On the other hand, the ZnF domain has been proposed to be essential for self-association of RAD18 and for it auto-ubiquitination capability (Miyase *et al*, 2005). We purified a RAD6-RAD18 mutant lacking the SAP domain and another mutant lacking the Zinc-finger domain to test their activity on PCNA in our in vitro reconstitutions (Fig.1a). We confirmed that deletion of

551327-L-bw-Dharadhar
Processed on: 30-12-2020
PDF page: 137

the SAP domain leads to complete loss of activity on PCNA but does not affect Rad18 auto-ubiquitination. However, the Zinc finger deletion in Rad18 did not affect either auto-ubiquitination or activity on PCNA in our assay (Fig.1d).

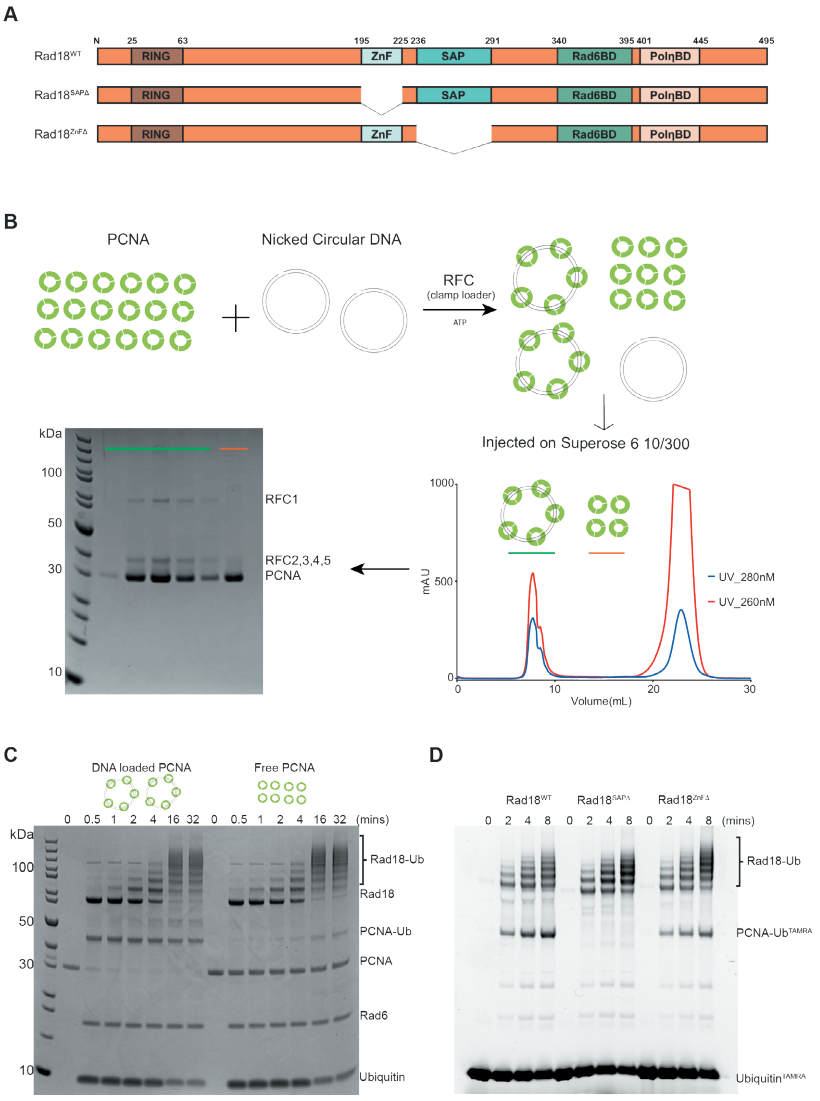

Fig.1) RAD6-RAD18 has enhanced activity on purified DNA-loaded PCNA
A) Schematic diagram of the RAD18 and RAD18 deletion mutants tested in this study.
B) Schematic representation of loading and purification of PCNA on nicked circular DNA. The DNA-loaded PCNA elutes in the void of the SEC column and this sample is collected and used for studying activity of RAD18 on DNA-loaded PCNA.
C) Coomassie stained gel of in vitro activity assay showing increased activity of RAD6-RAD18 on DNA-loaded PCNA compared to free PCNA (no DNA loading).
D) ^{TAMRA}UB signal of gel-based activity assays comparing activity of RAD18^{WT} with RAD18$^{\Delta ZnF}$ and RAD18$^{\Delta SAP}$.

The specific loss of activity in Rad18$^{SAP\Delta}$, only on PCNA, indicates the presence of a specific PCNA recognition element that is mediated by the RAD18 SAP domain. We analysed the sequence of the SAP domain in a multiple sequence alignment with different eukaryotes and identified a degenerate PCNA interacting peptide (PIP) motif (Fig.2a). Compared to traditional PIP motifs (Eissenberg *et al*, 1997), the new motif lacks the second of two aromatic residues (residue 285/286). We made three mutants within the PIP region, a double mutant (QV279AA: Q279A + V282A) and two single mutants (Q279A and Y285A). These mutants were co-purified with Rad6 and tested for activity on PCNA in a gel-based assay. The RAD18^{Y285A} mutant showed no activity on PCNA while the RAD18^{QV279AA} and RAD18^{Q279A} mutants showed reduced activity on PCNA compared to RAD18^{WT} (Fig.2b). We then tested DNA binding ability of the RAD18^{Y285A} mutant by performing electrophoretic mobility shift assays (EMSA) with a 65bp dsDNA. We observed that RAD18^{Y285A} had retained the ability to bind DNA similar to RAD18^{WT} (Fig.2c).

Several DNA binding mutants of the SAP domain that are more than 20 residues downstream of the PIP region have a severe effect on PCNA activity (Tsuji *et al*, 2008). We made four new mutants (NKQ270EEE: N270E+K271E+Q272E; K258E, K271E and K271E+K258E) to separate the DNA binding and PCNA activity functions. Additionally, we also made two mutants (HGL263AAA: H263A+G264A+L265A; GK269AA: G269A+K271A) which were known to affect DNA binding by the SAP domain, but their effect on RAD18 activity against PCNA had not been studied (Notenboom *et al*, 2007b). All these mutants were co-purified with RAD6 and their ability to bind DNA and mono-ubiquitinate PCNA was tested for DNA-binding (EMSA) and enzyme activity respectively. All of the mutants tested showed significant reduction in DNA binding compared to RAD18^{WT}. The RAD18^{K258E} and RAD18^{K271E} were less affected than RAD18^{HGL263AAA} and RAD18^{GK269AA} that almost completely lost DNA binding (Fig.2e). Similarly, none of these mutants was able to ubiquitinate PCNA as efficiently as RAD18^{WT}. The RAD18^{GK269AA} mutant showed complete loss of activity while low levels of PCNA mono-ubiquitination were observed in other mutants (Fig.2d).

551327-L-bw-Dharadhar
Processed on: 30-12-2020
PDF page: 139

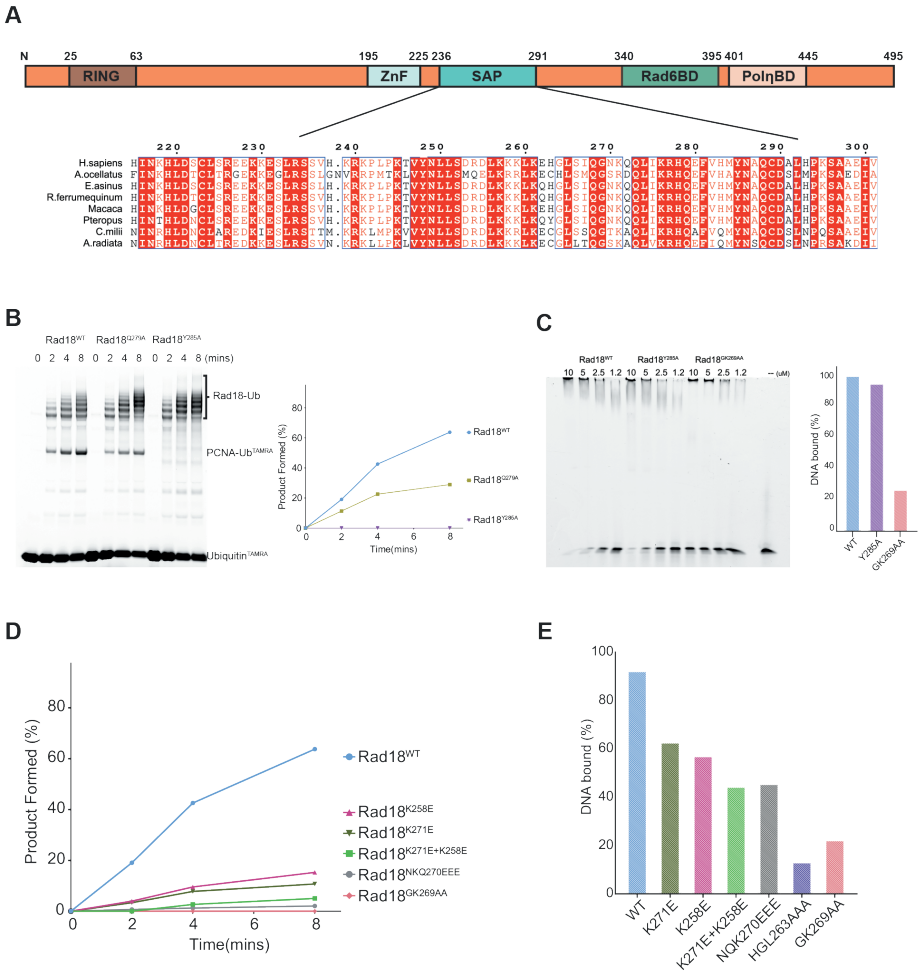

Fig.2) SAP domain is essential for RAD18 activity on PCNA
A) Multiple sequence alignment of RAD18 SAP domain which highlights the conservation of the DNA binding and the PCNA interaction region (PIP) across species.
B) Comparing activity of RAD18^{WT} and RAD18 PIP mutants on free PCNA in gel-based assays shows that RAD18^{Y285A} activity is severely reduced on PCNA. Left Panel: UB^{TAMRA} signal of gel-based activity assays; Right Panel: Quantification of gel-based activity assay.
C) EMSA based DNA binding experiment shows that RAD18^{Y285A} and RAD18^{WT} has similar DNA binding capability while RAD18^{GK269AA} has lost its ability to bind DNA. Left Panel: Gel-Red stained gel of the EMSA assay; Right Panel: Quantification of bound DNA at the highest concentration (10μM) used in this assay.
D) Quantification of gel-based activity assay that compare activity of RAD18^{WT} and RAD18 DNA binding mutants on free PCNA show that all RAD18 DNA binding mutants have reduced activity on free PCNA.
E) Quantification of bound DNA at the highest concentration (10μM) used in EMSA assay for analysing DNA binding of RAD18 DNA binding mutants compared to RAD18^{WT}.

551327-L-bw-Dharadhar
Processed on: 30-12-2020
PDF page: 140

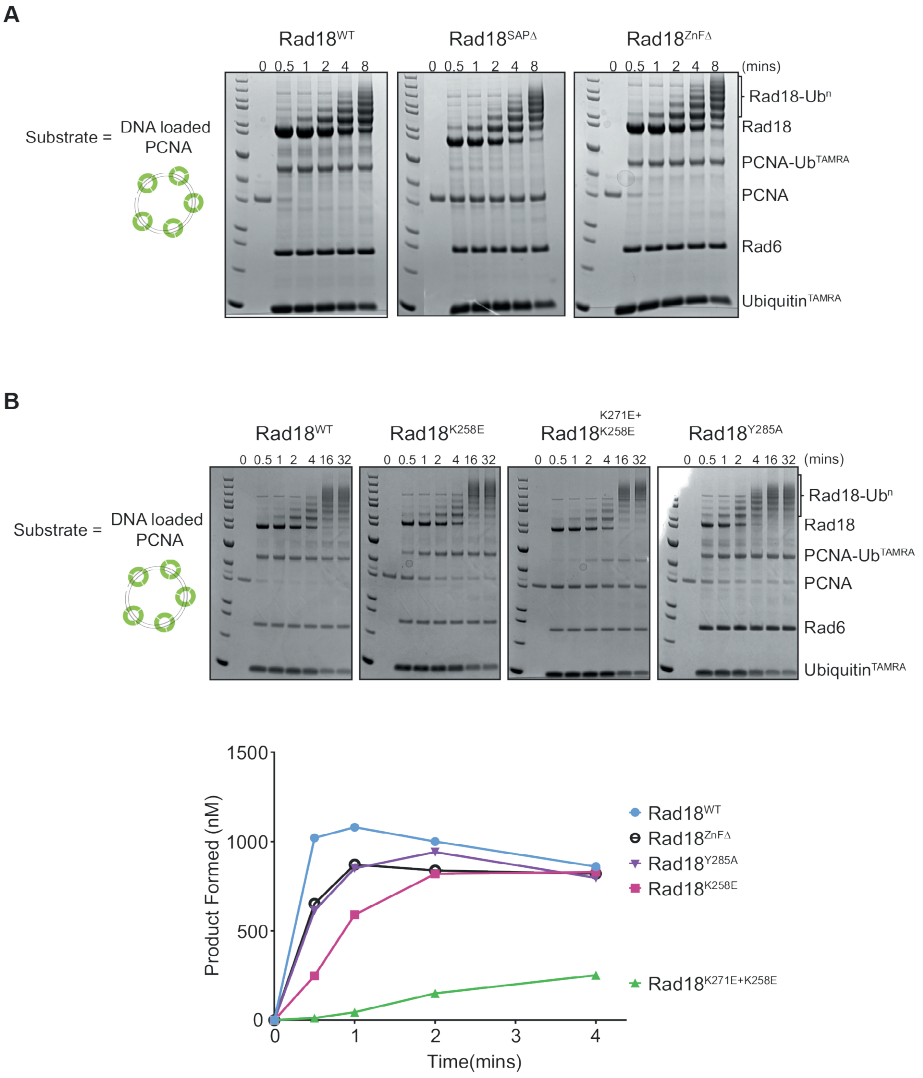

Fig.3) DNA binding function of SAP domain is essential for RAD18 activation on DNA-loaded PCNA.
A) Comparison of RAD18^{WT}, RAD18$^{\Delta ZnF}$ and RAD18$^{\Delta SAP}$ activity on DNA-loaded PCNA shows that deletion of SAP leads to complete loss of activity on PCNA whereas deletion of Zinc Finger has no effect on RAD18 mediated PCNA ubiquitination.
B) Comparison of RAD18^{WT}, RAD18^{Y285A}, RAD18^{K258E} and RAD18$^{K258E+K271E}$ activity on DNA-loaded PCNA shows that DNA binding is the only essential factor required for RAD18 activation. Upper Panel: Coomassie stained gels of in vitro activity assay on DNA-loaded PCNA; Bottom Panel: Quantification of amount of PCNA-UB formed versus time.

The RAD18 PIP mutant regains full activity on DNA-loaded PCNA

To analyse the role of individual domains in activation of RAD18 on DNA-loaded PCNA, we performed in vitro ubiquitination assays with the $RAD18^{\Delta SAP}$ and $RAD18^{\Delta ZnF}$. The $RAD18^{\Delta ZnF}$ showed similar activity like $RAD18^{WT}$ but the $RAD18^{\Delta SAP}$ had no activity on the DNA-loaded substrate (Fig.3a). To delineate the DNA and PCNA interaction functions of the SAP domain in RAD18 activation, we analysed several mutants of the SAP domain.

The $RAD18^{Y285A}$ mutant in the SAP domain is interesting as it has full DNA binding but has completely lost activity on free PCNA. We compared this PIP mutant ($RAD18^{Y285A}$) against two RAD18 DNA binding mutants ($RAD18^{K258E}$, $RAD18^{K271E+K258E}$) to see how it would act on DNA-loaded PCNA. Both DNA-binding mutants are less active, than WT, especially $RAD18^{K271E+K258E}$ (Fig.3b). Surprisingly, $RAD18^{Y285A}$ which lost activity on free PCNA (Fig.2b) now was able to modify DNA-loaded PCNA at similar levels as $RAD18^{WT}$ (Fig.3b). These experiments show that interaction of RAD18 PIP with PCNA is not important for efficient mono-ubiquitination of DNA-loaded PCNA whereas DNA binding by SAP domain is essential.

RAD18 employs a unique interface for ubiquitin transfer on DNA-loaded PCNA

The general mechanism of RING-mediated ubiquitination is thought to be conserved among members of the RING family. These E3 ligases mediate ubiquitin transfer by stabilization of ubiquitin into a catalytically competent state in the E2~Ub complex. This stabilization is mediated in dimer RING dimers by the RING domain that does not bind the E2 enzyme, as first shown for type 2 RING/RING dimer RNF4 at Y193 (Plechanovová *et al*, 2012). A similar stabilization was proposed for Type 1 RING ligases such as BRCA1/BARD1, RING1B-BMI1 and RAD18, and a charged residue present in the inactive RING was shown to affect activity in these enzymes (Densham *et al*, 2016). Upon superimposing the RAD18 RING domain structure on the RNF4-E2-UB structure (Plechanovová *et al*, 2012), R76 of RAD18 is found at the position corresponding to Y193 in RNF4 (Fig.4a). The $RAD18^{R76A}$ mutant was reported to have lower activity on PCNA compared to $RAD18^{WT}$ in HEK293 cells (Densham *et al*, 2016). We observed a similar effect of this mutant on PCNA activity. Somewhat surprisingly, however, it still carried out auto-ubiquitination with the same efficiency as $RAD18^{WT}$ (Fig.4b). This indicates that RAD18 has a distinct mechanism for auto-ubiquitination, either employing a different Ub-interaction surface which does not require the R76 residue or a completely different mechanism altogether.

551327-L-bw-Dharadhar
Processed on: 30-12-2020
PDF page: 142

To study the role of this residue in PCNA modification, we compared the activity of RAD18^{R76A} with RAD18^{WT} on DNA-loaded PCNA in our gel-based assays. Contrary to RAD18^{R76A} activity on free PCNA, RAD18^{R76A} ubiquitinates DNA-loaded PCNA as efficiently as RAD18^{WT} (Fig.4c). This shows that the mechanism of RAD18 RING activity is not comparable to other RING E3 ligases and that it employs a unique interface for ubiquitin interaction and its subsequent transfer to the target lysine. Intriguingly it also suggests that DNA-loaded PCNA may use a different mechanism than PCNA, implying that the activation process also changes the actual way that ubiquitin transfer is promoted.

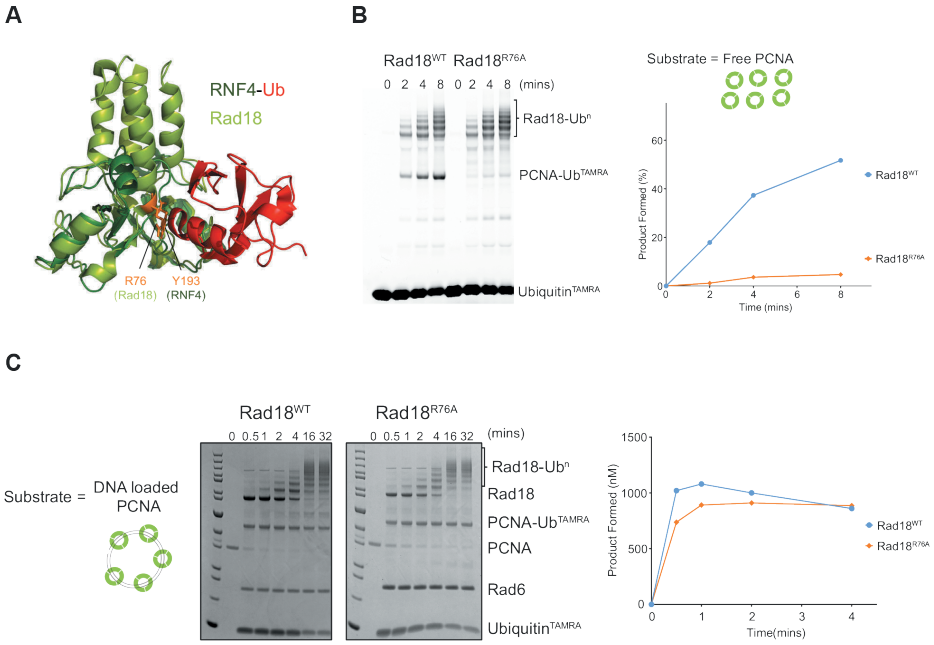

Fig.4) RAD18 employs a unique mechanism for ubiquitin transfer on DNA-loaded PCNA
A) Superimposition of RAD18 RING domain (dark green) on the RNF4 (light green)-E2 (not shown)-UB (red) structure shows the relative positioning of R76 on RAD18 with respect to Y193 on RNF4.
B) Comparison of RAD18^{WT} and RAD18^{R76A} activity on free PCNA shows the loss of activity of RAD18^{R76A} on free PCNA but no effect on its auto-ubiquitination activity. Left Panel: UB^{TAMRA} signal of gel-based activity assays comparing activity of RAD18^{WT} with RAD18^{R76A}; Right Panel: Quantification of gel-based activity assay.
C) Comparison of RAD18^{WT} and RAD18^{R76A} activity on DNA-loaded PCNA shows identical activity. Left Panel: Coomassie stained gels of in vitro activity assay on DNA-loaded PCNA; Right Panel: Quantification of amount of PCNA-UB formed versus time.

551327-L-bw-Dharadhar
Processed on: 30-12-2020
PDF page: 143

DISCUSSION

RAD18 is a member of the RING E3-ligase family and it plays a crucial role in the regulation of the translesion synthesis pathway. Several RING family members have been studied extensively, but a mechanistic understanding of RAD18 activity in TLS has not been reported yet. This study highlights the role of the SAP domain in RAD18 activity by identifying mutants that delineate its DNA and PCNA functions. We develop a protocol for large scale purification of DNA-loaded PCNA which is then used to study activity of $RAD18^{WT}$ and several mutants. We uncover several layers involved in the activation of RAD18 on DNA-loaded PCNA and also give mechanistic insight into RAD18-mediated ubiquitin transfer.

RAD6/RAD18-mediated PCNA mono-ubiquitination was significantly enhanced when PCNA is loaded on DNA (Haracska *et al*, 2006b). However, the true extent of activation caused by DNA loading of PCNA is not yet determined since the authors state that these assays contained a mixture of free and DNA-loaded PCNA. Additionally, the kinetic parameters involved in the activation of the ubiquitination reaction were not analysed. In our setup we have maximized the DNA-loaded PCNA, giving improved quantification of kinetic parameters, that allows analysis of the mechanism of this reaction. Any small amount of free PCNA will be reloaded by RFC. We have not carried out full kinetic analysis here, but current activity data shows that binding of RAD18 to DNA-loaded PCNA does not affect auto-ubiquitination of RAD18. This suggests that RAD18 activation is more likely due to increased affinity for its substrate rather than increased intrinsic activity.

The Zinc Finger and SAP domains are in close proximity to each other. Here, we show that RAD18 activity on PCNA is solely governed by the SAP domain and deletion of the Zinc Finger domain has no effect on RAD18 activity in vitro. We don't observe any defect in the ability of $RaAD18^{ZnF\Delta}$ to self-dimerize or perform auto-ubiquitination in contrast to earlier reports that implicate the ZnF domain for these functions (Miyase *et al*, 2005). The C207F mutation has been shown to have no effect on RAD18 dimerization in vitro (Notenboom *et al*, 2007a) whereas in vivo this mutation had lost self-association ability (Miyase *et al*, 2005). Thus, it is possible that the difference in assay conditions contribute to the conflicting results between in vitro and in vivo studies.

DNA interaction mutants within the SAP domain have a severe effect on RAD18 activity towards PCNA (Tsuji *et al*, 2008), but it is not known if this is due to inability to bind PCNA or due to reduced intrinsic activity of Rad18. Here, we identify a putative PIP motif at the end of the SAP domain and show that mutation within the PIP leads to complete loss of activity on PCNA. Due to the close proximity of the PIP motif to the DNA interaction

551327-L-bw-Dharadhar
Processed on: 30-12-2020
PDF page: 144

mutants it is likely that the DNA mutants distort the structure of the SAP domain which also affects the proposed PCNA-PIP interaction.

The RAD18^{Y285A} is the first SAP mutant that has no activity on free PCNA but it can still bind DNA as well as RAD18^{WT}. This allowed us to show that activation of RAD18 is mediated by the SAP domain only through its DNA binding function whereas PCNA interaction through the PIP motif is not necessary. Moreover, DNA loading makes the K164 on PCNA the most favourable target as PCNA mono-ubiquitination is much faster than RAD18 auto-ubiquitination which is contrary to what is observed in assays with free PCNA. Altogether, this suggests that DNA binding of RAD18 brings the ubiquitin charged RAD6 in an optimal position for ubiquitin transfer on K164 of PCNA.

RING-mediated ubiquitination relies on stabilization of the donor ubiquitin by positively charged residue in the 'other' RING domain (Densham *et al*, 2016). In RAD18, this Arg76 and mutation of the analogous residue in BRCA1-BARD1 and RING1-BMI1 significantly reduced RING activity. We did not observe reduced auto-ubiquitination of RAD18^{R76A} but ubiquitination of free PCNA is severely affected. Therefore, we propose that RAD18 employs two distinct mechanisms. This could be two distinct interfaces for ubiquitin transfer, one for auto-ubiquitination and another for free PCNA mono-ubiquitination, but it also possible that transfer is mediated in a different way. It is likely that interaction of RAD18 with its substrate causes conformational changes which leads to binding of the RING domain to donor Ub through the conventional charged residue interface. In the absence of substrate binding the RING domain utilizes another interface for interaction with donor Ub which remains to be identified.

Interestingly, on DNA-loaded PCNA the R76A mutant can mono-ubiquitinate PCNA as efficiently as RAD18^{WT}. This suggests two different mechanisms for ubiquitin transfer on free PCNA and DNA-loaded PCNA respectively, an idea that is supported by the different effect of the PIP mutation, which does affect PCNA modification, but not the DNA-loaded modification. Thus, we propose that RAD18 does not employ the R76 interface or the PIP for activity on DNA-loaded PCNA and it uses either the auto-ubiquitination mechanism or another unique mechanism as a result of conformational changes induced upon DNA binding.

551327-L-bw-Dharadhar
Processed on: 30-12-2020
PDF page: 145

REFERENCES

Bailly V, Lauder S, Prakash S & Prakash L (1997) Yeast DNA repair proteins Rad6 and Rad18 form a heterodimer that has ubiquitin conjugating, DNA binding, and ATP hydrolytic activities. *J. Biol. Chem.* **272:** 23360–23365

Choe KN & Moldovan GL (2017) Forging Ahead through Darkness: PCNA, Still the Principal Conductor at the Replication Fork. *Mol. Cell* **65:** 380–392

Davies AA, Huttner D, Daigaku Y, Chen S & Ulrich HD (2008) Activation of Ubiquitin-Dependent DNA Damage Bypass Is Mediated by Replication Protein A. *Mol. Cell* **29:** 625–636

Densham RM, Garvin AJ, Stone HR, Strachan J, Baldock RA, Daza-Martin M, Fletcher A, Blair-Reid S, Beesley J, Johal B, Pearl LH, Neely R, Keep NH, Watts FZ & Morris JR (2016) Human BRCA1-BARD1 ubiquitin ligase activity counteracts chromatin barriers to DNA resection. *Nat. Struct. Mol. Biol.* **23:** 647–655

Dou H, Buetow L, Hock A, Sibbet GJ, Vousden KH & Huang DT (2012) Structural basis for autoinhibition and phosphorylation-dependent activation of c-Cbl. *Nat. Struct. Mol. Biol.* **19:** 184–192

Eissenberg JC, Ayyagari R, Gomes X V & Burgers PM (1997) Mutations in yeast proliferating cell nuclear antigen define distinct sites for interaction with DNA polymerase delta and DNA polymerase epsilon. *Mol. Cell. Biol.* **17:** 6367–6378

Garg P & Burgers PM (2005) Ubiquitinated proliferating cell nuclear antigen activates translesion DNA polymerases η and REV1. *Proc. Natl. Acad. Sci. U. S. A.* **102:** 18361–18366

Haracska L, Unk I, Prakash L & Prakash S (2006a) Ubiquitylation of yeast proliferating cell nuclear antigen and its implications for translesion DNA synthesis. *Proc. Natl. Acad. Sci.* **103:** 6477–6482

Haracska L, Unk I, Prakash L & Prakash S (2006b) Ubiquitylation of yeast proliferating cell nuclear antigen and its implications for translesion DNA synthesis. *Proc. Natl. Acad. Sci. U. S. A.* **103:** 6477–6482

Hedglin M & Benkovic SJ (2017) Eukaryotic Translesion DNA Synthesis on the Leading and Lagging Strands: Unique Detours Around the Same Obstacle. *Physiol. Behav.* **176:** 139–148

Hoege C, Pfander B, Moldovan GL, Pyrowolakis G & Jentsch S (2002) RAD6-dependent DNA repair is linked to modification of PCNA by ubiquitin and SUMO. *Nature* **419:** 135–141

Huang A, Hibbert RG, De Jong RN, Das D, Sixma TK & Boelens R (2011) Symmetry and asymmetry of the RING-RING dimer of Rad18. *J. Mol. Biol.* **410:** 424–435

Miyase S, Tateishi S, Watanabe K, Tomita K, Suzuki K, Inoue H & Yamaizumi M (2005) Differential regulation of Rad18 through Rad6-dependent mono- and polyubiquitination. *J. Biol. Chem.* **280:** 515–524

Nakajima S, Lan L, Kanno SI, Usami N, Kobayashi K, Mori M, Shiomi T & Yasui A (2006) Replication-dependent and -independent Responses of RAD18 to DNA damage in human cells. *J. Biol. Chem.* **281:** 34687–34695

Notenboom V, Hibbert RG, van Rossum-Fikkert SE, Olsen J V., Mann M & Sixma TK (2007a) Functional characterization of Rad18 domains for Rad6, ubiquitin, DNA binding and PCNA modification. *Nucleic Acids Res.* **35:** 5819–5830

Notenboom V, Hibbert RG, van Rossum-Fikkert SE, Olsen J V., Mann M & Sixma TK (2007b) Functional characterization of Rad18 domains for Rad6, ubiquitin, DNA binding and PCNA modification. *Nucleic Acids Res.* **35:** 5819–5830

Plechanovová A, Jaffray EG, McMahon SA, Johnson KA, Navrátilová I, Naismith JH & Hay RT (2011) Mechanism of ubiquitylation by dimeric RING ligase RNF4. *Nat. Struct. Mol. Biol.* **18:** 1052–1059

551327-L-bw-Dharadhar
Processed on: 30-12-2020
PDF page: 146

Plechanovová A, Jaffray EG, Tatham MH, Naismith JH & Hay RT (2012) Structure of a RING E3 ligase and ubiquitin-loaded E2 primed for catalysis. *Nature* **489:** 115–120

Pruneda JN, Littlefield PJ, Soss SE, Nordquist KA, Chazin WJ, Brzovic PS & Klevit RE (2012) Structure of an E3:E2~Ub Complex Reveals an Allosteric Mechanism Shared among RING/U-box Ligases. *Mol. Cell* **47:** 933–942

Tateishi S, Niwa H, Miyazaki J-I, Fujimoto S, Inoue H & Yamaizumi M (2003) Enhanced Genomic Instability and Defective Postreplication Repair in RAD18 Knockout Mouse Embryonic Stem Cells. *Mol. Cell. Biol.* **23:** 474–481

Tateishi S, Sakuraba O, Masuyama S, Inoue R & Yamaizumi M (2000) Dysfunction of human Rad18 results in defective postreplication repair and hypersensitivity to multiple mutagens. *Proc. Natl. Acad. Sci. U. S. A.* **97:** 7927–7932

Tsuji Y, Watanabe K, Araki K, Shinohara M, Yamagata Y, Tsurimoto T, Hanaoka F, Yamamura K ichi, Yamaizumi M & Tateishi S (2008) Recognition of forked and single-stranded DNA structures by human RAD18 complexed with RAD6B protein triggers its recruitment to stalled replication forks. *Genes to Cells* **13:** 343–354

Watanabe K, Tateishi S, Kawasuji M, Tsurimoto T, Inoue H & Yamaizumi M (2004) Rad18 guides polη to replication stalling sites through physical interaction and PCNA monoubiquitination. *EMBO J.* **23:** 3886–3896

Yoder BL & Burgers PMJ (1991) Saccharomyces cerevisiae replication factor C. I. Purification and characterization of its ATPase activity. *J. Biol. Chem.* **266:** 22689–22697

551327-L-bw-Dharadhar
Processed on: 30-12-2020
PDF page: 147

CHAPTER 6

GENERAL DISCUSSION

DISCUSSION

The genomic integrity of the cell is maintained by a host of repair pathways that employ enzymes from different families. Ubiquitin E3 ligases and deubiquitination enzymes (DUBs) are often involved in the regulation of these pathways and have emerged as potential drug targets in several diseases. This strategy of modulating ubiquitin modifying enzymes can lead to specific targeting of pathways resulting in less toxicity. Development of specific inhibitors for this group of enzymes has proven to be complex due to which most current inhibitors target the active site. Since most DUBs and E3 ligases share identical active site grooves within their respective families the active site inhibitors often lack specificity. Therefore, development of compounds that target enzyme activity via an allosteric mechanism could lead to greater specificity and reduced off-target effects. Moreover, allosteric inhibitors are more likely to avoid resistance and they can be used in combination with more traditional inhibitors to increase their clinical potential (Wylie *et al*, 2017). In this thesis, we study the ubiquitin modifying enzymes involved in the translesion synthesis pathway and gain a mechanistic understanding of how these enzymes are regulated allosterically.

Stalling of replication forks due to damaged DNA is overcome either by repairing the impeding damage or by DNA damage tolerance (DDT) pathways. Translesion synthesis is a DDT pathway where the damaged DNA is bypassed by specialized translesion polymerases thereby preventing the formation of toxic DNA damage induced by fork stalling. Mono-ubiquitination of PCNA is an essential regulatory step of this pathway as it leads to the recruitment of the translesion polymerases to the replication fork (Hedglin & Benkovic, 2015). The E2-E3 ligase pair of RAD6-RAD18 and the DUB USP1 regulate the (de)modification on DNA-loaded PCNA (Hoege *et al*, 2002; Huang *et al*, 2006). Here, we looked at the mechanisms involved in the regulation of catalytic activity of USP1 and RAD18 by the substrate i.e. DNA-loaded PCNA-Ub. We also investigated the activation of USP1 and two closely related paralogs, USP12 and USP46 by a WD40 repeat protein called UAF1.

USP1, USP12 and USP46 belong to the largest family of DUBs called the Ubiquitin specific proteases (USPs). USP12 and USP46 are mainly composed of the USP catalytic domain and have a sequence similarity of 88%. They are amongst the smallest members of the USP family which are mostly large multi-domain proteins with a conserved catalytic fold. USP1 is much larger compared to USP12 and USP46 mostly due to the presence of several inserts within its catalytic domain but the function of these inserts is so far unknown. The role of inserts on USP catalytic activity has not been studied in a systematic manner but it is known that several USPs contain domains that are involved

551327-L-bw-Dharadhar
Processed on: 30-12-2020
PDF page: 150

in self-regulatory mechanisms which affect intrinsic activity or substrate recruitment (Nijman *et al*, 2005; Ye *et al*, 2009; Sahtoe & Sixma, 2015). In Chapter 4, we have investigated the role of these inserts in USP1 activity on the minimal substrate. We found that the large insert 1 along with insert 3 auto-inhibit USP1 activity in the absence of UAF1. This auto-inhibition is not observed in the presence of UAF1 suggesting that UAF1 binding leads to a rearrangement of insert 1 and insert 3 resulting in the loss of auto-inhibition.

The insert 3 of USP1 is a small insert of approximately 20 amino acid residues and is located on the backside of the ubiquitin binding cleft. This is a functionally intriguing location as USP12 and USP46 bind to their secondary activator, WDR20, in this region (Li *et al*, 2016). Unlike USP12 and USP46, USP1 does not interact with WDR20 (Kee *et al*, 2010) but instead carries the insert 3 which we show plays an important role in USP1 activity together with insert 1. We went a step further and showed that insert 1 and 3 mediated activation in USP1 resembles the WDR20-mediated activation of USP12 and USP46. Moreover, our activity studies revealed that UAF1 binding to USP1 compensates for the lack of WDR20 binding as USP1-UAF1 reaches the same catalytic state as the USP12/USP46-UAF1-WDR20 complex. This compensation is brought about in part by the rearrangement of the insert 1 and insert 3 upon UAF1 binding. In the absence of any structural information of the USP1-UAF1 complex it is difficult to fully understand the effect of UAF1 binding but our studies have identified a defined region for allosteric activation in USP1. Many other USPs contain inserts (Nijman *et al*, 2005; Ye *et al*, 2009) whose function is still not known and a systematic approach of probing USP activity upon insert deletion could lead to more examples of such allosteric mechanisms.

Structural information on the USP-UAF1 complex could be vital to understand how this class of USPs is activated by UAF1. In chapter 3, we have solved the crystal structure of the USP12-UAF1 complex bound to ubiquitin and found two sites for UAF1 binding. We show that the USP12-UAF1 complex exists in a 1:2 stoichiometry in solution where UAF1 binds USP12 on the finger subdomain and on the backside of the ubiquitin binding cleft (Dharadhar *et al*, 2016). We confirmed previous findings that UAF1 binding on the fingers of USP12 leads to catalytic activation in spite of the binding site being distant from the USP catalytic center (Yin *et al*, 2015). We did not observe any significant structural changes in USP12 upon UAF1 binding as the enzyme was trapped in the activated state with Ubiquitin Propargyl for structural studies. We tried determining the structure of the USP12-UAF1 complex in the absence of ubiquitin but failed to do so. However, another group was able to determine the structure of USP12-UAF1 without ubiquitin and also the structure of the USP12-UAF1-WDR20. They identified several subtle rearrangements in

551327-L-bw-Dharadhar
Processed on: 30-12-2020
PDF page: 151

USP12 upon UAF1 binding and proposed that the allosteric activation was a sum of all these changes (Li *et al*, 2016). Interestingly, one prominent location was the small helix and loop at the base of the fingers which is where insert 3 is located in USP1.

In Chapter 3, we also show that UAF1 binds to a second site on USP12 which does not have an effect on its catalytic activity. Our binding studies confirm that this two-step binding is also conserved in both USP46 and USP1 which could imply an important role that is independent of activation. In case of USP12 and USP46 this second binding could have a direct impact on WDR20-mediated activation as there is a partial overlap between the two interfaces. The binding kinetics of UAF1 for the two binding sites is different as the fingers binding has high affinity with low off rates while the backside binding has relatively low affinity with high off rates. This could indicate a more dynamic role in regulation of USP1/12/46 function for the backside binding but the exact function remains to be determined. So far, we have been unable to develop disruptive mutations in USP12 for the backside binding as it is dominated by backbone interactions. The lack of site-specific mutations has made it difficult to perform any functional studies for the role of backside binding but its conservation in the sub-family indicates an important role for USP activity.

The activation of USP12 by UAF1 is a dynamic process where several elements undergo small changes that allow for greater catalytic activity. This has become apparent from the set of USP12-UAF1 structures which show marked differences amongst themselves. Thus, new emerging techniques will have to be used to fully understand the UAF1 activation mechanism as crystal structures alone will only serve as snapshots of a highly mobile system. In the case of USP1 this is more important since it has longer flexible regions which we have shown to be essential for UAF1 mediated activation of USP1. We know that the finger subdomain of USP1 is important for UAF1 binding and it is likely that the allosteric effect observed is relayed from the fingers to the rest of the molecule similar to what is seen in USP12. Homology models of the USP1-UAF1 complex based on the USP12-UAF1 structures show that insert 3 of USP1 lies at the base of the fingers which could explain how UAF1 binding leads to the loss of the insert 1 and insert 3 mediated auto-inhibition. Structural information of the full-length protein or insert 1 alone could help in obtaining more details of the activation mechanism as any further correlation from the USP12 structures is difficult due to the large size of the USP1 inserts.

Enzymatic analysis of DUBs has been mostly carried out on minimal substrates which leads to a limited understanding of the enzyme in several areas. One such aspect is

551327-L-bw-Dharadhar
Processed on: 30-12-2020
PDF page: 152

the effect of enzyme-substrate interactions on the catalytic state of the enzyme. In the case of USP1, the natural substrate is mono-ubiquitinated PCNA (PCNA-Ub) but since it carries out its role in TLS the ideal substrate should be PCNA-Ub loaded on DNA. In Chapter 4, we establish a workflow to purify DNA-loaded PCNA-Ub and perform quantitative enzymatic assays with USP1-UAF1. We show that USP1-UAF1 undergoes a 5-fold activation on DNA-loaded PCNA-Ub compared to free PCNA-Ub whereas USP1 alone undergoes a 2-fold activation on the DNA-loaded substrate. The role of DNA binding in USP1 activity on FANCD2 has been studied before and conflicting results have emerged with one report claiming that FANCD2-UB is shielded by DNA leading to reduced deubiquitination (Twest *et al*, 2017) while the other reports shows that the presence of DNA stimulates USP1-UAF1 activity on FANCD2-UB (Liang *et al*, 2019). The increase in activity of USP1 and USP1-UAF1 complex on DNA-loaded PCNA-Ub was solely due to an increase in affinity for the substrate. Combining USP1 activity data from three different substrates allowed us to develop a comprehensive model for USP1 activity regulation with defined kinetic parameters. Our analysis identified two distinct mechanisms of USP1 activation involving UAF1 activation by increased catalytic turnover and through DNA-loaded PCNA by increased substrate binding.

The DNA binding ability of both USP1 and UAF1 has been described in literature before but their role in TLS remains to be investigated (Lim *et al*, 2018; Liang *et al*, 2019). In Chapter 4, we have provided an impetus to this process by identifying mutations that disrupt both DNA and PCNA interactions respectively. Using a combination of mutagenesis and in vitro activity assays we show that insert 1 of USP1 is essential for not only DNA binding but also for activity on PCNA. Identification of a PCNA interaction mutant in USP1 allows us to specifically affect USP1 function in the TLS context as the region that interacts with FANCD2 resides in the N-terminal extension of USP1 and deletion of USP1 inserts does not affect activity on FANCD2 (Arkinson *et al*, 2018). Additionally, the PCNA interaction mutant is proficient in DNA binding which allows us to delineate the role of DNA binding and PCNA interaction within TLS. Based on our enzymatic assays of these mutants on DNA -loaded PCNA-Ub, we propose that both the DNA and PCNA interactions of insert 1 are necessary to achieve full activation on DNA- loaded PCNA. The effect of these mutants in cell-based functional assays remains to be tested and work in this direction is currently ongoing. Insert 1 of USP1 has emerged as a vital component for USP1 activity regulation by UAF1 and for USP1 activation on DNA- loaded PCNA. It is a large insert of 200 amino acids and currently there is no structural information available but this is a promising target for development of allosteric inhibitors to specifically inhibit USP1 function.

551327-L-bw-Dharadhar
Processed on: 30-12-2020
PDF page: 153

USP1 deubiquitination of PCNA-Ub in TLS is counteracted by the E2-E3 ligase couple RAD6-RAD18. It is known for more than a decade that RAD6-RAD18 mediated ubiquitination is more efficient (100 folds) when PCNA is loaded on DNA (Haracska *et al*, 2006) but several mechanistic questions remain unanswered. In Chapter 5, we uncover the molecular determinants involved in this activation and also shed light on the mechanism of this substrate mediated activation. Similar to insert 1 of USP1, we show that the SAP domain of RAD18 has both DNA and PCNA interaction regions. Our data confirms the presence of a previously unidentified PCNA interaction region which contains a PIP motif commonly found in PCNA interacting proteins. Presence of the PIP motif in both USP1 and RAD18 indicates the likelihood of both these enzymes competing with each other for access to PCNA which will be governed by factors such as local concentration of the enzymes and their affinity to the substrate.

In RAD18, the SAP domain is comprised of approximately 50 residues and both DNA and PCNA interaction regions are close to each other. We observed that all our DNA binding mutants which are outside the PIP motif had a severe effect on PCNA activity. However, we could delineate the two roles of the SAP domain as the RAD18 PIP mutant lacked any PCNA activity but was still proficient in DNA binding. The in-house setup for purification of DNA-loaded PCNA allowed us to test a large set of RAD18 mutants in quantitative gel-based enzymatic assays. These assays also enabled us to follow RAD18 auto-ubiquitination and we observed that there is no change in RAD18 auto-ubiquitination in the presence of DNA-loaded substrate. This suggests that the observed activation on DNA-loaded PCNA is due to an increase in affinity for the substrate rather than an intrinsic activation of the RAD18 ubiquitination process. Upon testing a combination of DNA and PCNA interaction mutants for activity on DNA-loaded PCNA, it was apparent that unlike USP1, activation in RAD18 was solely due to DNA interactions of the SAP domain. This suggests that upon DNA binding the RAD18 molecule is arranged in such a manner that the RAD6-loaded ubiquitin molecule is positioned optimally for transfer to K164 on PCNA. It is likely that the DNA-mediated positioning of RAD18 with respect to PCNA allows for RAD18-PCNA interaction making the PIP mutant redundant. Overall, our data confirm the role of DNA binding in the activation of RAD18 on DNA-loaded PCNA.

In Chapter 5, we also investigated the mechanistic details of RING-mediated ubiquitin transfer in RAD18. We show that RAD18 uses a unique RING-ubiquitin interface for auto-ubiquitination and for mono-ubiquitination on DNA-loaded PCNA. However, RAD18 needs the traditional charged residue interface (R76) (Densham *et al*, 2016) for efficient mono-ubiquitination of free PCNA which indicates the presence of a change in mechanism in RAD18 between substrates. Since the PIP interaction of RAD18 is only essential for

551327-L-bw-Dharadhar
Processed on: 30-12-2020
PDF page: 154

activity on free PCNA it is possible that this interaction leads to conformational changes in RAD18 that engages the traditional charged interface for ubiquitin transfer. The RAD18 interface involved in ubiquitin transfer to DNA-loaded PCNA and for auto-ubiquitination remains to be identified. Until now dimeric RING E3 ligases have been shown to rely on the "arginine lynchpin" for stabilizing the closed conformation of E2-Ub, which enables the efficient transfer of ubiquitin to the substrate (Plechanovová *et al*, 2012; Dou *et al*, 2012; Densham *et al*, 2016). However, the RING domain of Arkadia depends on secondary ubiquitin-RING binding to stabilize the closed confirmation and enhance ubiquitin transfer (Wright *et al*, 2016). A similar mechanism could exist in RAD18 where the donor ubiquitin interacts with additional RING or non-RING elements of the E3 ligase. Further biochemical and structural studies would help in determining these regions within RAD18 and also reveal details on how the nature of the substrate can alter catalytic activity by switching interfaces involved in ubiquitin transfer.

In this thesis, we have uncovered several molecular mechanisms involved in the regulation of ubiquitin modifying enzymes. The role of USP1 inserts in activation by UAF1 sheds light on self-regulatory mechanisms that are involved in controlling USP1 enzymatic activity. Several other USP proteins contain inserts whose functions are still unknown, thus research in this direction could lead to an understanding of several such self-regulatory mechanisms. In addition to self-regulation of catalytic activity we have also uncovered mechanistic details of substrate-mediated activation in both USP1 and RAD6-RAD18. Biochemical characterization of these enzymes using natural substrates has led to the identification of molecular determinants that are involved in this activation. Our studies show that both USP1 and RAD6-RAD18 contain PIP interaction regions, this could have an important role to play in TLS pathway as both would compete for the same site on PCNA and depending on upstream stimuli they could dislodge each other from the substrate. (De)-Ubiquitination assays of other E3 ligases and DUBs with their respective substrates could offer several more examples of substrate mediated alterations in catalysis. The regions involved in the allosteric regulation of E3 ligases and DUBs have immense potential for the development of potent inhibitors that target regions other than the conserved active site of these proteins. If detailed molecular mechanisms are understood then specific perturbation of ubiquitin modifying enzymes can be achieved.

551327-L-bw-Dharadhar
Processed on: 30-12-2020
PDF page: 155

REFERENCES

Arkinson C, Chaugule VK, Toth R & Walden H (2018) Specificity for deubiquitination of monoubiquitinated FANCD2 is driven by the N-terminus of USP1. *Life Sci. Alliance* **1:** 1–15

Densham RM, Garvin AJ, Stone HR, Strachan J, Baldock RA, Daza-Martin M, Fletcher A, Blair-Reid S, Beesley J, Johal B, Pearl LH, Neely R, Keep NH, Watts FZ & Morris JR (2016) Human BRCA1-BARD1 ubiquitin ligase activity counteracts chromatin barriers to DNA resection. *Nat. Struct. Mol. Biol.* **23:** 647–655

Dharadhar S, Clerici M, Dijk WJ Van, Fish A & Sixma TK (2016) A conserved two-step binding for the UAF1 regulator to the USP12 deubiquitinating enzyme. *J. Struct. Biol.*

Dou H, Buetow L, Sibbet GJ, Cameron K & Huang DT (2012) BIRC7-E2 ubiquitin conjugate structure reveals the mechanism of ubiquitin transfer by a RING dimer. *Nat. Struct. Mol. Biol.* **19:** 876–883

Haracska L, Unk I, Prakash L & Prakash S (2006) Ubiquitylation of yeast proliferating cell nuclear antigen and its implications for translesion DNA synthesis. *Proc. Natl. Acad. Sci. U. S. A.* **103:** 6477–6482

Hedglin M & Benkovic SJ (2015) Regulation of Rad6/Rad18 Activity During DNA Damage Tolerance. *Annu. Rev. Biophys.* **44:** 207–228

Hoege C, Pfander B, Moldovan GL, Pyrowolakis G & Jentsch S (2002) RAD6-dependent DNA repair is linked to modification of PCNA by ubiquitin and SUMO. *Nature* **419:** 135–141

Huang TT, Nijman SMB, Mirchandani KD, Galardy PJ, Cohn M a, Haas W, Gygi SP, Ploegh HL, Bernards R & D'Andrea AD (2006) Regulation of monoubiquitinated PCNA by DUB autocleavage. *Nat. Cell Biol.* **8:** 339–347

Kee Y, Yang K, Cohn MA, Haas W, Gygi SP & D'Andrea AD (2010) WDR20 regulates activity of the USP12.UAF1 deubiquitinating enzyme complex. *J. Biol. Chem.* **285:** 11252–11257

Li H, Lim KS, Kim H, Hinds TR, Jo U, Mao H, Weller CE, Sun J, Chatterjee C, D'Andrea AD & Zheng N (2016) Allosteric Activation of Ubiquitin-Specific Proteases by β-Propeller Proteins UAF1 and WDR20. *Mol. Cell* **63:** 249–260

Liang F, Miller AS, Longerich S, Tang C, Maranon D, Williamson EA, Hromas R, Wiese C, Kupfer GM & Sung P (2019) DNA requirement in FANCD2 deubiquitination by USP1-UAF1-RAD51AP1 in the Fanconi anemia DNA damage response. *Nat. Commun.* **10:** 1–8

Lim KS, Li H, Roberts EA, Gaudiano EF, Clairmont C, Sambel LA, Ponnienselvan K, Liu JC, Yang C, Kozono D, Parmar K, Yusufzai T, Zheng N & D'Andrea AD (2018) USP1 Is Required for Replication Fork Protection in BRCA1-Deficient Tumors. *Mol. Cell* **72:** 925-941.e4

Nijman SMB, Luna-Vargas MPA, Velds A, Brummelkamp TR, Dirac AMG, Sixma TK & Bernards R (2005) A genomic and functional inventory of deubiquitinating enzymes. *Cell* **123:** 773–786

Plechanovová A, Jaffray EG, Tatham MH, Naismith JH & Hay RT (2012) Structure of a RING E3 ligase and ubiquitin-loaded E2 primed for catalysis. *Nature* **489:** 115–120

Sahtoe DD & Sixma TK (2015) Layers of DUB regulation. *Trends Biochem. Sci.* **40:** 456–67

Twest S van, Murphy VJ, Hodson C, Tan W, Swuec P, O'Rourke JJ, Heierhorst J rg, Crismani W & Deans AJ (2017) Mechanism of Ubiquitination and Deubiquitination in the Fanconi Anemia Pathway. **:** 1–13

Wright JD, MacE PD & Day CL (2016) Secondary ubiquitin-RING docking enhances Arkadia and Ark2C E3 ligase activity. *Nat. Struct. Mol. Biol.* **23:** 45–52

Wylie AA, Schoepfer J, Jahnke W, Cowan-Jacob SW, Loo A, Furet P, Marzinzik AL, Pelle X, Donovan J, Zhu W, Buonamici S, Hassan AQ, Lombardo F, Iyer V, Palmer M, Berellini G, Dodd S, Thohan S, Bitter H, Branford S, et al (2017) The allosteric inhibitor ABL001 enables dual targeting of BCR-ABL1. *Nature* **543:** 733–737

551327-L-bw-Dharadhar
Processed on: 30-12-2020
PDF page: 156

Ye Y, Scheel H, Hofmann K & Komander D (2009) Dissection of USP catalytic domains reveals five common insertion points. *Mol. Biosyst.* **5:** 1797–1808

Yin J, Schoeffler AJ, Wickliffe K, Newton K, Starovasnik MA, Dueber EC & Harris SF (2015) Structural Insights into WD-Repeat 48 Activation of Ubiquitin-Specific Protease 46. *Structure* **23:** 2043–2054

551327-L-bw-Dharadhar
Processed on: 30-12-2020

ADDENDUM

Summary
Samenvatting
Stellingen
Curriculum Vitae
PhD Portfolio
List of Publications
Acknowledgements

SUMMARY

DNA damage is a continuous process that needs to be countered effectively by the cell to ensure a healthy genome. The cell uses DNA repair pathways to remove damaged sites on DNA but during replication it also makes use of DNA damage tolerance (DDT) pathways to prevent stalling of the replication fork. Translesion synthesis is a DDT pathway that is regulated by the attachment and removal of a single ubiquitin molecule on PCNA. The E2-E3 pair RAD6-RAD18 mono-ubiquitinate PCNA at K164 residue and USP1 deubiquitinates the mono-ubiquitinated PCNA. The catalytic activity of both these enzymes is regulated by different mechanisms, especially USP1, which binds a WD40 repeat protein called UAF1 leading to a significant increase in its activity.

Ubiquitin specific proteases (USPs) form the largest class of DUBs and many have been implicated in crucial cellular processes. **In Chapter 2**, we provide a template for studying Ubiquitin specific protease (USP) function in vitro. The purification of a few USP proteins is described here along with detailed procedures for studying enzymatic activity of USPs. This chapter shows how activity studies could be used to identify different layers of regulation in USPs, which could be mediated by internal domains, interacting modulators or even the substrate itself. Since, all these regulatory factors could contribute together it is useful to perform quantitative analysis which can tease apart individual contributions of different factors.

In Chapter 4, we perform quantitative analysis of USP1 activity on 3 different substrates of increasing complexity, i.e., Ub-Rhodamine, PCNA-Ub and DNA-loaded PCNA-Ub. We show that USP1 activity is stimulated on DNA-loaded PCNA compared to free PCNA-Ub. Our quantitative kinetic modelling of USP1 activity shows that the activation on the DNA-loaded substrate is solely due to an increase in affinity for the substrate. Using deletion mutants of USP1, we identify insert L1 as the domain responsible for the activation on the DNA loaded substrate. We also identify regions within insert L1 which are important for DNA and PCNA interaction, and we show that both these interactions are important for stimulation of USP1 activity on DNA-loaded PCNA.

USP1 has low intrinsic activity alone but it gets activated upon binding a WD40 repeat protein called UAF1 which increases the catalytic turnover of USP1. Two closely related paralogs of USP1, i.e. USP12 and USP46 also bind UAF1 and get activated by an increase in catalytic turnover. **In Chapter 3**, we show how UAF1 binds this class of USPs by solving the crystal structure of the USP12-UAF1 complex with ubiquitin. We identify a conserved two step binding of UAF1 to USP12 and USP1 as well as confirm the presence of a 1:2 stoichiometry of the USP12-UAF1 complex in solution. Using mutational analysis, we

551327-L-bw-Dharadhar
Processed on: 30-12-2020
PDF page: 160

show that the high affinity UAF1 binding on the fingers of USP12 is important for the activation of the enzyme whereas the low affinity backside binding does not play a direct role in activation. Since the backside UAF1 binding site overlaps with another activator of USP12 called WDR20, we propose that the backside binding of UAF1 might play a role in regulation of USP12 by competing with WDR20.

USP1 unlike USP12 and USP46 has several inserts whose role in USP1 function is poorly understood. **In Chapter 4**, we identify a self-regulatory mechanism in USP1 involving the combined action of insert L1 and insert L3. We show that insert L1 and L3 together auto-inhibit USP1 activity and this gets relieved upon binding of USP1 to UAF1. We also observe that removal of insert L1 and L3 mediated auto-inhibition brings USP1 to a catalytic competent state similar to what is observed in USP12/USP46 upon WDR20 binding. Our analysis demonstrates how UAF1 binding leads to activation of USP1 by relieving insert L1 and L3 mediated auto-inhibition.

In Chapter 5, we uncover the mechanisms involved in RAD6-RAD18 activity on DNA-loaded PCNA. We confirm the importance of the SAP domain in RAD18 for activity on both free and DNA-loaded PCNA. We identify a PCNA interaction site within the SAP domain and by mutational analysis show that it is important for activity of RAD18 on free PCNA. Activity assays on DNA-loaded PCNA with RAD18 mutants show that RAD18 activation is entirely dependent on SAP-DNA interactions. Finally, we propose that RAD18 uses two different RING-ubiquitin interfaces for ubiquitin transfer depending upon the type of substrate. We show that RAD18 uses a common arginine residue (R76) for ubiquitin stabilization and transfer on free PCNA but for transfer on DNA loaded PCNA or RAD18 itself, it uses a unique RING-ubiquitin interface.

In **Chapter 6**, we discuss the results presented here in the context of existing research from the ubiquitin field and provide future directions for research in the regulatory mechanisms of DUBs and E3 ligases.

551327-L-bw-Dharadhar
Processed on: 30-12-2020
PDF page: 161

SAMENVATTING

DNA schade is een voortdurend proces dat de cel continu moet herstellen, om zo een gezond genoom te behouden. De cel gebruikt de DNA reparatieroutes om schade in DNA te verwijderen. Maar tijdens DNA replicatie, wanneer herstel te lang zou duren, wordt door de cel het *DNA damage tolerance* (DDT) mechanisme gebruikt, om te voorkomen dat de replicatie vork vastloopt. Een belangrijke vorm van DDT is de translesie synthese. Deze wordt gereguleerd door het plaatsen en verwijderen van een enkel ubiquitine molecuul op PCNA. Het E2-E3 paar, RAD6-RAD18, plaatst een enkele ubiquitine op lysine 164 (K164) in PCNA en USP1 haalt deze mono-ubiquitine weer weg. De katalytische activiteit van deze beide enzymen wordt op diverse manieren gereguleerd Dit geldt met name voor USP1, waar binding aan een WD40-*repeat* eiwit, genaamd UAF1, een significante activatie geeft.

Ubiqiutine-specifieke proteases (USPs) vormen de grootste klasse van de-ubiquitinerende enzymen (DUB), en zijn betrokken bij vele cruciale cellulaire processen. In **Hoofdstuk 2**, tonen wij een template voor het bestuderen van USP functies *in vitro*. De zuivering van een aantal USP eiwitten wordt besproken, samen met gedetailleerde procedures voor de bestudering van enzymatische activiteit in USPs. Dit hoofdstuk laat zien hoe activiteit-experimenten gebruikt kunnen worden om verschillende niveaus van USP-regulatie te identificeren. Diverse factoren kunnen bijdragen aan de activiteit, zoals interactie met interne domeinen, met externe modulatoren of zelfs met het substraat zelf. Aangezien al deze factoren kunnen samenwerken is het belangrijk om kwantitatieve analyses uit te voeren waarmee de individuele invloeden van de verschillende factoren van elkaar gescheiden kunnen worden.

In **Hoofdstuk 4**, laten we kwantitatieve analyses van USP1-activiteit zien op drie verschillende substraten, oplopend in complexiteit; Ub-Rhodamine, PCNA-Ub en PCNA-Ub geladen op DNA. We tonen aan dat USP1 activiteit gestimuleerd wordt door PCNA-Ub op DNA, vergeleken met vrij PCNA-Ub. De kwantitatieve modelering van USP1 activiteit laat zien dat de activatie op het DNA-geladen substraat uitsluitend komt door een toename in affiniteit voor het substraat. Door gebruik te maken van deletiemutanten van USP1, hebben we de insertie L1 geïdentificeerd als het domein dat verantwoordelijk is voor de activatie op het DNA-geladen substraat. Ook hebben we regio's in insertie L1 gevonden die belangrijk zijn voor de interactie met DNA en PCNA. We tonen aan dat deze interacties met DNA en PCNA belangrijk zijn voor de stimulatie van USP1 activiteit op het op DNA-geladen PCNA.

USP1 heeft een lage intrinsieke activiteit. Deze wordt versterkt door de binding aan een WD40-*repeat* eiwit, genaamd UAF1, door een hogere katalytische *turnover*. Twee

551327-L-bw-Dharadhar
Processed on: 30-12-2020
PDF page: 162

gerelateerde paralogen van USP1, USP12 en USP46, binden ook aan UAF1, en worden ook geactiveerd via een toename in de katalytische *turnover*. In **Hoofdstuk 3**, laten we zien hoe UAF1 deze klasse van USPs bindt door het oplossen van de kristalstructuur van het USP12-UAF1 complex gebonden aan ubiquitine. We hebben een geconserveerd twee-staps binding van UAF1 aan USP12 en USP1 geïdentificeerd, en daarnaast een 1:2 stoichiometrie van USP12-UAF1 in oplossing. Door gebruik te maken van mutatie analyses, kunnen we de hoge affiniteit van UAF1 voor de 'vingers' van USP12 aantonen, en het belang hiervan voor de activatie van de enzymactiviteit. Dit terwijl de binding aan de 'achterkant' een lage affiniteit heeft en geen directe rol spelt in de activatie. Aangezien de 'achterkant' van UAF1 overlapt met een andere activator van USP12, genaamd WDR20, stellen we voor dat de binding met de 'achterkant' van UAF1 mogelijk een rol speelt in de regulatie van USP12 door competitie met WDR20.

USP1 heeft, in tegenstelling tot USP12 en USP46, een aantal inserties waarvan de rol niet volledig begrepen is. In **hoofdstuk 4**, hebben we een zelfregulerend mechanisme ontdekt in USP1, wat verzorgd wordt door de gecombineerde activiteit van inserties L1 en L3. We tonen aan dat inserties L1 en L3 samen een automatische rem vormen op USP1 activiteit, en deze remming wordt opgeheven na de binding van UAF1 aan USP1. Ook laten we zien dat het afnemen van de automatische rem van inserties L1 en L3, USP1 in een katalytische competente status brengt die vergelijkbaar is aan de toestand van USP12/USP46 na binding aan WDR20. Onze analyses tonen hoe UAF1 binding leidt tot activatie van USP1 door het afnemen van de automatische rem, door L1 en L3.

In **Hoofdstuk 5**, ontdekken we de mechanismen die betrokken zijn bij RAD6-RAD18 activiteit op DNA-geladen PCNA. We bevestigen het belang van het SAP domein in RAD18 voor de activiteit op zowel vrij als DNA-geladen PCNA. We identificeren een bindingsplaats voor PCNA in het SAP domein, en door middel van mutaties tonen we aan dat deze binding belangrijk is voor de activatie van RAD18 op vrij PCNA. Activatieproeven op het DNA-geladen PCNA met RAD18 mutanten laat zien dat de activatie van RAD18 volledig afhankelijk is van de interacties tussen SAP en DNA. Tenslotte poneren we de hypothese dat RAD18 twee verschillende RING-ubiquitine bindingsplekken heeft, die overdracht van ubiquitine mogelijk maken en dat het gebruik hiervan afhankelijk is van het type substraat. We laten zien dat RAD18 een bekende arginine (R76) gebruikt voor het stabilisaties van ubiquitine op de E2 en katalyse van de overdracht naar vrij PCNA maar voor dit proces, op DNA-geladen PCNA of op RAD18 zelf, gebruikt het een unieke bindingsplaats op het RING-ubiquitine oppervlak.

551327-L-bw-Dharadhar
Processed on: 30-12-2020
PDF page: 163

In **Hoofdstuk 6,** plaatsen we de resultaten in de context van bestaande literatuur van het ubiquitine-veld. Daarnaast geven we voorstellen voor toekomstig onderzoek naar mechanismen van DUBs en E3-ligases.

551327-L-bw-Dharadhar
Processed on: 30-12-2020

STELLINGEN

1. UAF1 binding to the finger sub-domain of USP12 leads to increased catalytic activity while the second binding event does not affect catalytic activity on a minimal substrate. (this thesis)

2. The primary mechanisms by which USP1 is activated by UAF1 is through relieving the auto-inhibition caused by the joint action of insert L1 and L3. (this thesis)

3. USP1 deubiquitinates PCNA-Ub more efficiently when it is loaded on DNA and this effect is strengthened when in complex with UAF1. (this thesis)

4. Insert L1 is an important regulatory hub within USP1 necessary for both substrate mediated activity enhancement and allosteric activation upon UAF1 binding. (this thesis)

5. RAD18 employs two distinct interfaces for ubiquitin transfer on free PCNA and DNA loaded PCNA respectively. (this thesis)

6. Successful *in vitro* characterization of de(ubiquitination) enzymes requires pure and stable protein.

7. Quantitative analysis of enzymatic activity on natural substrates is essential for mechanistic understanding of enzyme function and regulation.

8. Structural information alone is not enough to understand dynamic regulatory systems involving flexible elements.

9. A lot of good scientific research is lost due to a lack of time to pursue unexpected results.

10. While differing widely in the various little bits we know, in our infinite ignorance we are all equal. (Karl R. Popper)

11. We must accept finite disappointment, but never lose infinite hope. (Martin Luther King, Jr)

551327-L-bw-Dharadhar
Processed on: 30-12-2020
PDF page: 165

CURRICULUM VITAE

Shreya Dharadhar was born on January 22, 1988 in Mumbai, India. In 2009 he graduated from Mumbai University with a Bachelor of Science in Biotechnology and enrolled in the same Master program of Mumbai University. He was awarded the Master degree in 2011. In September 2011, he enrolled in the Masters of Biomolecular science program at the Vrije University Amsterdam. He performed his first internship in the lab of Dr. Yves Bollen at Vrije University Amsterdam where he studied membrane localization of proteins. In February 2013, he joined the group of Prof. Titia Sixma at the Netherlands Cancer Institute in Amsterdam for his second internship project. He worked on bacterial mismatch repair proteins and was awarded the Master degree by the end of the internship. In October 2013, he started to work as a PhD student under the supervision of Prof. Titia Sixma at the Netherlands Cancer Institute. The research presented in the thesis were performed in the Netherlands Cancer Institute, Amsterdam.

551327-L-bw-Dharadhar
Processed on: 30-12-2020
PDF page: 166

PHD PORTFOLIO

Name of the PhD student: Shreya Dharadhar
Erasmus MC Department: Genetics
Graduate School: Onderzoekschool Oncologie Amsterdam
PhD period: 2013-2020
Promoter: Prof. dr. Titia K. Sixma

1. PHD TRAINING

Courses:

2015 Basic Microscopy Course 'In the footsteps of Antoni van Leeuwenhoek', OOA, a Amsterdam
2016 X-Ray methods in Structural biology, Cold Spring Harbor Laboratories, NY, USA
2018 Scientific writing course 'Getting your manuscript out for review and your work the a attention it deserves', OOA, Amsterdam
2019 iNEXT workshop on Integrated methodologies and approaches for Structural biology

Seminars:

2013-2020 NKI Research club seminars, Amsterdam (oral presentations)
2013-2020 Weekly division research meeting (oral presentations)
2013-2020 International NKI seminars, lunchmeetings with speakers
2015 X-Ray techniques in biology, SyNeW mini school, Utrecht

(Inter)national conferences:

Oct 2013 Annual Graduate Student retreat; Renesse, NL (poster)
Dec 2013 NWO-CW Study Group Meeting 'Chemistry in Relation to Biology and Medical a Sciences', Veldhoven, NL (poster)
Oct 2014 Annual Graduate Student retreat; Renesse, NL (oral presentation)
Oct 2016 CPH-Bioscience conference, Protein signaling; Copenhagen, Denmark
Dec 2016 NWO-CHAINS, Veldhoven, NL (oral presentation)
Oct 2017 Annual Graduate Student retreat; Renesse, NL (oral presentation)
Apr 2018 Dutch Replication meeting, Delft, NL (poster)
Sep 2019 EMBO workshop, The ubiquitin system: Biology, mechanism and role in disease, Cavtat, Croatia (poster)

551327-L-bw-Dharadhar
Processed on: 30-12-2020
PDF page: 167

2. TEACHING

Student Intern Supervision

2015: Supervision Master student, Anna Chertkova (5 months)
2016: Supervision Master student, Tom Rappol (9 months)
2018: Supervision Master student, Ivette Aarsman (5 months)
2018: Supervision Master student, Ishita Gupta (3 months)

551327-L-bw-Dharadhar
Processed on: 30-12-2020

LIST OF PUBLICATIONS

Dharadhar S, van Dijk W.J, Scheffers S, Fish A, Sixma T.K (2020) Insert L1 is a central hub for allosteric regulation of USP1 activity. Manuscript accepted, EMBO Reports

Dharadhar S, Kim R.Q, Uckelmann M, and Sixma T.K (2019). Quantitative analysis of USP activity in vitro. Methods in enzymology

Dharadhar S, Clerici M, van Dijk W.J, Fish A, and Sixma T.K (2016). A conserved two-step binding for the UAF1 regulator to the USP12 deubiquitinating enzyme. J. Struct. Biol. 196.

Gupta I, **Dharadhar S**, Sixma T.K, and Khan S (2020).Biochemical characterization of TRIM72 E3 ligase and its interaction with the insulin receptor substrate 1. Biochem. Biophys. Reports 21, 100729.

Bhairosing-Kok D, Groothuizen F.S, Fish A, **Dharadhar S**, Winterwerp H.H.K, and Sixma T.K (2019). Sharp kinking of a coiled coil in MutS allows DNA binding and release. Nucleic Acids Res. 47.

Hiruma Y, Koch A, **Dharadhar S**, Joosten R.P and Perrakis A (2016). Structural basis of reversine selectivity in inhibiting Mps1 more potently than aurora B kinase. Proteins Struct. Funct. Bioinforma. 84.

551327-L-bw-Dharadhar
Processed on: 30-12-2020
PDF page: 169

ACKNOWLEDGEMENTS

During the many years of completing my PhD there were several people who have helped me finish this thesis and made the whole process enjoyable.

Firstly, I would like to thank **Titia** for giving me the opportunity of working in her lab. I am very grateful for your guidance and the confidence that you have showed in me. You were supportive and understanding of my personal struggles and your suggestions have helped in clearing many scientific obstacles. I have learnt a lot from you and I wish you more success in the future.

This work would have not been possible without the help of **Pim**. I was lucky that I got a chance to work with you. Thank you for the endless protein preps and also for running the lab smoothly. Special thanks to **Sasha** for the training on various biophysical techniques and for the help with Biacore and the modelling of USP1 activity. It was a lot of fun working with you and chatting about a variety of things. I also want to express my sincere thanks to **Tassos** and **Heinz** for their help and suggestions during the yearly progress meetings.

Another person who has made a big contribution to the work presented here is **Serge**. I am grateful for all the help with preps and cloning. You adapted very quickly in the lab which made our collaboration fruitful and I am sure that you will do very well in managing the lab. Apart from the science, I had a lot of fun spending time with you inside and outside the lab and I am sure we will remain in touch since we are neighbors now. This brings me to all the other office members who have played an important role in making the lab enjoyable. **Nassos**, I had a great time with you especially our trip to Greece and all the amazing dinners. I will definitely miss all the fun and long chats that we had in the office. Thank you for your generosity with everything and I wish you all the best in getting that Cryo-EM structure in Brno. **Doreth**, I will miss the nice time we had in the office and the discussions about all the lab stuff to vent out our frustrations. Thank you for all the help during the thesis writing and I am sure we will continue to meet at many more lunches. **Misbah**, I am grateful for all the help both inside and outside the lab. I will miss the conversations we had on many different topics (mainly Indian politics) during our customary tea breaks. I hope we can continue to do this outside the lab and i wish you good luck for your new job in Leiden.

I would also like to thank some of my lab mates who have now left the department. **Robbert,** thank you for all the fun moments we had during our PhD journey, it was great

551327-L-bw-Dharadhar
Processed on: 30-12-2020
PDF page: 170

to see you handle all the PhD stress with so much ease. **Luca**, it was great fun having you in the office and I really enjoyed our chats about music and food. **Tati,** thank you for all the help in the lab especially with the crystals.

Special thanks to **Flora** who trained me when I started in the lab as a graduate student and **Marcello** who helped me with kick starting my PhD. I also want to thank all the other past members of the Sixma and Perrakis lab, **Herrie, Michael**, **Danny**, **Thanga, Roy, Elli, Yoshi, Bart, George, Willem-Jan** for all the help and the good times in the lab.

I would like to wish all the current members of the Sixma and Perrakis lab (**Xiahou**, **Yvette**, **Andrea**, **Bogac**, **Shun**, **Anu**, **Susanne**, **Niels, Razvan, Jitske and Fernando)** good luck with their respective projects and thank you for all the help and suggestions during the group meetings. Thank you to all the past and present members of the Brummelkamp lab (**Thijn**, **Lisa**, **Lucas**, **Joppe**, **Vincent**, **Marcus**, **Jaqueline**, **Astrid**, **Lisa**, **Abdel**, **Gian-Luca**, **Peter**) and good luck for all the future endeavors. I also want to thank all members of the Protein facility (**Patrick**, **Magda**, **Justina** and **John**), especially **John** for all the help with providing insect cells.

Many people outside the lab have helped me in various ways during this journey. Firstly, I would like to thank all my friends and family members back home for their constant support and encouragement. **Onkar and Radhika**, it will be difficult to list everything here with the limited space so thank you for all the help. Thanks to **Anirudh** for being a great roommate and friend.

I want to thank my parents for all sacrifices that they have made to make all of this possible. This thesis is dedicated to the both of you. Finally, thanks to the most special person in my life, my wife. **Mayuri**, you have been a pillar and I have relied on you during the most testing times that came during my PhD. I don't know how all of this could be done without you. I am looking forward to the next phase in our life and I am sure that it will be even more beautiful.

551327-L-bw-Dharadhar
Processed on: 30-12-2020
PDF page: 171